Heat and cold recovery, a PV/ Thermal experiment

A case study done at
the Coolworld Waalwijk
cooling systems test facility

Master Thesis: MSc Sustainable Energy Technology

Lars Meeuwisse

TUDelft

Heat and cold recovery, a PV/ Thermal experiment

A case study done at the Coolworld Waalwijk cooling systems test facility

by

Lars Meeuwisse

Student Name	Student Number
Lars Meeuwisse	4317815

Thesis Supervisor:	Dr. R. Santbergen
Daily Supervisor Assistant:	P. Bruijstens
External Supervisor:	Professor K. Hooman
Thesis Committee:	Professor A. Smets
Project Duration:	06, 2023 - 05, 2024
Faculty:	Faculty of EEMCS, Delft

Cover:	Test setup with PVT panels attached to rest cold circuit at Coolworld Rentals BV Waalwijk.
Style:	TU Delft Report Style, with modifications by Daan Zwaneveld

T̂U Delft

Preface

During this master's thesis for the study programme Sustainable Energy Technology (SET) I have had the privilege to combine both an academic background with a practical implementation in developing solutions for the testing facility for cooling systems of Coolworld Waalwijk. This has triggered me to further explore the world of cooling and heating energy systems and by this message, I want to thank Coolworld Rentals B.V. in Waalwijk for giving me the opportunity to explore this curiosity. The unique blend of industry insight and academic guidance I received has profoundly influenced both my educational experience and my ideas for my future career path.

First, I would like to express my gratitude to Paul Bruijstens, my daily supervisor at Coolworld Rentals. His guidance was crucial in navigating the challenges and our out-of-the-box thoughts have certainly pushed me in the right direction multiple times, for new possibilities within the current system. His mentorship was invaluable, providing both support and encouragement as well as enjoyment throughout my research.

My sincere thanks also go to Dr. Rudi Santbergen from the PMVD department, whose expertise and insightful feedback have greatly enriched this thesis. His dedication to academic excellence has been inspirational, pushing me to refine my research.

Special thanks are owed to Professor Kamel Hooman, who facilitated my research at Coolworld Rentals B.V. His support in making this collaboration possible is greatly appreciated, as it allowed me to bridge theoretical knowledge with practical application in a real-world setting.

This thesis represents not just an academic achievement but also a chapter of personal growth, brought about by the challenges and learning that accompanied my research. I am grateful for the opportunity to work with such distinguished individuals and for the support provided by both the TU Delft and Coolworld Rentals B.V.

Lastly, I hope this research contributes valuable insights to the field of testing cooling machines and the use of rest cold, in lifting energy efficiencies for PV panels. May the outcome of this report serve as a stepping stone for future studies. I look forward to the continuous journey of learning and discovery in the vast field of sustainable technology.

Lars Meeuwisse
Delft, May 2024

Summary

Coolworld Waalwijk, a cooling machines rental service experiences marginal growth due to the rise of cooling systems for temporarily use. Their testing facility is heavily occupied for testing systems up to 800 kW. Due to regulations by the Dutch government, risen energy prices, and potential energy grid congestion, besides the willingness to more sustainable practices, the urge rises for implementation of new energy solutions to their 500 MWh annual consumption. Part of this demand is heat demand for warming residual cold, which insinuates the investment in a combined solution.

Currently, investments in solar-generated energy have become cheaper than fossil fuel alternatives and the rise of newly developed technology such as PVT panels is ever-increasing. This is especially relevant when considering the PV energy generation losses that occur when exposed to high temperatures. This is where Coolworld comes in. In seeking a sustainable alternative energy resource, their residual cold could actively cool solar panels, enhancing their performance.

This master's thesis aims to gain insight into the energy-intensive processes and losses at Coolworld Waalwijk's testing facility and to identify sustainable solutions. With the outcome, an Energy Management Strategy (EMS) will be created, to to offer key sustainability opportunities for other cooling machines testing facilities. Additionally, it includes an analysis of a PV/Thermal system, with Coolworld as a case study.

This study investigated all individual components, cooling machines, and testing methods to identify areas where energy consumption could be reduced or losses prevented. The findings show significant losses from current systems, such as an antifreeze floor heating system and an insulated warm water vessel maintained at 25°C, losing 420 and 976 kWh per week respectively during winter. Additionally, there is a loss of 342 kWh per week due to incorrect usage of heat recovery exchangers on the facility's roof. A test setup demonstrated that no external heating is required when heat from the cooling machines' exhaust is properly captured. Based on this recommendations are made for installing a professional heat capture system, adjusting testing procedures, implementing controllers to prevent heat leakage during tests, and investigating processes running outside working hours.

Additionally, a study was conducted on reusing residual cold produced during testing. Both a numerical model and an experimental setup were built. The model and current energy demand (split into heat and electricity) created and validated system sizing for standalone PV, solar collector, and PVT systems. For the PVT system, it was shown that active cooling of PV panels could increase efficiency by 0.0140% per degree Celsius compared to uncooled panels. The thermal efficiency could reach higher values when the mean fluid temperature inside the collector is much lower, suggesting that thermal performance in temperature profiles below STC could be even higher.

The built strategy for heat recovery research in other testing facilities, along with the identified energy losses and corresponding recommendations, and the gained knowledge on thermal performance in below STC conditions, demonstrate the potential benefits for this and other testing facilities with rest cold.

Contents

Nomenclature

Abbreviations

Abbreviation	Definition
AOI	Angle of Incidence
BV	Buffer Vessel Sequence
CAGR	Compound Annual Growth Rate
CC	Circuit Sequence
CFC	Chlorofluorocarbons
CW	Coolworld Rentals B.V.
DB	Duffie-Beckman
DHI	Diffuse Horizontal Irradiance
DNI	Direct Normal Irradiance
DTU	Data Transfer Unit
EG	Ethylene Glycol
EPR	Electronic Pressure Regulators
EMS	Balance Management Strategy
EW	East-West
GHG	Greenhouse Gas
GHI	Global Horizontal Irradiance
GWP	Global Warming Potential
HCFC	Hydrochlorofluorocarbons
HFC	Hydrofluorocarbons
HVAC	Heating, Ventilation, and Air Conditioning
IEA	International Energy Agency
IEEE	Intelligent Energy Europe Programme
INOCT	Installed Nominal Operating Cell Temperature
IPCC	Intergovernmental Panel on Climate Change
LCoE	Levelised Cost of Electricity
LNG	Liquified Natural Gas
LTC	Low Temperature Chiller
LU	Luchtbehandeling (Air Handler)
KNMI	Royal Netherlands Meteorological Institute
MEG	Monoethylene Glycol
MPG	Monopropylene Glycol
MS	Microsoft
NL	The Netherlands
NOCT	Nominal Operating Cell Temperature
PO	Pomp (Pump)
PV	Photovoltaic
PVT	Photovoltaic Thermal
QDT	Quasi Dynamic Testing
RM	Remote Monitoring
RVO	Rijksdienst Voor Ondernemend Nederland
SET	Sustainable Energy Technology
SF	Shading Factor
SS	Steady State
SST	Steady State Testing
STC	Standard Test Conditions

Abbreviation	Definition
SVF	Sky View Factor
TEDCW	Total Energy Demand CW
Wp	Wattpeak
WW	Warmtewisselaar (Heat Exchanger)

Latin Symbols

Symbol	Definition	Unit
A	Area, of the solar collector	[m^2]
A_module	Module azimuth angle	[°]
C_p	Specific heat capacity	J/(kg.K)
d	Differential or distance	[m]
D	Diameter	m
Gb	Beam (direct) solar irradiance	[W/m^2]
Gd	Diffuse solar irradiance	[W/m^2]
h_c	Convective heat transfer coefficient	[W/(m^{2}K)]
I	Solar irradiance	[W/m^2]
k	Thermal conductivity	[W/(mK)]
L	Length of an object or system	[m]
m	Mass	[kg]
N	Number of units or modules	[-]
P	Power or Pressure	[W], [Pa]
$Q_{consumption}$	Consumed heat quantity	[J]
Q_{loss}	Heat loss quantity	[J]
$Q_{storage}$	Stored heat quantity	[J]
r	Radius	[m]
t	Thickness of the material	
T_{air}	Ambient air temperature	[K]
$T_{surface}$	Temperature of the collector surface	[K]
$T_{surroundings}$	Temperature of the surroundings	[K]
T_1	Initial temperature	[K]
T_2	Final temperature	[K]
T_a	Ambient temperature	[K]
T_m	Module temperature	[K]
T_{NOCT}	Temperature under Nominal Operating Cell Conditions	[K]
T_{fluid}	Fluid temperature within a system	[K]
T_{inside}	Temperature inside a structure or device	[K]
$T_{outside}$	Temperature outside a structure or device	[K]
T_{wall}	Wall temperature	[K]
U	Overall heat transfer coefficient	W/(m$^2 \cdot$ K)
u'	Modified wind speed	[m/s]
V	Velocity, Voltage or Volume	[m/s], [V] or [m^3]

Greek Symbols

Symbol	Definition	Unit
α	Reflectivity of the collector surface (dimensionless), Albedo	[-]
β	Beta, temperature coefficient or angle	[-]

Symbol	Definition	Unit
Δ	Symbol for difference/change	
γ	Gamma, coefficient or angle	[-]
λ	Lambda, wavelength	[m]
ρ	Density	[kg/m^3]
ϵ	Emissivity of the material	
ε	Emissivity of the collector surface (dimensionless)	[-]
η_{aux}	Efficiency of auxiliary components	[-]
η_{el}	Electrical Efficiency at Maximum Power Point	[-]
η_{inv}	Conversion efficiency of the inverter	[-]
η_{MPP}	Maximum Power Point efficiency	[-]
θ	Theta, temperature or angle	[°or K]
θ_L	Low incidence angle	[°]
θ_m	Module angle	[°]
θ_T	High incidence angle	[°]
ϕ	Phi, phase or angle	[°]
ψ	Psi, function or angle	[°]
ϑ_a	Ambient temperature in specific context	[K]
ϑ_m	Modified temperature notation	[K]

Constants

Symbol	Definition	Value
e	Base of natural logarithm	≈ 2.71828
π	Pi, mathematical constant	≈ 3.14159
σ	Stefan-Boltzmann constant	$5.670374419 \times 10^{-8}\,\text{W/(m}^2\text{K}^4)$

Introduction

1.1. Solar energy and development

The global energy transition we are currently in, has resulted in an 89% decline in the photovoltaic (PV) solar energy price per MW, making it now even more interesting to invest in solar panel generation, than investments in coal plants [1]. The price for one MW installed solar powered energy generated electricity has reduced from 359$ in 2014 to 40$ in 2019, surpassing even the most optimistic predictions set by the Intergovernmental Panel on Climate Change (IPCC). Therefore it can be said that these IPCC reports will have to be reviewed again.

Also in the Dutch energy market, this transition can be seen. The total energy production from solar panels rose by 46% in 2022, compared to 2021, mainly due to the introduction of new solar panels and solar panel techniques. This growth can be seen in Figure 1.1, which both show the growth in solar energy production in the Netherlands (NL) from 2019 to 2022. This figure shows that the total energy production from solar energy has been more than 3 times the size in 2019. Economic growth and innovations go hand in hand, and the TU Delft plays a pivotal role in this. At the Photovoltaic Materials and Design (PVMD) department of the Electrical Engineering faculty these solar-specific developments are closely followed and new ideas are designed, manufactured and tested.
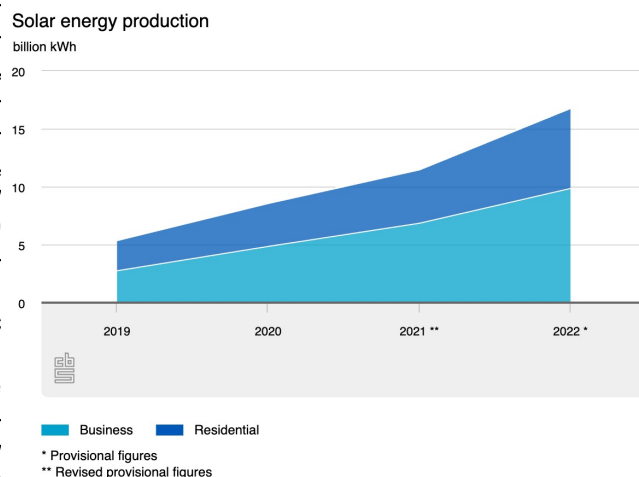
Figure 1.1: Solar Energy Production in NL (source: [2])

One of these is the fast development of PV Thermal (PVT) panels. A new group of students and PhD students along with professors recently looked at these developments but the focus lies on modelling. Nevertheless, the urge is there to do real-time tests to validate these. The outcome of this could be useful for manufacturers which then can result in an economic impulse and investments by people and companies to a more sustainable energy mix.

1.1.1. Solar panel performances

In the world of solar energy, efficiency is one of the most important parameters which is mainly based on design aspects. Different heat transfer and PV panel structures are modelled, to showcase efficiency to temperature outcome since heat generation results in efficiency losses for PV panels. To understand this phenomenon, a brief explanation of the electrical charge of a PV panel will be described. PV technology converts solar energy into electricity. A PV cell acts as a p-n junction diode, whose electrical properties, such as voltage, current, or resistance, alter under light exposure. Solar cells, when

combined into panels, can produce energy, with single-junction silicon cells generating a maximum open-circuit voltage of around 0.5 to 0.6 V. The operation involves light photons from sunlight reaching the p–n junction, penetrating the thin p-type layer, and energising the junction to create electron-hole pairs, thereby disrupting thermal equilibrium and allowing electrons and holes to move across the junction, generating voltage. More on this is elaborated in section J.1.

Temperature increases impact the PV cell performance by raising circuit resistance, reducing electron velocity, and thus lowering open-circuit voltage, quantified by the temperature coefficient. This effect also badly influences the cell material which leads to a reduction in longevity, which is not investigated further in this study.

In essence, a PV cell is designed to generate an electric current when exposed to sunlight. The cell operates across a spectrum of voltages, ranging from zero to open-circuit volts V_{OC}, where it experiences a short-circuit condition where the voltage is zero, and so is Power ($P = I * V$). Therefore, the point at which a PV cell or panel delivers its maximum power output, known as the Maximum Power Point (MPP), does not coincide with either the short-circuit or open-circuit conditions. Instead, it is found at an intermediate point where the product of current (I) and voltage (V) is at its highest. This is typically determined under conditions of full sunlight, where the solar cell's voltage and current output are such that they yield the greatest possible power output, effectively harnessing the solar energy.

Since the V_{OC}, as described below in Equation 1.1, related to equation 9.1 from the Solar Energy book [3], is depending on temperature, this also manipulates the efficiency. Namely, when temperature T rises, V rises as well, rising closer towards V_{OC} turning eventually in a power output of zero with I being zero, which can be seen in Figure 1.2a following the Power Curve. So this temperature increment lowers the efficiency.

$$V_{oc} = \frac{k_B \cdot T}{q} \ln\left(\frac{J_{ph}}{J_0} + 1\right) \approx \frac{k_B \cdot T}{q} \ln\left(\frac{J_{ph}}{J_0}\right) \tag{1.1}$$

Besides this, when looking at the I-V characteristics with different temperatures lower than Standard Testing Conditions (STC), as shown in Figure 1.2b, the MPP can increase. This study is on the temperature efficiency when cooled below STC. With a physically built testing setup.

(a) Current - Voltage characteristics for Solar Panels

(b) Current - Voltage characteristics for solar panels at different temperatures
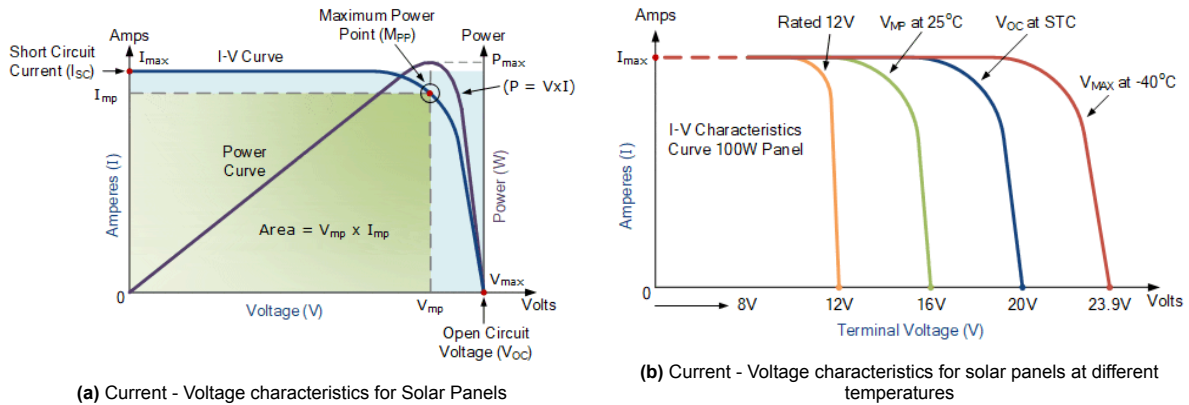
Figure 1.2: Current - Voltage diagrams, source: Alternative Energy Tutorials [4]

1.2. Coolworld Rentals B.V. Waalwijk

Coolworld Rentals B.V. (Coolworld), a prominent provider of cooling systems spread over 7 countries in Europe, recognises the urgency of sustainable practices. Currently, they have an energy consumption of over 450 MWh per year. This energy consumption is mainly due to their testing facility. The facility runs cooling machines 5 days a week day during working hours, ranging from 20 to 800 kW, with machines which have just returned from, or, are going to a new rental contract. The machines produce cold glycol-water (varying from ± -10°C until -30°C, from warm glycol-water, which is the inlet to the machines. Below, this is schematically drawn. In Figure 1.3, a 3D version of the cooling circuit and

both the heating circuits are shown. An external vessel BV20, is used to warm up the cold BV06 vessel, to ensure a consistent cooling test process.
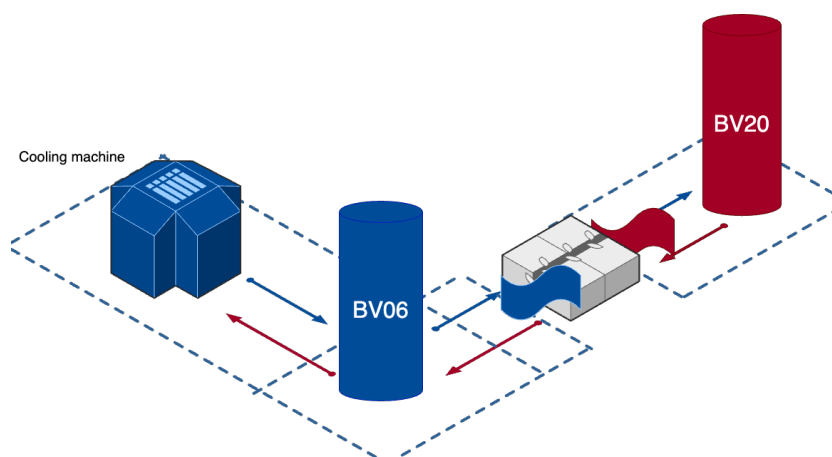
Figure 1.3: The cooling process, the main process of the testing facility, a cooling machine cools down a vessel, whereafter this gets heated again with the heat, from another filled with warm liquid to cold liquid, its evaporator blows out warm air to do this, the process is very energy consuming

This process consists of 3 main subprocesses, starting with the cooling machine producing cold, as Figure 1.4 below shows.
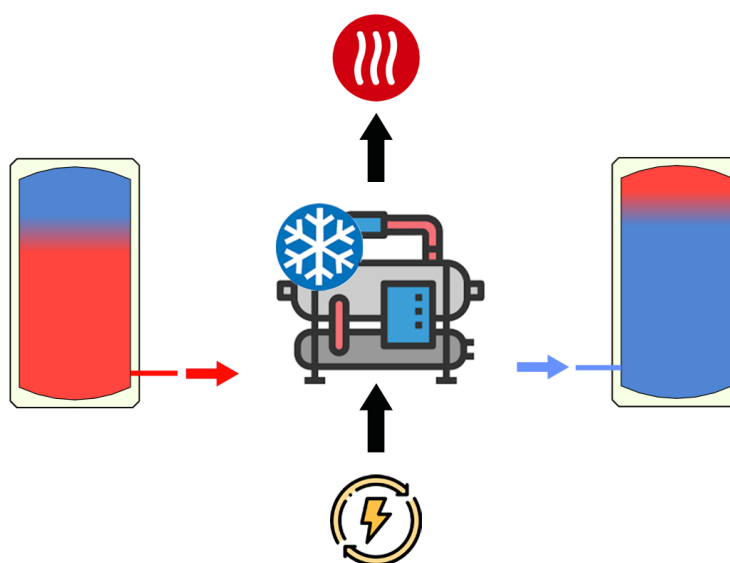
Figure 1.4: The cooling process, the main process of the testing facility, a cooling machine cools down a vessel filled with warm liquid to cold liquid, its evaporator blows out warm air to do this, the process is very energy consuming

After the cooling process, a residual cold output remains, which is then reheated to prepare it for the next cooling cycle. This is done with a heat exchanger and another buffer vessel that is kept on 25 °C. Currently, this second buffer vessel is reheated with a 300 kW heater powered by grid electricity. The process is schematically shown in the figure below in Figure 1.5.
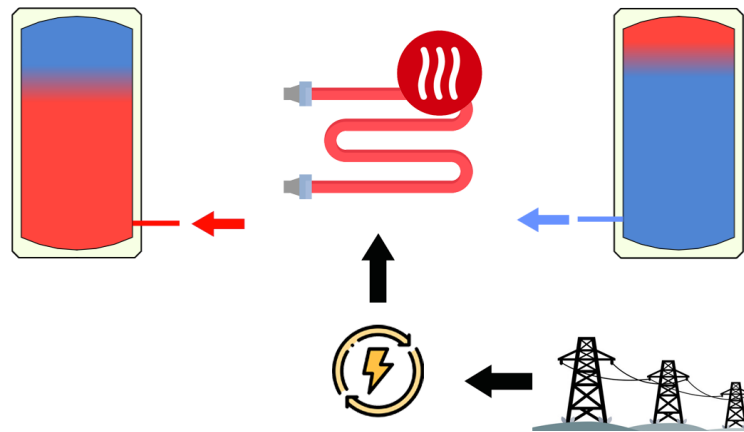
Figure 1.5: The heating process, the main counterpart of the cooling process. A heating element produces heat that is used to warm up the tank in the cooling circuit, powered by energy from the grid.

This heat is needed in order to check their cooling performances. As one can imagine, the energy-consuming process of cooling, is now assisted with another energy-consuming process, namely heating the residual cold liquid. This indicates a significant area for potential efficiency improvements. The combination of high electricity and heat demand brings up the possibility of implementing the formerly named, solar heat and electricity generation with PVT panels. A setup as such is schematically drawn in Figure 1.6.
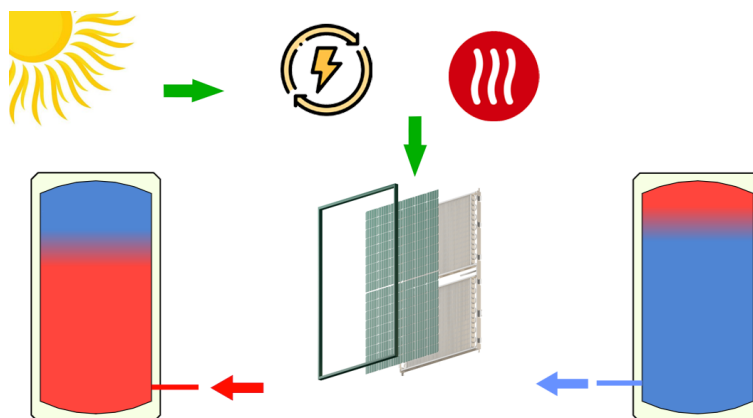
Figure 1.6: The heating process, now by the use of PVT panels instead of a heating element attached to the grid. The panels produce both heat and electricity, making it a win-win in this process.

The combination of both energy supplies can ensure that part of both heat and the electrical energy demand of Coolworld, could be covered more sustainably. Besides this, the current energy grid in the Netherlands tends to become subject to net congestion, making it a serious consideration to create net independent electricity generation for their demand. An integrated sustainable energy solution will be made including transforming the rest cold. Waalwijk will act as a case study for other cooling systems facility energy solutions and the outcome of this can also be interesting for other testing facilities for cooling systems outside Waalwijk, making it a versatile solution in exploring possibilities for lowering CO_2 emissions in the cooling process industry. Another interesting side effect that comes with this, is the possibility of actively cooling the PV panels to see what this does to the energy yield of these. A literature study on this is done in the next section.

1.3. Literature Review

A literature study is conducted on rest cold reuse and how the application of this on PVT systems setups could impose new insights into the thermal and electrical performances of both PV panels and solar collectors.

1.3.1. From rest cold to a new purpose

Cold production in the testing facility can be split up into two different forms, depending on two types of cooling machines (chillers), Mono-Ethylene Glycol (MEG), for glycol with a minimum temperature of -50 °C ([5]), used in very low-temperature application such as CO_2 refrigeration cycles, and Mono-Propylene Glycol (MPG) for temperatures until -32°C. MEG application is not discussed further in this study since these machines are very rarely used, and therefore tested. It could be interesting to use their rest cold in further research. The warming process of this rest cold is mainly done with environmental heat, captured when the ambient temperature is above 10 °C. At the output of the air-cooled machines, cold is produced and heat is exhausted on top of the machines. Research is done on finding a completely new purpose for the residual cold. It is not very common to have a cold as a residuum, normally heat is more usual. A specific process in which a lot of rest cold occurs is the process of liquifying Liquified Natural Gas (LNG). "The large amount of cold energy stored in LNG presents an opportunity for sustainable technologies to recover and utilize this energy", as can be read in [6]. During the regasification of LNG, the transition back to its gaseous state liberates the stored cold energy. This phase change occurs when the LNG is warmed, leading to its vaporisation and the discharge of energy. There is unfortunately not a separate process to which the rest cold could be used known, and therefore investigating this is another research topic of this paper. Related to this research a few examples of papers showed up when searching for terms in "rest", "cold" and "heat" provided examples of research in the field of the cooling process of data centres, which produce a lot of heat, but that would mean that rest cold could be applicated to it, it did not show any solutions possible other than that.

Transform residual cold to heat - Heat Exchangers

The energy intensive process from section 1.2 induces finding a solution to reheat the cold glycol to warm glycol in a sustainable way, by replacing the current heating elements. Currently, little measurements are taken to reduce the energy needs as described above, at least, the intentions are there but these are not fully checked. Further details on this can be read in subsection 2.6.1. More heat capture possibilities need to be investigated.

Solar powered systems - ISO/ EN norms

During this research, while knowing that the potential implementation of PVT modules should be considered, the ISO: "ISO 9806-2017 Solar energy — Solar thermal collectors — Test methods",[7] has been consulted. The creation of this ISO is done by a guide, the: "GUIDE TO STANDARD ISO 9806:2017 - A Resource for Manufacturers, Testing Laboratories, Certification Bodies and Regulatory Agencies"[8]. Within this guide, a certification is named, the Solar Keymark Certification, which can only be issued in European standards which are named in "EN 12975: Quality Assurance in solar thermal heating and cooling technology – keeping track with recent and upcoming developments", [9] which on its own has a guide, "A guide to the standard EN 12975", [10]. All these papers/ certificates have been read carefully and many other different options for solar energy generation or collection are named as can be seen in Figure 1.7. It has been chosen not further to define every single one of them [8].
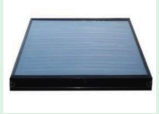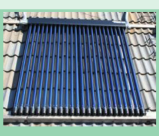
Collector type	Characteristics	Typical applications
WISC liquid heating collectors *(Picture source: RISE)*	- High performance at low temperatures and highly dependent on wind speed and thermal irradiance; - Can often withstand freezing; - Sometimes designed for working under dew-point of ambient air (heat pumps).	- Swimming pools - Evaporators for heat pumps
Flat plate collector *(Picture source: QAiST - IEE/08/593/SI2.529236)*	Good performance at higher temperatures (typical temperatures for domestic hot water)	- Domestic hot water systems - Combi- systems - District heating
Vacuum tube collector *(Picture source: RISE)*	Good performance at higher temperatures (typical temperatures for domestic hot water and above)	- Domestic hot water and Combi-systems - District heating - Solar assisted cooling - Process heat
Stationary concentrating collector *(Picture source: RISE)*	Good performance at high temperatures	- Domestic hot water and Combi-systems - District heating - Solar assisted cooling - Process heat

Figure 1.7: Table from GUIDE TO STANDARD ISO9806-2017 with different collector types, source: [8]

PV, solar thermal and PVT: Existing research
Not mentioned in the above scheme, but named in the guide is the combined PV and thermal collector. The thermal collector as we know it behind the panels, is a heat exchanger, and its main function is collecting heat from ambient air. This means that it is not intended as a stand-alone solar collector, apart from the solutions mentioned above. But, it figures as a hybrid. The PV panel generates electrical power and absorbs heat. The thermal collector has a medium to transfer this heat with, in the form of liquid pumped through it. The liquid in cold form, as residua from a cold liquid process, has not been applied before in existing research. Nevertheless interesting information was captured from former study *"Model Validation of an Empirical Photovoltaic Thermal (PV/T) Collector"*, by Ben Cheikh el hocine et al. [11]. Zondag et al. [12], [13] carried out energy performance evaluations for a PVT/w system through the creation of a range of steady-state and dynamic simulation models. Many studies and calculations are based on this paper. Kalogirou et al. [14] provided simulation outcomes using TRNSYS for hybrid photovoltaic/thermal (PVT) solar systems tailored for domestic hot water usage, comparing their functionality in both passive (thermosyphon) and active (pump-circulated) operating modes. This study provided insights into how a model could be built for a flat plate numerical model, Only, in this case, this syphon is replaced by a rest cold vessel.

As described in *"Detailed analysis of the energy yield of systems with covered sheet-and-tube PVT collectors"* [15] the absorption factor of a thermal collector is based on its electrical efficiency, defined in the equation below and it is by definition lower than the thermal efficiency of a flat plate collector, due to the higher emissivity factor of a PV laminate compared to that of a flat plate panel.

$$A_{\text{eff}} = A - \eta_e \tag{1.2}$$

In which A_{eff} is the absorption factor and η_e the electrical efficiency of the PV panel. For different solar cell types, total absorption factors were found to range from 85% to 93%, while effective absorption factors varied between 70% and 82%, see also Santbergen, Rindt, and Zolingen [16]. So a glazed PVT collector typically has a lower electrical efficiency than a standalone PV module due to the extra cover. The heat collected by the fluid also affects the cell temperature, which, when lower, can enhance the electrical yield due to the cells' negative temperature coefficient. However, the impact of system sizing, like the collector area to storage size ratio—and thermal load on cell temperature varies, making it unclear whether electrical gain or loss will occur. Previous studies have not systematically explored how system sizing and fluid temperature influence electrical efficiency this will shortly be elaborated. Part of this study will investigate the improvement of PVT collectors by cold temperature influences.

Interesting research has been that of K. Touafek [17] who made a new approach for the current existing PVT collector. Instead of the ambient air mainly interfering with the PV cells' generated heat, it insinuates to use of a cooling liquid only to capture the heat from it, by insulating the rest of the thermal collector on the backside. This type of panel is not forehand in the Netherlands but would be very interesting within this study. It is therefore recommended to further investigate this. In an innovative experiment by Col [18], a water circulation system was implemented at the rear surface of a photovoltaic panel for cooling purposes. An aluminium radiator served as the heat exchanger within this setup, effectively removing heat from the photovoltaic surface. demonstrated 32% reduction in the photovoltaic surface temperature from and an increase in electrical efficiency by 57%, which is considerably high.

PVT: New research approach
Normally when energy efficiency over module temperature is determined, room temperature in a testing facility is raised so that with the same inlet temperature for the fluid, different efficiencies can be measured.[7] The outcome used for temperatures rising above STC (25 °C), but it has not been validated yet, what this does with temperatures below STC, as can be seen in Figure 1.8 below. No study has yet shown what could happen to the efficiency when the temperature of the inlet of the PVT is further below zero, actively cooled. Therefore this research will include further details on this. Research that is found on ethylene glycol tests showed a decrease in efficiency. This study was to show efficiency commpared to pure water, [19]. However, no conclusion was made on using glycol substances with temperatures below zero or STC. This study will include this, but then with a Propylene-Glycol mixture.

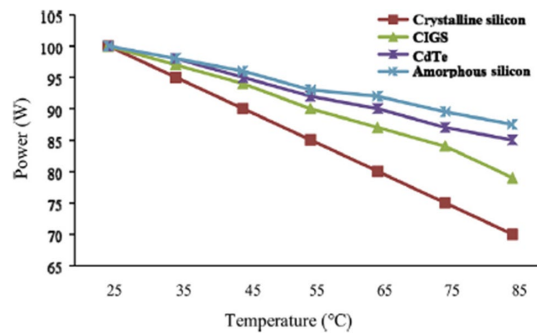**Transform "rest" cold to heat - Other solutions**

Figure 1.8: Different solar panel types, and their power over temperature differences (source: [20])

Research on other sources for stand-alone energy generation methods, such as wind or geothermal energy, is done, but is out of the scope of this study. Future studies could define what other possibilities in the transformation from rest cold to heat could be used. Geothermal could be an interesting one in this topic, but is due to difficult implementation not an option for Coolworld Waalwijk.

1.3.2. Knowledge gaps
In literature, it was found-or rather-not found, what a new purpose for rest or residual cold could be. The only process in which a direct purpose can be found is that of liquifying LNG, and then the thermal process along with it. Which on its own cannot be linked with testing cooling systems. Generally, there seems to be a lack of applications for residual cold. Besides this, there is no existing current literature on what the application of "rest" cold to the PVT panels' efficiency could do. Most former research on PVT and its efficiency has been studied in residential showcases, as well as with the use of water, mainly with temperatures around room temperature, and not with temperatures below STC or 0 °C.
Most literature describes solutions for waste heat reuse or the cooling of heat during other energy-intensive processes in for example the chemical industry. The later-named field is an example that is currently a growing industry, and partly the reason for Coolworld's recent growth. This led to more energy consumption within Coolworld Waalijk, and a request to investigate this was created in the form of this study. At the testing facility of Coolworld, a high heat and electricity demand exists and cold is a surplus. However, the specific distribution of energy and potential areas for reducing losses are not clearly defined.

1.4. Problem Statement
For cooling systems, testing facilities play a pivotal role performance evaluation and research. However, the increasing energy demands of these facilities, pose significant environmental and economic challenges. The IEA states the following: "As incomes rise and populations grow, especially in the world's hotter regions, the use of air conditioners is becoming increasingly common. In fact, the use of air conditioners and electric fans already accounts for about a fifth of the total electricity in buildings around the world – or 10 % of all global electricity consumption." Compared to the residential cooling demand, the industrial growth tends to be even bigger. It has been shown that between 2018 and 2023 the market growth was significant with a Compound Annual Growth Rate (CAGR) of 5.5 %. This trend is predicted to grow to 6.1 % from 2023 to 2033. [22] This growth has led to an increase in energy demand at cooling machine testing facilities, a trend clearly observed at Coolworld's test site, which consumes 50,000 kWh per month. Due to this consumption, Coolworld has been policed by the Dutch government to do research on energy-saving measurements. This is written in a law, introduced by the *Rijksdienst Voor Ondernemend Nederland (RVO)*. This law describes that companies with an energy consumption of 50.000 [kWh] per year or more, should take energy-saving measurements [23]. Figure 1.9 below shows their entire energy consumption for the past year, 2023. This master thesis aims to address the challenges and opportunities previously mentioned, by analysing the opportunities in reducing energy and reusing waste energy in testing facilities in the cooling systems industry. Besides this, the above-mentioned literature study has shown that there are many ambiguities in actively cooling PVT systems, to see what this does to their thermal and electrical performances.
Which, together with the former paragraph, led to the following problem statements:
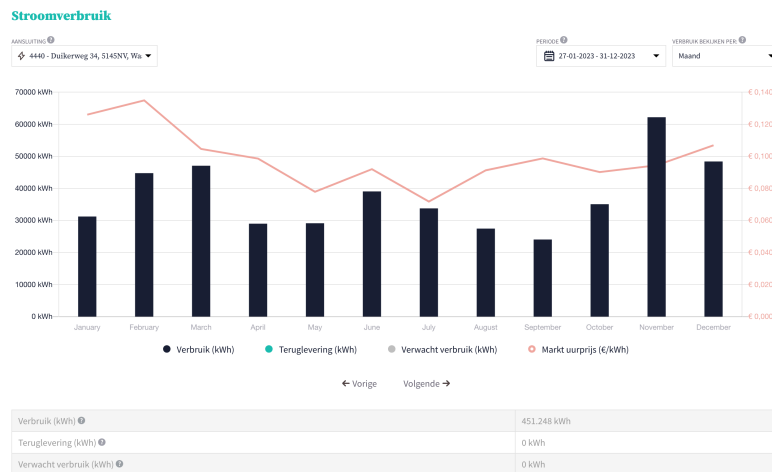
Figure 1.9: Picture of Coolworld's annual energy use, source: [24]

1. **At Coolworld Waalwijk's energy-intensive testing facility, the specifics of energy consumption, where losses occur, and possible solutions to these are not yet known.**
2. **It is unknown what actively cooling (below STC temperature) PVT panels, will do to their electrical and thermal performances.**

1.5. Research Objectives

To address the two problems outlined above, two research objectives have been established. This section will detail these objectives, which have each led to separate chapters on methodology and results. The research objectives are:

1. **Gain insight into the energy-intensive processes and losses at Coolworlds testing facility and identify sustainable solutions, to develop an Energy Management Strategy (EMS) based on these findings.**
2. **Analysis of PV/ Thermal system, with Coolworld as a case study**

1.5.1. Gain insight into the energy-intensive processes and losses at Coolworlds Testing site and identify sustainable solutions, to develop an Energy Management Strategy based on these findings.

One of the primary objectives of this master's thesis is investigate the current energy processes within the testing facility of Coolworld Waalwijk and search for current energy losses that could be reduced. With this outcome, a description will be made on how research for heat recovery, can be done in other testing facilities. An energy management strategy is built and the research outcome can be found in chapter 2 and chapter 3.

With this strategy, one will be able to create an overview of components, determine energy consumption and losses, visualise this and test energy saving solutions for heat recovery for a cooling systems testing facility, to which Coolworld in Waalwijk figures as case study. This strategy will serve as a research method, to be universally implementable in any other cooling systems testing facility and other research topics on this are the following.

Find out what components the testing facility consists of
A study on the existing components in the facility is needed to be able to determine energy consumption and flows. Therefore, first, an overview of these components needs to be created.

Assessing the energy requirements of the testing facility

An analysis is conducted to understand the energy consumption (patterns) and demands of the testing facility. This assessment will provide insights into the specific energy needs and if needed an approximation per asset will be made to complete the total energy balance. A daily and weekly consumption pattern will be established. With these numbers, it is disclosed which current processes are highly energy-consuming and with this, it is decided which components need further investigation, in order to reduce energy consumption.

Create an overview of the currently (temporary) energy-saving solutions
In order to build energy management overview, the current, already installed, energy solutions are also part of above's mentioned study, and where possible improved.

Developing an energy management strategy manual
A comprehensive strategy will be formulated to create insight into the energy flows within a testing facility. This strategy will include the effective use of a sustainable energy system.

Design of energy saving solutions to current energy losses
Universally applicable energy solutions will be designed based on above's mentioned research topic together with Waalwijk's specific solutions.

1.5.2. Analysis of PV/ Thermal system, with Coolworld as a case study
The second objective is to create a model that includes a sustainable energy generation solution to reduce dependence on energy from the grid and find a sustainable alternative to it. Besides, the thermal and electrical performances of a PVT system are investigated when active cooling with fluid temperatures below STC are used in the system. Both numerically in a model and experimentally. The method to this can be found in chapter 4 and the results to this in chapter 5. The goal is to build an independent energy solution for a cooling systems testing facility. The following sub-researches support this.

Conduct research in reusing rest cold
Since the testing facility has a lot of rest cold, which is produced without any further purpose, a literature study is done.

Conduct research in the field of PV, solar collector and PVT energy solutions
To minimise energy consumption from the grid both electrical and thermal, research is done on what systems i s a possible solution to implement at Coolworld. It is chosen to do research in the PVT field, but a comparison to stand-alone photovoltaic (PV) and thermal solar energy will be discussed.

Create a model of PVT modules to be implemented at Coolworld Waalwijk
Based on boundary conditions such as weather and climate during the year as well as cold inlet to the PVT system, an empiric model will be made to predict the possible efficiency increments due to the cold inlet to the system, as well as a total energy generation with the system.

Model validation
With the use of several test method descriptions values found are validated. Besides, a test setup with four PVT panels is built to do thermal and electrical performance tests with, by actively cooling them with rest cold.

1.6. Thesis Structure
This paper is organised into eight chapters. Chapter 2 and chapter 3 explain *"Investigating the energy structure of Coolworld Waalwijk's testing facility"*, and chapter 4 and chapter 5 elaborate on the *"Analysis of a PV/ Thermal system, with Coolworld as a case study"*. Chapter 6 discusses the implications of both methods' and results' chapters. Chapter 7 concludes the paper by summarising the main findings, and at last provides chapter 8 recommendations for future research and implementation of the outcome.

2

Investigating the energy structure of Coolworld Waalwijk's testing facility

Research is done on the current setup in the facility (section 2.1) of which the needed energy definitions can be found in (section 2.2). Then overviews of the facility are defined in (section 2.3). With this more constructive research could be done on the existing fluid circuits in the facility (section 2.4), hereafter more information on the fleet of cooling machines (section 2.5), their working principle, and the accompanied components that exist in the test setup ((section 2.6) according with solutions to these are created. At last is the testing procedure reviewed (section 2.7) and are solutions calculated, designed, implemented and tested, resulting in overviews on the energy consumption (section 2.8) and a booklet on how this is done is built.

2.1. Background

Small research on energy-saving solutions is done by employees at Coolworld, but many unknowns remain. PV panels are considered for installation, but a new purpose for the rest cold has not been studied. In the roof section above the facility, heat exchangers (Figure 2.1) are installed, formerly used together with a tarp on one side, but these not tested properly to see what heat exhausted from the machines can be recovered. Furthermore, insulation of the heating vessel is considered, but not pushed through.

(a) Cooling machine positioned under heat exchangers

(b) Frozen BV06 Cooling circuit vessel

Figure 2.1: Picture of the testing facility, taken from the eastern side, left all electrical connections, on the right all water-glycol

On the left side of Figure 2.1a all the electrical connections can be found. In the back on the left, one finds a door to the big vessel with warm water-glycol. On the right side, one can find all the water glycol

connections for the machines. In the back, the cold circuit testing vessel can be found, which is shown in Figure 2.1b. Currently, the vessel is iced on the outside during a test. The target is to find solutions to heating this vessel as sustainable as possible now that the urge for a greener image rises, the price per solar panel has decreased, the price of electricity per [kWh] has risen and the energy grid in the Netherlands tends to become subject to net congestion. Investing in sustainable solution could now be very interesting in line with the current growth that exists at Coolworld.

2.2. Energy definitions

For all the measured and calculated data shown in this paper, some major approaches/ rules are considered. Energy will be defined in kWh. A short overview with the incorporated calculations is shown below, more in-depth information on these can be found in Appendix A. These definitions are mainly based on studies on Mills and Coimbra [25] and Smets, Jäger, et al. [3] and the glycol-water characteristics found in VDI-Verlag GmbH [26] Only sensible heat $\dot{Q}$, in [W], is used in the calculations, which can be written as:

$$\dot{Q} = \dot{m} \cdot C_p \cdot (T_2 - T_1) \tag{2.1}$$

Where m the body's massflow in [kg/s], C_p the heat capacity in [J/(K*kg)] an T_1 and T_2 are temperature differences in °C. Heat transfer within a material is calculated with the **conductive** heat transfer $\frac{dQ_{cond}}{dt}$ [W] (is $\dot{Q}_{cond}$), written as:

$$\frac{dQ_{\text{cond}}}{dt} = -k \cdot A \cdot \frac{dT}{dx}, \tag{2.2}$$

Wherein k is the thermal conductivity in (W/(m K)), A is the surface area over which heat is passing, measured in square meters [m^2], and $\frac{dT}{dx}$ is the temperature gradient in in [K/m]. **Convective** heat transfer $\frac{dQ_{\text{conv}}}{dt}$ [W] (is $\dot{Q}_{conv}$) is:

$$\frac{dQ_{\text{conv}}}{dt} = -h \cdot A \cdot (T_1 - T_2) \tag{2.3}$$

Where h s the convective heat transfer coefficient [W/(m^{2}K)], A is the contact surface area, and $\Delta T = T_1 - T_2$ is the temperature differential in [°C]. The coefficient h [W/(m²·K)] depends on the fluid's velocity, surface characteristics, and flow type (laminar or turbulent), calculated from the Reynolds number Re (dimensionless) [-]

$$Re = \frac{\rho \cdot u \cdot L}{\mu} \tag{2.4}$$

With: Re: Reynolds number, ρ: fluid density [kg/m³], u: fluid velocity [m/s], L: characteristic length [m], μ: dynamic viscosity [Pa·s]. With which the Nusselt number is calculated:

$$Nu = C \cdot Re^m \cdot Pr^n \tag{2.5}$$

C, m, n: material-specific constants, Pr: Prandtl number. The heat transfer h is then:

$$h = \frac{Nu \cdot k}{L} \tag{2.6}$$

At last, the **Radiative** heat transfer Q_{rad} [W] is:

$$\dot{Q_{\text{rad}}} = \epsilon \cdot \sigma \cdot A \cdot (T_{\text{surface}}^4 - T_{\text{surroundings}}^4) \tag{2.7}$$

With ϵ: emissivity [-], σ: Stefan-Boltzmann constant ($5.670374419 \times 10^{-8}$ [W/(m^{2}K^4)]), A: surface area [m^2].

2.3. Testing site overview

The total structure of the testing facility and all its components is not specified on paper. It has therefore been decided to make an overview of this facility including all components. Many changes have been made to the site since its completion in 2006, but not everything is clearly stated in overviews. First a logical overview of all components needs to be created. So a schematic overview: **component-wise**. The second is the **top-view** overview which gives more explanation to positioning of components. In chapter 3 more details of this can be found in the booklet that is built on the strategy. All upcoming parts are included in this. To showcase the facility from top, a picture is made, as can be seen in Figure 2.2.
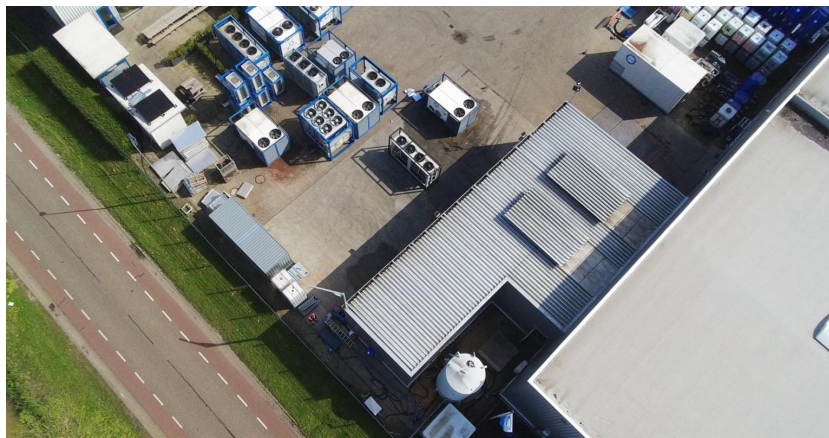

Figure 2.2: Topview from the testing facility. On the top left a, later explained, PVT test setup, on the right lower corner, a big buffer silo and in the middle-right the testing facility itself with roof placed heat exchangers. The concrete floor in the middle with two machines on them is the wash street, besides that are machines not in use.

2.4. Circuits

The testing facility consists of multiple circuits. Each circuit is an open- or closed-loop cycle with at least one pump, one buffer vessel, and a heat exchanger, cooling machine or other object. Every circuit has its own working fluid and temperature and for each, an overview with components will be made .

2.5. Cooling machines

To understand the testing site 's purpose a refrigeration cycle is shortly explained first, followed by the actual machines types at Coolworld, to later determine the accompanied components, so that an energy study can be performed.

2.5.1. Refrigeration cycle

The refrigeration cycle is a process used in various industries and applications to remove heat from a particular space or substance, thereby lowering its temperature. This cycle involves the circulation of a refrigerant, such as Hydrofluorocarbons HFC's (R-134a), Hydrocarbons or Natural Fluids (CO_2) through a closed loop system consisting of the four main components: compressor, condenser, expansion valve, and evaporator, see Figure 2.3 for a numbered schematically drawing, corresponding with the enumeration down below. A more detailed explanation is written in Appendix B.

1: **Compressor**: Increases the pressure and temperature of the refrigerant vapour, and acts as a pump for the loop as well.

2: **Condenser**: Condenses the high-pressure, high-temperature vapour into a liquid. Also known as the outdoor unit, it can be compared to a heat exchanger.

3: **Expansion Valve or Restriction**: Regulates the flow of refrigerant into the evaporator, allowing for a controlled drop in pressure and temperature, also known as the metering device, since it measures the amount of refrigerant entering the evaporator (4).

4: **Evaporator**: Absorbs heat from the substance or space being cooled, causing the refrigerant to evaporate, also known as the indoor unit and comparable to a heat exchanger.
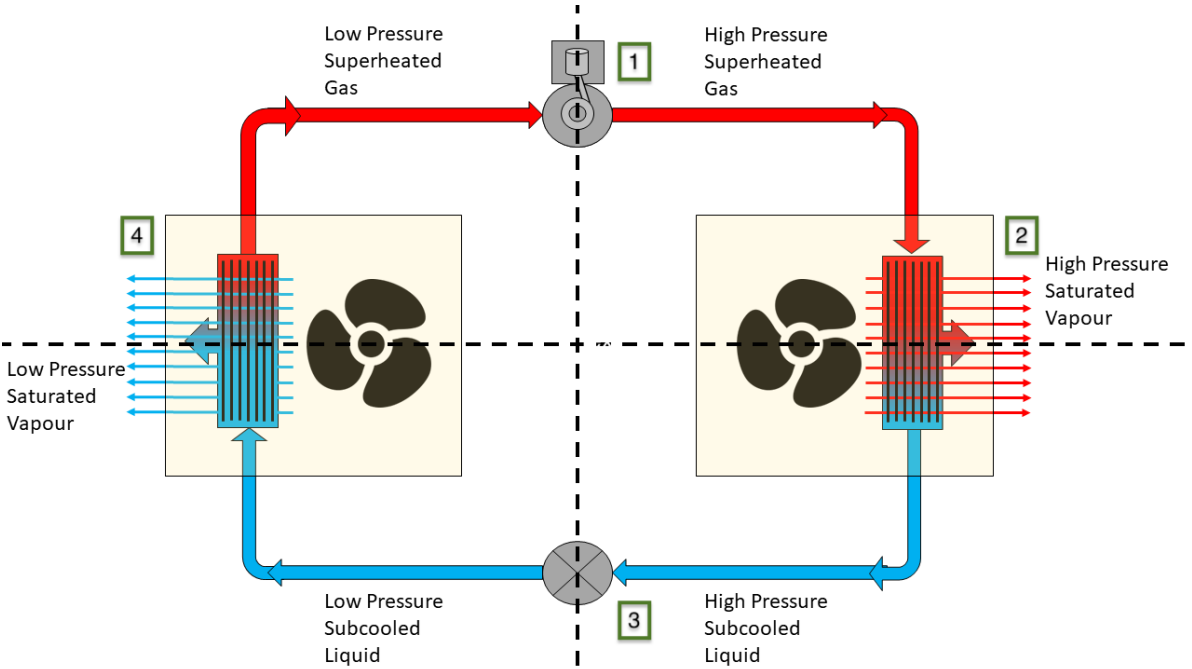
Figure 2.3: Schematic diagram of the refrigeration cycle (Torr [27])

2.5.2. Cooling machine types

The current fleet of cooling machines within the Coolworld assortment can be divided into 3 different types. In the table below (2.1) these are named and categorised, and named if they are taken into consideration in this study or not. Next, an explanation per category is given.

Table 2.1: Cooling machines fleet Coolworld Rentals Waalwijk

Category	Machine types	Included in study
Refrigeration Unit	Fridges, Freezers	No
Climate Controllers	Air-conditioners (HVAC), Airhandlers	No
Process Installations	Chillers	Yes

At Coolworld Waalwijk mainly in HFC's are used in standalone cooling machines, such as refrigeration units and climate controllers. This is due to the regulations that are made in presuming the usage of CFC's and HCFC's. These cooling liquids are inside a closed loop system and not used in the testing facility, which only runs on a glycol and water mixture.

Refrigeration Unit
These are both complete units, as well as dis-mountable units that come with a specific cooling or freezing unit delivered inside the housing. The Figure 2.4a below shows what they look like.
These machines produce immediate cold air inside the housing of the unit, which therefore has no transfer of refrigerants with the test facility. Therefore, these systems are not taken into account during this study, as they are not tested in the facility itself.

Climate Controllers
This includes fully functioning air conditioning systems that can interchange with existing setups, as well as mobile AC units and ventilation control. These also, do not interchange a liquid within the facility and are therefore not taken into consideration during this study. Besides, these systems are a small part of the fleet since they mainly cover small requests, are tested rarely and testing is not energy-intensive. An example of a Climate Controller system can be found in Figure 2.4b.

(a) A Refrigeration Units

(b) A Climate Controller

Process Installations

Systems such as, run a separate glycol-water cycle that is made part of the cooling system. The machine itself, called chiller, has a refrigeration fluid inside, which chills a separate working fluid that needs to be attached separately. The liquid is a mixture of MPG, or MEG in several colder temperature cases, depending on the demands. This cooling fluid is then used as working fluid to control air or liquid treatment systems which then can cool down complete industrial buildings such as warehouses or liquid-based setups such as ice rinks. Such a combination of systems can be seen in Figure 2.5.
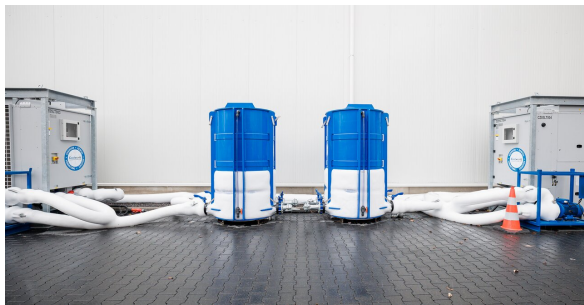
(a) Buffer vessels and chillers outside of warehouse

(b) Air handlers inside of warehouse

Figure 2.5: Pictures of Coolworld's Process Installation

These systems are tested in the testing facility and are therefore the main cause of this study. These produce a cold energy flow consisting of glycol-water substances which flow in the facility in multiple different circuits as stated in section 3.2. Besides, the cooling capacity of chillers, extends to much larger applications and energy consumption, making it more interesting to have sustainability measures to it. A schematic drawing of this installation can be found below in Figure 2.6.
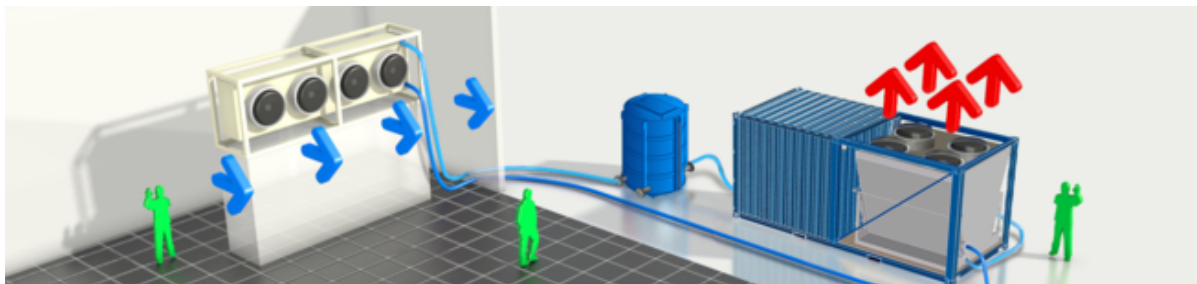
Figure 2.6: Schematic drawing of water-glycol based cooling machine circuit, source: Coolworld [28]

2.6. Components

Besides the circuits that exist in the testing facility, heat loss can occur in a few specific elements in the facility itself as well. All components in the facility are taken into consideration and summed up in the following sum-up in Table 2.2, describing whether or not they are included in this research.

Table 2.2: Overview of the component types in the testing facility setup

| Category	Description	Included in study
Heat Exchangers	All exchangers are here taken into consideration, so both water to water as well as water to air	Yes
Silos	Vessels, tanks, and other liquid storage options	Yes
Hoses and pipings	Based on a business point of view, in which hoses are a big part of Coolworld's market, these are expected to be deliberately chosen and therefor not further investigated	No
Pumps	Each circuit includes a pump which can build a consistent flow during operation	No
Couplings	Couplings are in two types, permanent and easy detachable/attachable	No
Valves/ Taps/ Liquids/ Other	All places where flow can be adjusted with a tap	No

2.6.1. Heat-exchangers

An important part of the cooling and heating circuits are heat exchangers. These are responsible for the exchange of heat between the two main circuits. The cooling circuit consists of a cooling machine and a big storage vessel (BV06).

WW1600 heat exchanger

During tests, the cooling machine cools the BV06 content. To maintain testing, this liquid must be warmed up, which is managed by the heating circuit with vessel BV20. Both circuits run simultaneously, with the same flow, enabled by wirelessly connected pumps. Figure 1.3 schematically shows the heat exchanger between the two vessels. The pump in the warm liquid circuit is not coupled.

Roof section heat exchanger

Another direction for this heating circuit is by using a separate circuit that flows through heat exchangers that are placed on the roof of the testing facility. These heat exchangers have been installed in 2016, and a schematic drawing of them can be found in Figure 2.7a. These collect hot air that is exhausted from the machines during their testing procedure. Figure 2.7b shows the heat exchangers in the roof with the pipelines directed towards them.
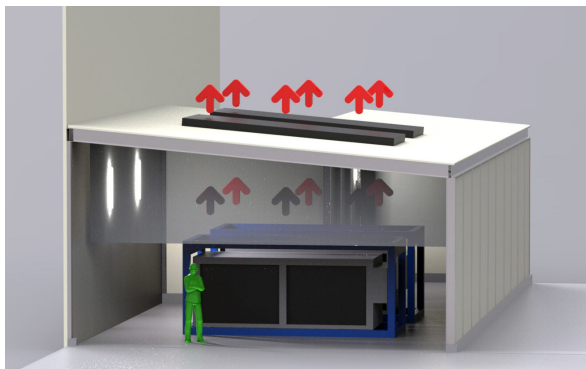
(a) A schematic drawing of the heat exchangers in 2016

(b) Picture of the heat exchangers, with BV06 on the right

Figure 2.7: Both a schematic drawing and picture of the heat exchangers in the roof

As one can see in this picture, on the back right end of this picture the cold BV06 vessel is currently partly iced. The cooling machine is producing cold, and the heaters in the roof should be collecting hot air. However, excessive testing on how to use them has not been performed. As a result, it is unknown how to get the highest returns from them and tests on them will be done.

Washing street, floor heating
This is the floor heating that is positioned right next to the testing facility at the washing street. As can be seen on in Figure 2.8a. There is constant water on the surface, which can freeze on cold winter days. This circuit consists of a small pump and liquid from the big BV20 vessel. Heat loss from this component when freezing would not happen, is calculated with calculations based on section 2.2, given as follows. The heat convection coefficient for tubes $h_{c,tube}$ is based on the Reynolds number (Re):

$$Re = \frac{V \cdot D}{\nu} \tag{2.8}$$

where V_{flow} is the flow speed [m/s], D_{in} is the inner diameter [m], and $\nu_{glycol\text{-}water}$ is the kinematic viscosity [m^2/s]. Next comes friction factor (f) for $10^4 < Re_D < 5 \times 10^6$:

$$f = (0.790 \cdot \ln(Re) - 1.64)^{-2} \tag{2.9}$$

Following with the Nusselt number (Nu):

$$Nu = \frac{\left(\frac{f}{8}\right)(Re - 1000)Pr}{1 + 12.7\sqrt{\frac{f}{8}}\left(Pr^{2/3} - 1\right)} \tag{2.10}$$

Finally, the heat transfer coefficient ($h_{c,tube}$) is:

$$h = \frac{Nu \cdot k}{D} \tag{2.11}$$

Including the thermal conductivity k of the fluid inside (glycol-water). Next, with the help of table 3.2 from [25] different Shape Factors (S), as described in Table 2.3 calculate the heat resistances R, in Table 2.4, for each layer between the surface of the street and fluid inside the tubes. This gives the $R_{tot} = R_{concrete} + R_{tube} + R_{conv}$ with: r: outer radius [m], L: length [m], h: distance to surface [m], $k_{concrete}$: thermal conductivity of concrete [W/(m·K)], k_{tube}: thermal conductivity of tube material [W/(m·K)], h_c: convective heat transfer coefficient [W/(m²·K)], A: surface area [m²]. The surface temperature T_s can then be calculated. A more detailed calculation is given in section A.1

Table 2.3: Shape Factors for Different Configurations

Description	Shape Factor (S)
Concrete	$S_{concrete} = \frac{2\pi L}{\ln\left(\frac{2h}{r}\right)}$
Tube	$S_{tube} = \frac{2\pi L}{\ln\left(\frac{r_{out}}{r_{in}}\right)}$

Table 2.4: Generalized Thermal Resistance Equations

Description	Equation
Conduction	$R = \frac{1}{Sk}$
Convection	$R_{conv} = \frac{1}{h_c A}$

2.6.2. Silo's

The working fluid and temperature for each silo is different. One vessel is highlighted since this one has an external heating element. This heating element is the main internal temperature factor on the whole energy system of the facility, besides ambient temperature influences. The other two vessels in the facility BV06 and BV02 are not considered any further since these have no energy losses.

Warm water buffer vessel (BV20)
This tank can be found in Figure 2.8b. It is assumed that the silo losses a lot of its heat, which you can feel when walking around. Little research on insulating it has been done, but not yet been performed. The calculations are based on *Steady State conditions* with **convective**, **conductive** and **radiation** heatloss as described in section 2.2. First the total thermal resistance for the vessel is built with the following area calculations

(a) The testing facility's washing street

(b) The warm 20 m^3 vessel, outside, without insulation.

$$A_{cyl} = \pi \times 2.4\,\text{m} \times 2.6\,\text{m} \tag{2.12}$$

$$A_{hemi} = 2\pi \times (2.4\,\text{m})^2 \tag{2.13}$$

$$A_{total} = A_{cyl} + 2 \times A_{hemi} \tag{2.14}$$

The Re_D Reynolds number for a cylinder is:

$$Re_D = \frac{VD}{\nu} \tag{2.15}$$

where V is the air velocity, D is the characteristic length, and ν is the kinematic viscosity of the fluid, based on air conditions. Which gives (when $4 \times 10^5 < Re_D < 5 \times 10^6$), average Nusselt number, Nu_D, of:

$$Nu_D = \frac{0.3 + 0.62 \cdot Re_D^{1/2} \cdot Pr^{1/3}}{\left(1 + \left(\frac{0.4}{Pr}\right)^{2/3}\right)^{1/4} \cdot \left(1 + \left(\frac{Re_D}{282000}\right)^{5/8}\right)^{4/5}} \tag{2.16}$$

With this the $h_{\text{avg,air}}$ is calculated and a total thermal resistance is made including internal thermal conductivity in the glycol-water substance, when in still condition. Second a calculation is made for the vessel including internal flow, which occurs during working hour, which gives heat transfer coefficient h_{in}. R for conduction and convection is described in Table 2.4 and $R_{2,\text{total}} = R_{2,\text{cyl}} + 2 \times R_{2,\text{sphere}}$. Which gives the thermal resistance of the steel wall with S_{steel} as follows for the spherical part, cylindrical part and total respectively in:

$$R_{2,\text{cyl}} = \frac{2\pi \times 2.6\,\text{m} \times \ln\left(\frac{r_2}{1.2\,\text{m}}\right)}{45\,\text{W/mK}} \tag{2.17}$$

$$R_{2,\text{sphere}} = \frac{4\pi \times (1.2\,\text{m})}{1} \tag{2.18}$$

$$R_{2,\text{total}} = R_{2,\text{cyl}} + 2 \times R_{2,\text{sphere}} \tag{2.19}$$

Using the temperature difference between the internal and the ambient ($\Delta T = T_i - T_a$), Q can be calculated with

$$Q = \frac{\Delta T}{R_{total}} \tag{2.20}$$

A validation on this is made with an online tool from *Rockassist™*. Other silos are not considered since these are not having energy losses to the surroundings, but, instead, energy wins. Such as the BV06, which needs to be warmed up, and therefore would not need any insulation.

2.6.3. Hoses and pipings
Hoses and pipings are one major part of Coolworld's assets. It is both for rental service as well as in the facility a sufficient part of the infrastructure. As a rental service, the hoses must be rugged, and for the facility as well. Losses are assumed to be negligible.

2.6.4. Pumps
Pumps can be seen as the heart of the flow capacity for each circuit. The facility consists of multiple circuits, and thus multiple pumps, each in an individual circuit. They are energy-consuming, so therefore they are included in the total energy consumption overview. However, replacing them or searching for a new product is out of the scope of this study.

2.6.5. Couplings
A differentiation can be made between two types of couplings. There is a permanent coupling, the flange joint and the easy dismountable version is the Bauerconnection. More details are in

2.6.6. Valves/ taps/ liquids/ other
Components that will not be further considered in the energy consumption, but which do exist in the total overview will be covered in this section. A summary can be found in Table B.1.

2.7. Machine testing
It is of importance to know what the actual testing procedure consists of, and what will be tested. There will be no in-depth reconsideration of tests, but for sustainability purposes, this is something that Coolworld should look after. Results on this are in section 3.5.

2.7.1. Testing purposes
The testing purposes are written down in an overview each time a machine is coupled, and will be reviewed. This overview is shown in Appendix C. It insinuates that possibilities are there to look after them more sustainably. Especially measurements in a longer period of time are more easily to recover energy from.

2.7.2. Current testing procedure
The testing procedure as stated in the database of Coolworld is mainly built for training purposes, but not looked after with an sustainable eye. Herewith, things could be done differently. In broad terms, the procedure is as follows:

1. The cooling machine is positioned in the facility, not perfectly aligned with the roof exchangers, but place as many as possible.
2. Every electrical and water connection is connected, one inlet, one outlet, and sometimes an extra outlet. Depending on the number of circuits within the machine
3. Cooling machine is turned on to prepare oil temperature
4. Test checklist will be consulted
5. Pump is started and taps opened
6. Flow is determined and set
7. The heater in BV20 is turned. Depending on its temperature, $T_{ambient}$, and the size of the cooling machine, if $T_{ambient}$ is high enough, air handlers can be used instead
8. Machine turns on (mostly spontaneously after oil is heated)
9. The three-way-valve is turned on, to ensure 16 °C water flows through the heat exchangers in the roof, so that no condensation lead to 'rain' from pipings.
10. After heat is starting to develop in the test facility, the heat exchangers' fans are turned on in the roof section.

11. Testing will be done and a continuous flow of cooling is produced

12. After the test is done everything is shut off and disconnected

Currently, there is no knowledge of how most energy could be extracted from the roof heat exchangers, although the mechanic in the facility is aware of sustainable practices, it is unsure how this is done best. Therefore it is decided to measure the current energy recovery.

2.8. Energy management: Strategy

To define all the above-mentioned characteristics and components and ways to manage these it has been decided to create an Energy Management Strategy (EMS) that create the now-how for new sustainable solutions. This strategy will define all tools, software and literature needed to make measurements. The testing facility of Coolworld Waalwijk figures as a case study to this final result. All details can be found in section 3.6.

2.9. Energy management: Outcome

The outcome for energy measurements will be defined after consolidating the booklet and this paper.

2.9.1. Consumption

An overview of energy consumption will be provided and is based on the current energy consumption. Idle energy consumption is determined from the overall energy consumption profile, and by extracting that, a profile per day and per week can be created. Findings on the idle energy consumption are also named in section 3.7.

2.9.2. Sankey Diagram

The total energy flows within the testing facility can be drawn in the form of a Sankey diagram, of which the results are shown in section 3.7 It has been decided to make a Sankey diagram, that shows all in and outflows for energy that exist in the testing facility. This overview will be made per day and week, for storage of energy purposes. It is suggested too difficult to store energy for a longer period.

2.10. Payback time

Investments in energy saving solutions should be considered economic feasible before investing. Even though the investment on its own can be very relevant to reduce the current carbon footprint. One measurement tool is Equation 2.21:

$$\text{payback time} = \frac{\text{initial investment}}{\text{annual return}}. \tag{2.21}$$

With this calculation one can define payback time of the initial investment.

2.11. Conclusion

With the method described, all the components of the facility will be mapped. After this, each item is reconsidered for research or not if the consumption is either neglectable, or the component is irreplaceable. Besides, calculations are made for stand-alone components that have energy losses. Also, the energy intensive processes, such as the cooling machine running tests and its incorporated components are reviewed. The testing method will be investigated and calculations are made on potential and measured energy losses. A validation for each of them is made by measuring or by the use of a calculation tools. A strategy on heat recovery is built, to have other testing facilities replicate this study. In the end, a total energy consumption overview, with potential economical savings is projected, based on 0.22 €/kWh

3

The energy structure of Coolworld Waalwijk's testing facility

This chapter elaborates on the research objectives, described in subsection 1.5.1.To gain insight in the energy structure, an overview is made (section 3.1) and circuits are defined (section 3.2. Hereafter energy consumption and losses are mapped out and solutions are presented in the chapters 3.3, 3.4 and 3.5 respectively on components, machines and testing procedures. To which the outcome is a strategy (section 3.6) and the energy outcome (section 3.7). Electrical leakages have been considered, but none were actively found in the form of electrical charge that is leaking, based on the research done by a secondary party (*Elektricien Waalwijk*).

3.1. Testing site overview

3.1.1. Schematic components drawing
Two types of overviews are made. The first overview drawn schematically is shown in Appendix D. This one includes all the different components. This was firstly made to define all components and component types that exist in the facility. However, this is not easy to understand. Therefore it has been decided to make a more convenient version as top-view.

3.1.2. Top-view drawing
The second overview is drawn as a top-view of the facility. This is easier to follow and to find the connection between each different subpart in the facility. Based on a version that was made by a colleague from Coolworld, this version is made. It can be found in Appendix E.
The top view drawing consists of multiple components, hoses, etc. which have specific names. For better understanding all types of components will be named in a general overview, this can be found in Table 3.1. The naming is done by Coolworld and will be used in this paper as well. By the help of this overview, all other parts with the same indicated names can be derived. The important ones are included in the total energy consumption overview in Table 3.12

3.2. Circuits
The circuits all intermingle within the testing facility, making it difficult to draw all of them. They do not interfere and are all closed-loop. An overview of all circuits is named in Table 3.2
A drawing of each circuit is made, based on the earlier mentioned top-view of the testing facility. As can be found below in Figure 3.1. Each circuit will be discussed below.

3.2.1. CC01: Heating circuit (> 20°C)
This is a warm circuit that is meant to warm up the cold circuit named in the above paragraph. This circuit is partly built to capture heat from the heat exchangers on top of the facility. This temperature is held above 16°C otherwise the humid ambient air around the exchangers, and piping to and from them, will condense and cause 'rain' in the testing facility. This circuit consists of the big 20 m^3 buffer vessel
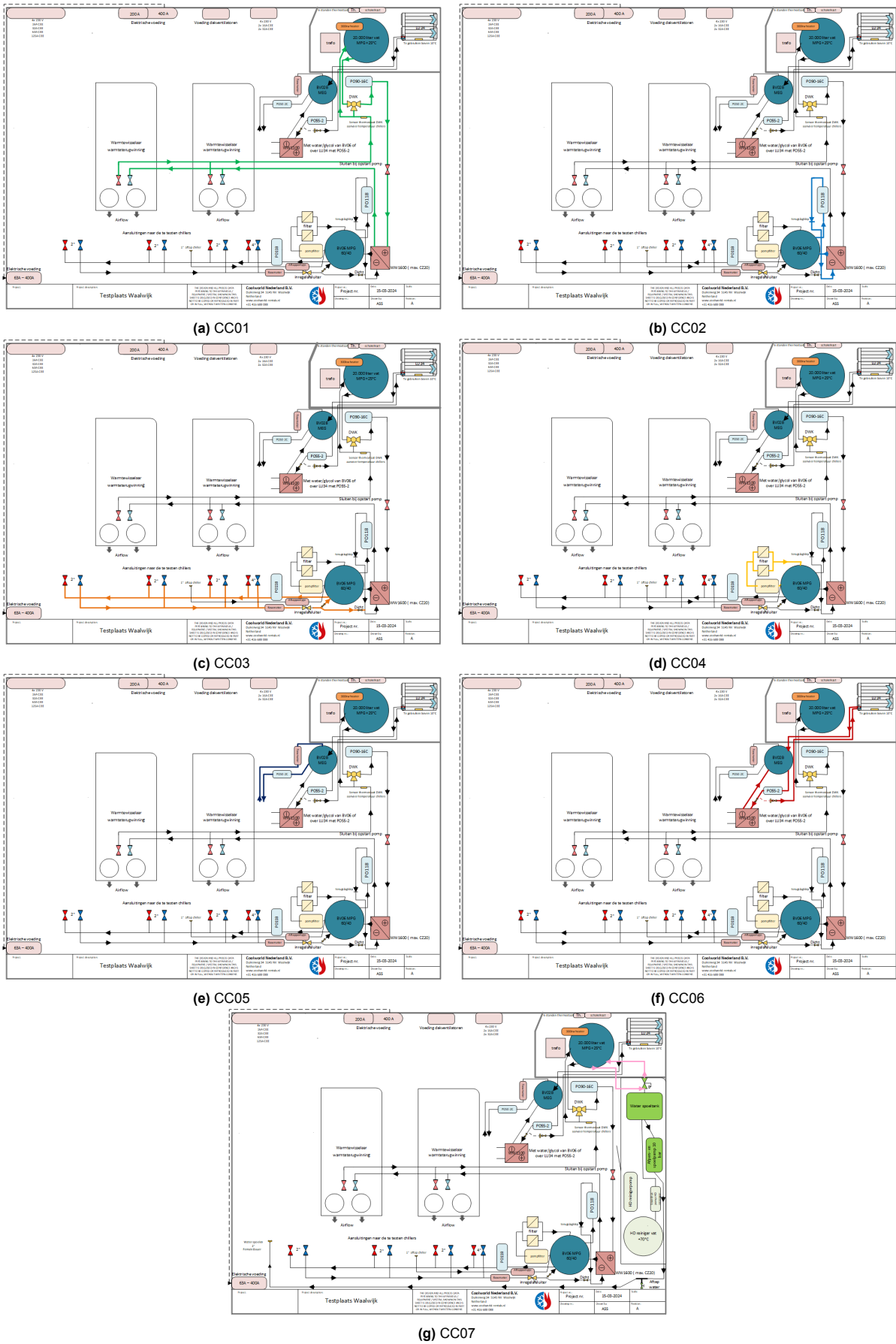
(a) CC01

(b) CC02

(c) CC03

(d) CC04

(e) CC05

(f) CC06

(g) CC07

Figure 3.1: All existing circuits in the testing facility

Table 3.1: Names of all the component types in the overview of the testing facility

Name (Coolworld)	Meaning	Number	Description
BV06	Buffervat (barrel/ silo)	Content in m^3	Silo for the distribution of water and MEG (-24 °C)in coldest circuit
CC01	Circuit	Sequence numbering	Combines all components in test setup
LU	Luchtbehandeling (Air handler)	power in kW	
PO	Pomp (Pump)	power in kW	
WW1600	Warmtewisselaar (Heat exchanger)	kW	Couples different cold and warm circuits to exchange heat/ cold

Table 3.2: Names of circuits in the setup of the testing facility, as current state

Name (CW)	Color	Description
CC01	Green	The heating water-glycol (MPG +25 °C) circuit, from the BV20 vessel
CC02	Blue	The heated cold water-glycol (MPG until -10 °C) circuit, from the BV06
CC03	Orange	The Cooling Machines water-glycol (MPG until -24 °C) circuit, from the BV06
CC04	Yellow	The cold water-glycol filter (MPG until -10 °C) circuit, from the BV06
CC05	Dark Blue	The colder water-glycol (MEG until -24 °C) circuit, from the BV02B
CC06	Dark Red	The heating water-glycol (MEG until -24 °C) circuit, from the LU34 or BV06
CC07	Pink	Floor Heating water-glycol (MPG +25 °C) circuit, from the BV20 vessel

which is kept at 25 °C, the rooftop heat exchangers, the three-way valve (DWK), pump PO90-16C and the floor heat exchanger WW1600.

3.2.2. CC02: Heated cold circuit MPG until -10 °C)

This circuit is being heated in the heat exchanger (WW1600) by the heating circuit CC01. This is to exchange cold liquid from the buffer vessel BV06 during cooling machine testings.

3.2.3. CC03: Cold refrigeration circuit (< -10°C)

This cycle is the cooling machines cycle. The temperature is mainly based on the power the cooling machine delivers, which is been tested at that moment. This can range between 20 to 800 kW. It is coupled to the cold buffer vessel B06.

3.2.4. CC04: Filtering circuit (< $\pm$-10°C)

This circuit is created as a bypass to filter the working fluid, water glycol, for the cooling machines.

3.2.5. CC05: Cold refrigeration circuit (< -24°C)

This external cooling circuit is used for tests with cooling machines that need to reach lower temperatures, of which an example the CO_2 Low Temperature Chiller (LTC) machines are. This testing circuit is used very little, and can be reheated with ambient air (if above 10°C), due to its low-temperature application.

3.2.6. CC06: Heated cold circuit MEG until -24 °C)

This is the heating circuit to warm up the cold BV02 barrel when this is in use during testing of LTC machines. A LU34, does the heating process.

3.2.7. CC07: Floor heating (< +25°C)

This is the floor heating circuit, that is used to antifreeze the washing street during winter.

3.3. Cooling machines

If heat on top of the machines would be fully captured, this could be enough to warm op the cold produced liquid again. But now, part of the heat loss (leakages) are assumed to take place there, when considering, that the testing facility is in the open air.

3.3.1. Cooling machines energy consumption

Energy consumption for different cooling machines setups is measured with information from DaikinOnsite. With this online tool, one is able to see the energy consumed by machines, during tests. For different machines is the actual energy consumption determined and included in subsection 3.7.2

DaikinOnsite

With DaikinOnSite, multiple parameters are visible. The most interesting ones are named below. It could be of interest to have certain characteristics checked from a distance. One can find them on the site at "Data Points":

- **Unit Status**

    - EvapLvgWTemp: leaving evaporator temperature
    - EvapEntWTemp: entering evaporator temperature
    - ActiveSetpt: Active Set Point
    - ActualCapacity: Capacity of
    - OATemp: Open Air Temperature

- **Power Conservation**

    - ChillerCurrent: Current at that moment in the chiller

With above-mentioned parameters one is able to determine energy consumption and cold production. With the help of the equations in section 2.2, a check can be made.

Heat capture

The possible heat recovery is also based on this, namely by looking at the temperature outlet of the machine, and the air flow this is done with. This is checked with a Testo anemometer with temperature sensor to confirm. Since this is not a study to find out the actual efficiency of the machine, other validations or methods have not been used.

3.4. Components

Mentioned in the method are also couplings, liquids, hoses and other components, but these are considered to not significantly influence energy consumption and are therefore not investigated thoroughly.

3.4.1. Heat-exchangers

Roof section heat exchanger

The installation of these is done by TMP Workgroup, Waalwijk. Formerly, no further documentation from them was shared, this has been checked with them, but unfortunately without further outcome. One of the main research goals of this study is heat recovery, but since this is also part of the testing method, further elaboration on these exchangers can be found in section 3.5.

Washing street, floor heating

Based on the paper "Karakterisatie van afgiftesystemen" by [29] and the book [25] an approach of the heat exchange in the concrete floor heating is made with the following assumptions:

1. Tubes within the floor heating are expected to be of PE-RT, Poly Ethylyn Raised Temperature wall thickness 2 mm
2. Wind is considered to be the annual averag windspeed of 3.7 (m/s).

3. The distance between the tubes is assumed to be at least 30 cm.
4. The depth of the tubes is assumed to be h 20 cm, since heavy machines need to load and unload cooling machines, this is the minimum.
5. The floor is considered concrete, the composition of stone and cement does not influence the specific heat capacity c [29].
6. The heat transfer to the underside area is considered zero, due to insulation
7. Concrete is assumed in wet conditions since at the washing street there is a constant layer of water, but since the thickness, conductivity is assumed to be, k = 2 W/m.K
8. The water temperature on top and influence by it is not taken into consideration.
9. Temperature pumped in the system is assumed to be 25 °C constant, on normal conditions
10. A mixture of 20 % glycol is considered
11. For smooth concrete with ambient wind speed of 3.7 m/s, $h_{c,air}$ around 20 W/m.K [30].

With a given outdoor temperature of 5, 10 and 15 °C and the calculation method from subsection 2.6.1, in detail in section A.1. At this temperature, the floor heating is of no purpose, but it also does not collect heat from the environmental air, since its input BV20 silo is at minimum around 25 °C. The diameter of the tubes in floor heating system is measured with an outer diameter being 20 [mm]. Furthermore, λ is the thermal conductivity coefficient, v is the viscosity, Pr is the Prandtl number and c is the specific heat of which the materials in the equation can be seen in the Table 3.3 below.

Table 3.3: Important characteristics of materials in the floor heating calculations

Material	λ (W/m.K)	v (m^2/s)	$Pr(-)$	c (J/kg.K)	ϵ [-]
Air	0.027	1.657 $\times 10^{-5}$	0.690	-	-
Glycol-water	0.478	1.203 $\times 10^{-6}$	8.600	-	-
Concrete (wet)	2.200	-	-	870.0	0.900
PE-RT (tubes)	0.400	-	-	-	-

With these parameters and the calculations stated earlier, an over, Table 3.4 gives an overview of the loss number considering area A is $8 \times 12 = 96$m

Table 3.4: Heat transfer numbers for different circumstances for the floor heating.

T_a (°C)	T_s (°C)	Q_{rad} (kW)	Q_{conv} (kW)	Q_{total} (kW)	Loss (8h) (kWh)
5.00	-5.00	11.00	6.476	17.47	139.8
10.0	0.00	8.249	6.165	14.41	115.3
15.0	5.00	5.500	5.801	11.30	90.39

Validation: measurement

Later it was found that a pump, with flow meter was installed. Herewith, and the simple heat transfer calculation from Appendix A, a measurement could be made on the calculations, which indicated that with a flow of 0.4 m^3 and ambient temperature of on average 10°C, on a very cloudy day, the T_{in} of 23.6 °C, resulted in an T_{out} of 18.2 °C. Which then gives a loss of 8.682 kWh/h, which is per 8 hours a day 69.41 kWh. This is much lower, and most probably due to much less radiation heat loss during the day, and without sunshine. Eventually is the total energy consumption based on this calculation for one day in spring and winter, and for one whole week considering 5 working days of 8 hours. Since is was found that the pump is not always turned on, see Table 3.5. With these numbers, an annual energy loss can be assumed. The floor heating will not be on during the whole year, but when considering only 3 winter months, the loss adds up to around 4323 kWh, which costs €951,-

Table 3.5: Energy consumption washing street in Spring and Winter

Season	T_a (°C)	Q_{day} (kWh)	Q_{week} (kWh)
Winter	5	84.14	420.7
Spring	15	54.40	272.0

3.4.2. Buffer vessels

Warm water buffer vessel (BV20)

The 20 m^3 glycol-water vessel that is standing outside is subject to environmental weather conditions, some assumptions are made for this calculation:

1. The temperature is measured in the inside of the silo T_{inside}
2. The silo consists of superposition of two speheres and a cylinder
3. The silo is completely filled
4. Small losses on the top of the open silo are negligeble
5. The height is H is 5.000m
6. The diameter is D is 2.400m
7. The inside temperature is constant at 25 °C and the water is not flowing
8. The thickness of the silo is 0.008m
9. Inside the silo the glycol-water is considered still in the first place.
10. No calculations are included for the actual heat transfer from the heating element to the glycol-water
11. It is considered that the surroundings have the same temperature as the ambient temperature
12. T_{wall} is considered (after measuring and averaging) T_{glycol} -8 °C is 17°C for the radiation calculations
13. For the working hours (wh) a constant flow in the tank due to processes gives an internal heat transfer coefficient of h_{inside} =

Based on these and the calculations from subsection 2.6.2 and section A.2 and the following parameters as stated in Table 3.6, calculations are done:

Table 3.6: Important characteristics of materials in the floor heating calculations

Material	λ (W/m.K)	υ (m^2/s)	$Pr(-)$	ϵ [-]
Air	0.027	1.65×10^{-5}	0.690	-
Glycol-water	0.478	1.223×10^{-6}	8.60	-
Steel (painted white)	45.00		-	0.900

A calculation is made for glycol water in still condition, outside working hours, including convection, conduction and radiation based on formula's from Appendix A, with the following outcome Table 3.7:

Table 3.7: Heat Loss at Different Ambient Temperatures

Ambient Temperature (°C)	Heat Loss (conv/ cond) (kWh/day)	Radiation Heat Loss (kWh/day)
5	12.14	110.0
15	2.021	47.81

This does not seem much, but when considering a flow inside the vessel, as normally is during working hours (wh), the thermal loss is much higher, with a heat transfer coefficient h_{inside} of 35 W/m^2.K, see all numbers below in Table 3.8

Table 3.8: Heat transfer numbers for different circumstances for BV20, the big buffer vesel

T_a (°C)	T_{wall} (°C)	Q_{rad} (kW)	$Q_{conv,wh}$ (kW)	$Q_{conv,night}$ (kW)	Loss (24h) (kWh)
5	17	3.210	6.780	0.505	139.4
10	17	1.921	5.084	0.379	92.84
15	17	0.563	3.390	0.253	44.69

Solution

Insulating the tank brings up the thermal resistance. By taking an example of a thermal resistance

material such as rock wool, the heat loss in the above-mentioned conditions, for 0.010m of insulation brings back the total heat transfer during 24 hours of 9.648 kWh/day, without radiation heat in 5 °C T_a and 4.824 kWh/day for T_a = 10 °C. This gives a total of 14 times less energy loss then when not insulated.

**Validation of calculation and insulation**
It has been decided to validate the outcome of the calculations for the silo by making a calculation with the ROCKASSIST by Rockwool, which shows with variable input parameters that the heat loss for 100mm insulation is around 7.9 W/m^2 while in 5 °C and with 3.7 m/s windspeed. For comparison, when considering the calculated 9.648 kWh/day, and take one hour, and the total area of the silo of 56.28m, this is 7.14 W/m^2, which indicates that the calculation is accurate. The calculation made with the tool that can be found in Appendix G.

Energy use measured
Besides the calculation, measurements have been done for the vessel. An example is taken in the period from 25-01-2024 to 05-02-2024. A graph from the measurement can be seen in the next figure 3.2a. The purple line shows the energy consumed outside working hours (4pm - 8am), the yellow during working hours (8am - 4pm).
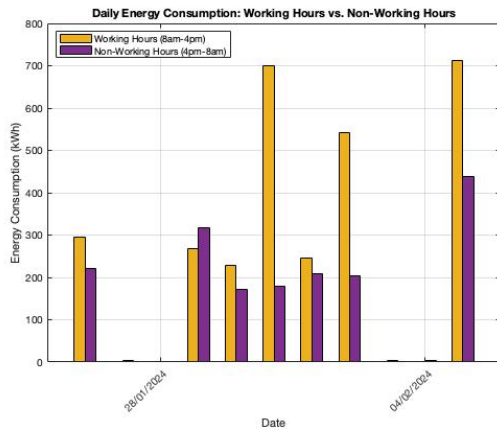
(a) The energy consumption of the buffer vessel when working hours is between 8am and 16pm
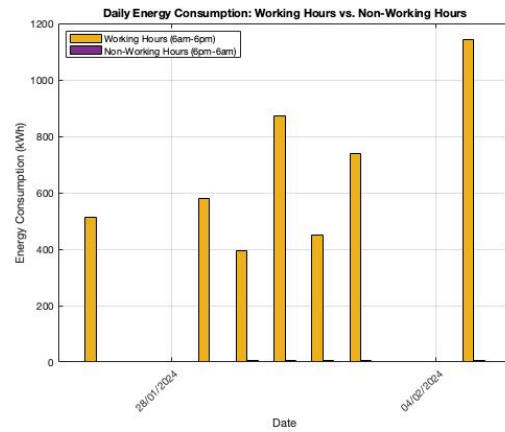
(b) The energy consumption of the buffer vessel when working hours is between 6am and 18pm

The vessel's energy consumption is higher than expected outside working hours and a more close look is taken. Comparison with working hours from 6am until 6 pm are made in Figure 3.2b. More details on this are summarised, besides the comparison between the total energy P_{fud} and energy consumption of the vessel P_{total} in Figure 3.3.:

1. Every half hour, the tank warms up, starting in the morning at 6:00 (am).
2. The tank still warms up after: 16:20 and even after 17:49, these moments are after testing, which is normally until 16:00, hereafter the next days' cooling machines setup is prepared
3. On holidays, the vessel's heater is not shut down, making it consume energy on days such as 01-01-2024 and 25-12-2023
4. Also, on days without testing the tank warms up, so not only on holidays, but every day.
5. After the weekend, the energy consumption is higher, which indicates in more energy loss during the weekend.
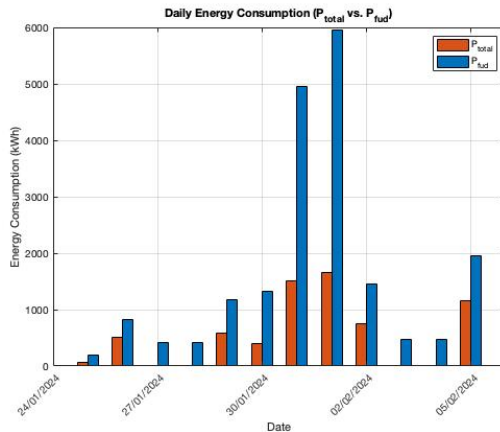
Figure 3.3: The energy consumption of the buffer vessel compared with the total energy consumption

The energy consumed by the vessel is 28.79% when taking the averaged consumption within the vessel, compared to the total energy consumed, so it is interesting to find a renewable energy source for this consumption. Besides, it was found that after a weekend with an average ambient temperature of 10 °C (03-02-2024 and 04-02-2024), the energy needed to warm up the vessel was around 120 kWh, with outside windspeed around 7 m/s on average. For a less warm weekend, around 3 °C, with around 2.5 m/s wind speed and more irradiation due to fewer clouds, the energy needed was around 150 kWh. This indicates a loss of around 75 kWh per day in winter weather when not in use. When in use with more internal flow, the losses increase. This suggests an annual consumption, considering 13.3 °C and an average wind speed of 3.7 m/s, of 52 kWh per day, which is lower than the performed calculation.

3.4.3. Hoses and pipings

Insulation is not important when considering piping and hoses in the testing facility, as the cold that flows through it must be warmed up. Since hoses are used for both cooling and heating circuits it is assumed that the total energy transfer in these hoses is in balance. Nevertheless, some recommendations are given in chapter 8.

3.4.4. Pumps

The energy for each pump has been measured or calculated. Most pumps are on nominal power, but they can differ a little when the liquid becomes less viscous when chilled. Nevertheless, nominal speed is considered and the pumps are summed up below.

Table 3.9: Overview of the component types in the testing facility setup

Circuit	Name (Coolworld)	Nominal Power [kW]	Included in study?
CC01	P090-16C	8.800	yes
CC02	P0118 (1)	8.700	yes
CC03	P0118 (2)	8.700	yes
CC04	Pedrollo HNAX5.4	1.100	yes
CC05	PO50 2C	5.000	yes
CC06	PO55-2	5.500	yes
CC07	Floor heating	0.005	no

Considering a testing duration of 4 hours per day, the pumps in circuit CC01, CC02, CC03 are used, which combined gives a consumption of: 52.4 kWh per day. The filter pump is running all day and night, which gives a total consumption of 26.4 kWh per day.

3.5. Machine testing

This paragraph will elaborate on the testing that has been done with the current setup at the testing facility in Waalwijk, first without adjustments.

3.5.1. Testing purposes

The most time and thus energy-consuming process is the so-called return check, with this check the machine is set to a set temperature of -10 °, and will be tested to see if it reaches this, all other tests are done in the meanwhile.

3.5.2. Data log findings: Daily use

During tests, the inlet temperature of the heat exchangers rises. This indicates that the exchangers work the other way around heating the surrounding cold air. When $T_{ambient}$ is lower than the T_{in}, and no machine is running, and the fans are turned off, the cold outdoor temperature cools down the heat exchangers water inlet each time $T_{water,in}$ (darkgreen) is higher than $T_{water,out}$ (lightgreen). See Figure 3.4 between 08:20 and 09:00.
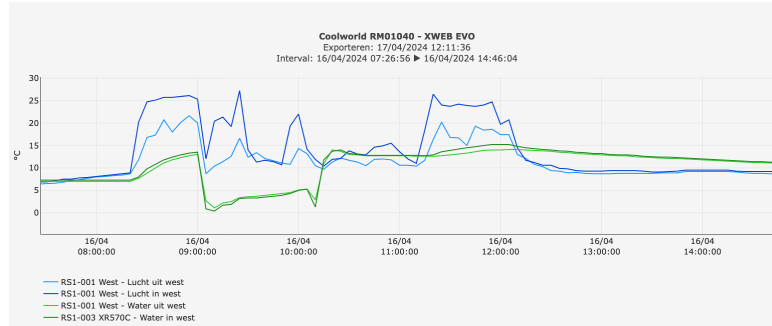
Figure 3.4: Graph from the sensor environment, showing a lower $T_{uit,water}$, then $T_{in,water}$ on 16-04-2024

Exhausted air of the cooling machine does not influence, due to turned off fans in the heat exchangers, or low water flow. This is better visible in Figure 3.5, when T_{in} is lower then $T_{ambient}$ between 11:45 and 14:20 the air temperature sensor below the exchanger is lower than that of the sensor on top of the exchanger. This did not result in a big ΔT, showcasing that the flow was not running.

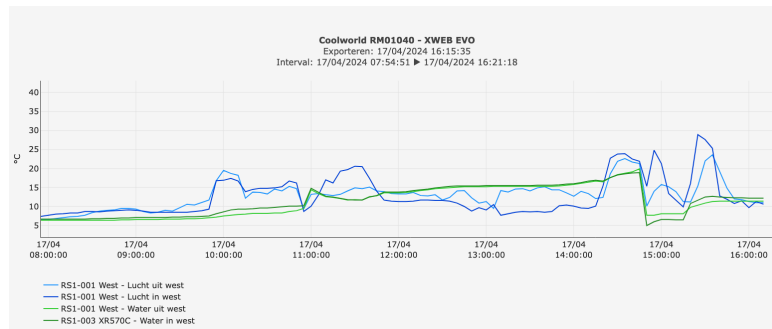**Figure 3.5:** Graph from the sensor environment, showing a lower $T_{uit,water}$, then $T_{in,water}$, for water on 17-04-2024

3.5.3. Data log findings: Weekly use

The findings mentioned above are supported by Figure 3.6, which shows a rising inlet temperature.
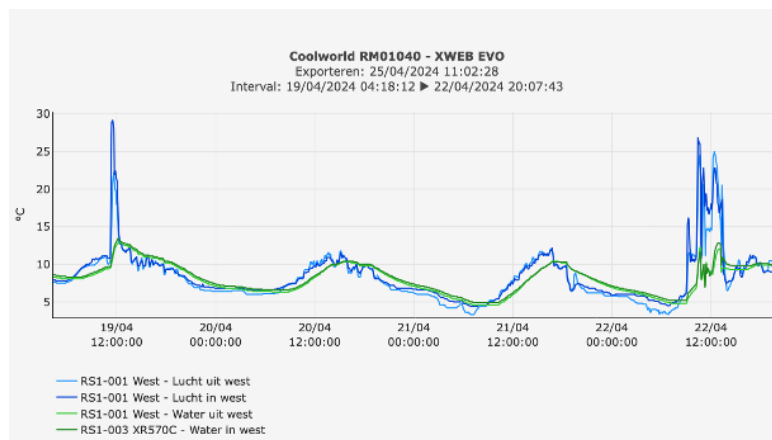

Figure 3.6: Graph showing an increasing $T_{uit,water}$ and $T_{in,water}$, for water, during the week 19-04 until 22-04

Since the repeated occurrence, the idea behind it was searched for. The reason is that the temperature in the roof cannot drop too much, since than condensation and rain occurs, besides this is the three way valve temperature control (to define how much is preheated with the big vessel) is not calibrated. It does make a 360°turn and then is calibrated by feeling, a picture of the button is shown in Figure 3.7. Due to this a lot of energy gets lost. Even during testing, more energy is lost than recovered. This is visible when showing the ΔT plot for the water-glycol through the exchangers see Figure 3.8a

Figure 3.7: The three way valve temperature button, not calibrated.
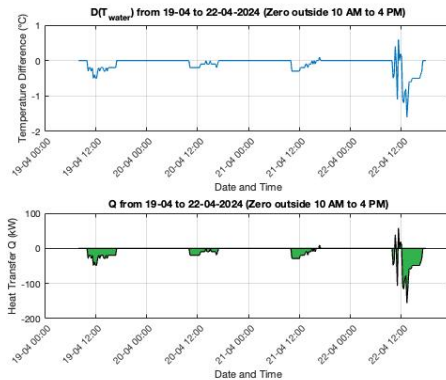
(a) The ΔT_{water} and Q profile from 19-04 to 22-04, only between 10am, and 16pm, considered the only testing periods.

(b) The positioning of the fans in the roof section of the testing facility.

Together with the approached 90 m^3/h volumetric flow (average flow for all machines) with the density of the glycol-water at 0 °C (average temperature) 1045 kg/m^3 and a specific heat capacity of 3.72 kJ/kg.K the heat loss profile is created, see Figure 3.8a. This gives the following losses of energy in this week in Table 3.10.

Table 3.10: Heat exchanger heat loss during a week of testing

Date	Daily Heat Loss Q (kWh)
19-04-2024	108.5
20-04-2024	55.07
21-04-2024	77.48
22-04-2024	199.3

The positioning of the fans is 45 degrees on top of the heat exchangers, which could therefore drag cold air over the exchangers, and cause energy loss. Below a figure of the positioning of the fans, in Figure 3.8b.

3.5.4. Data log findings: Overall, 29-02 until 24-04
When considering the period since 29-02-2024, it was visible that the water outlet temperature is most of the time lower than the temperature in. For data withing working hours, when the circuit is running, hours between 10 am and 16 pm are taken. Figure 3.9a and Figure 3.9b show that ΔT is still more often negative then positive. Heat loss is greater in the beginning of the year, which can be related to colder weather conditions. One moment has very positive ΔT. This is on the day that testing with a new method has been done, as elaborated below.

3.5.5. New heat recovery method: 10th and 11th of April
On the 10th and 11th of April, testing was done differently. Now, chilled glycol water was directly pumped into the heat exchangers, and the cooling machine were aligned under the heat exchanger. In the study conducted, the opportunity arose to evaluate the performance of the exchangers. The test
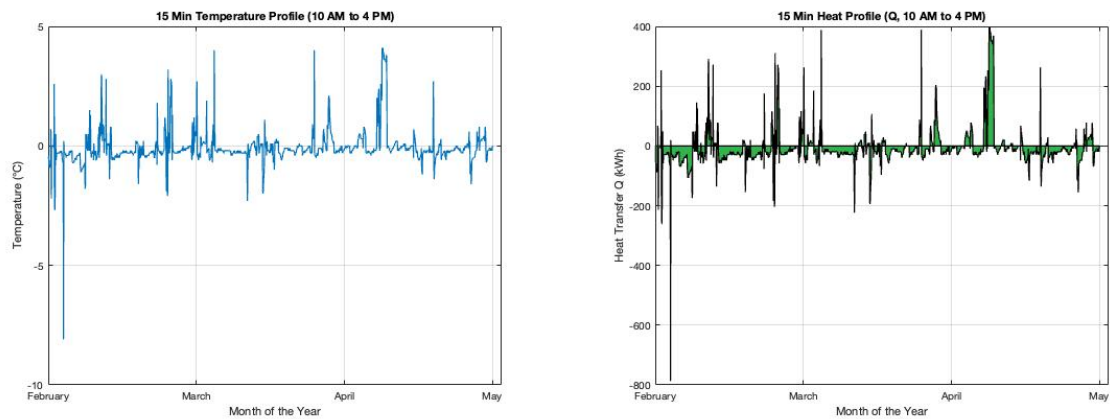
(a) The energy consumption of the buffer vessel when working hours is between 8am and 16pm

(b) The energy consumption of the buffer vessel when working hours is between 6am and 18pm

was done with a CZ62005 machine, which involves a 600 kW cooling power capacity. The initial phase of testing was carried out without any physical barriers surrounding the unit, hereafter can be seen in Figure 3.10, a sail was installed, but on one side only, as sometimes done in the past.

From this test, the temperature profile of Figure 3.11 was made. In these graphs, the curtain did capture a lot more energy. More information per time step is elaborated below in Table 3.11, based on videos and photos made during the test and by exploring the graphs. As can be read and seen, the heat collection is almost twice the amount when the exhaust fully enclosed compared to one side closed. The heat collected by the heat exchangers is even larger than the actually produced cold. Making it very useful to have the installation of the cooling machines differently when in testing mode. As can be seen, with 100% capacity, almost 600 kW is possible to recover, making this test method very efficient. Normally only in summer, with smaller machines, this could be achieved.

Figure 3.10: Installation of energy recovery solution
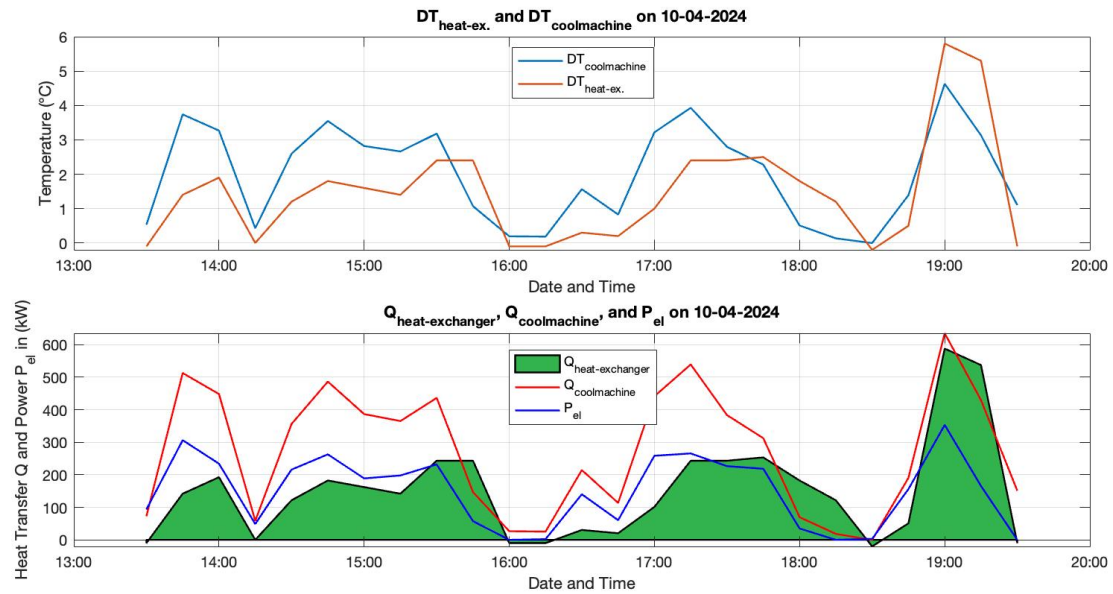
Figure 3.11: Testing day results, in the upper graph the ΔT for both the cooling circuit and heat exchangers, in the graph below the belonging $Q_{heat-exchanger}$ (recovered) in green and electrical energy needed in P_el, as well as the produced cold ($Q_{coolmachine}$).

Table 3.11: Heat exchanger heat loss during a week of testing

Time	Description	Findings
until 13:30	No testing	-
13:30 - 14:45	Testing is done without any sail attached	already more heat capture when aligning the machine.
14:45 - 15:45	Very low temperature in the pipelines in the roof section	Much more possible heat exchange.
15:45 - 16:15	Attachment of sail	No heat exchange
16:15 - 16:45	Sail attached at one side	Since the amount of air flow out of the machine, the sail was bulging, see Figure 3.12a, so the machine could not produce enough cold, since warm air is interfering with the inlet of air, which needs to be cold, to be able to exchange heat of the machine with.
16:45 - 17:00	Sail is attached more tightly to the upper part of the machine.	Now no air will be blown towards the air inlet of the machine, less heat in the facility now, see Figure 3.12b.
17:00 - 18:00	One side enclosed properly	More heat is collected by now.
18:00 - 18:45	Attaching second part of the sail	Sail is now enclosing the whole top of the machine, without interfering with the inlet, see Figure 3.12c
18:45 - 19:30	Fully attached sail and capacity	The machine is unable to produce enough cold while the heat exchangers work, so more collection of heat then production of cold.

(a) Bulging with one side of the sail closed the elastic attachment was not solid enough.

(b) Bulging when the side is closed of better with a beam on the sail,

(c) Sail is now fully enclosing the cooling machine.

3.5.6. Outcome new method

- **Improvement of Airflow Roof**: More airflow is needed to efficiently capture air from larger machines with high volumetric flows. This adjustment prevents over-pressure issues below the exchanger, such as with bulging curtains.
- **Roof Fan: Change of Positioning**: Most measurements were in winter, leading to the fans extracting cold air from the surroundings when activated without a machine running beneath them.
- **Roof Air Control**: A controller should be added to the fans on the roof to allow for more airflow than what is generated by the machines. Additionally, installing controllers in the heat exchange circuit on the roof would ease operations. These controllers could determine liquid temperature at the inlet, ambient temperature inside and outside the facility, and decide whether airflow should pass through the heat exchangers.
- **Inconsistent Air Temperature Flow**: Testing of the machines revealed highly inconsistent heated air inflow. This inconsistency arises mainly due to settings during machine startup, which are currently not adjustable.
- **Inconsistent Water Temperature Flow**: It was surprising to observe that the water temperature at the inlet also experienced significant rises during testing.
- **Electrical Power vs. Produced Cold (P_{el} vs. Q)** The electrical power needed to produce the observed cold is lower than the actual cold produced. This discrepancy might be due to a different circuit configuration or only one income (L1) of the total energy amount being displayed on DaikinOnSite, although the pattern matches the cold produced but at half the magnitude.

3.5.7. New heat recovery method, second test

Hypotheses:

With a smaller machine, less heated air is leaking, so that more actual capture on top of the facility would occur. Possibly leading to, shutting off of the machine since than more heat capture occurs, then cold is produced.

By definition a machine has more rest heat than it cools, this is due to the different other processes in the machines that generate heat. Such as the pump and compressor. Therefore when running on fully recovered heat, it will continuously try increasing its capacity, therefor not all the rest heat can be captured, and some will need to escape. Now sometimes the ΔT is higher in the heat exchangers on the roof, then it is in the cooling machine itself. So more heat is captured, than cooling is generated. Which is checked with a smaller, 300 kW (CZ30028), kW machine, see Figure 3.13a

Also with a smaller machine, the possible air suction in top of the facility is not strong enough, which results in curtains bulging again. Figure 3.13b shows that the heat capture was exceeding the machine's 300 kW power. Considering (by approach) the same mass flow in the heat exchangers, the cooling

(a) Testing with a smaller machine, the CZ30028, it is shown that still bulging occurs due to overpressure
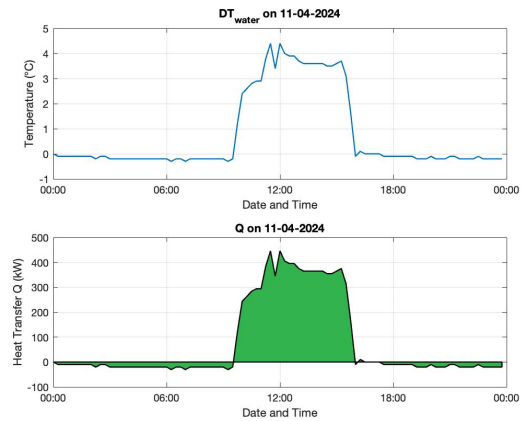
(b) Graphs showing the ΔT of the water-glycol in the heat exchangers and the heat captured with it, which is as much as its produced cold

machine was not able to produce more cold, see the stagnation in heat capture at 11:00. The heat exchanger also started to rain due to the amount of heated air collection and cold liquid flowing through it.

3.5.8. Adjusted testing procedure

Currently, there is no knowledge of how most energy could be extracted from the roof heat exchangers, although the mechanic in the facility is aware of sustainable practices, it is unsure how this is done best. A change in the test procedure as stated in subsection 2.7.2 would look as follows. The underscored text is changed or newly added; the striked-through has to be removed. It is now not being built in to attach the heat recovery options. But this should become part of the procedure, but it should be known when and how.

1. Every electrical and water connection is connected, one inlet, one outlet, and sometimes an extra outlet. Depending on the number of circuits within the machine
2. The heat capture roof /curtain will be lowered
3. Cooling machine is turned on to prepare oil temperature
4. Test checklist will be consulted
5. Pump is started and taps opened
6. Flow is determined and set for the tested machines' cooling circuit
7. The pump for flow through the heat exchangers in the roof is turned on and corresponding to the controller in the next step, OR the fans in the roof are responding on the controller
8. The controller in the heat exchanger roof determines the amount of flow through the heat-exchangers, so that chilling still occurs in the cooling circuit [1]
9. Either the fans in top
10. ~~The heater in BV20 is turned. Depending on its temperature, $T_{ambient}$ and the size of the cooling machine, if $T_{ambient}$ is high enough, air handlers can be used instead~~
11. Machine is turned on, manually
12. ~~After heat is starting to develop in the test facility~~ the heat exchanger fans are turned on.|
13. The three way valve is not in use, and as cold as possible is transported through the heat exchangers in the roof
14. After the test is done everything is shut off and disconnected

The controllers in the testing facility's' roof need to respond continuously on one another to define the flow needed in either the water or air section. Especially when multiple machines are turned on and off. A better solution can be found in chapter 8

---

[1]This is due to a higher amount of heat that can be recovered by capturing, in the process, therefore the flow within the exchangers is needed to adjust such that the cooling machine is still able to produce cold

3.6. Energy management: Strategy

A strategy booklet has been carried out as a product of the later named heat exchangers test that has been applied to the testing facility of Coolworld Waalwijk. This strategy is made to perform comparable tests and measurements as a standardisation for other facilities that include comparable warm and cold liquid and air flows. This booklet can be found in Appendix I.

3.7. Energy management: Outcome

3.7.1. Energy consumption

Energy is purchased from Nieuwstroom™. With Figure 1.9 showing 2023's consumption. Stand-by energy consumption at days that the location of Coolworld Waalwijk is closed is defined by choosing national holidays, such as 01-01-2023, and eastern and the weekends. Multiple things are noticeable from these.

1. During holidays, energy consuming processes such as the heater of the vessel are not turned off, this visible due the time schedule on which this turns on, normally around 6/ 7 am,
2. During weekends, an amount of +/- 416 kWh is normally being used
3. The average energy consumption in 2024 is 1450 kWh, and when not counting weekends 2015.77 kWh.
4. The average weekly consumption is 10.26 MWh.
5. The energy consumed on days without testing is around 752 kWh, this is higher per week average, due to more losses in the weekend of the buffer vessel.

3.7.2. Sankey Diagram

The main components in the testing facility and in circuits are: Pumps, hoses, buffer vessels and the cooling machines itself. For the hoses, the actual consumption is brought to a 1 % of the total testing consumption of energy. Another 1 % is considered for measuring items such as the flow meters, three way valve and sensor applied in the testing facility. All others are filled in below inTable 3.12, distinguished in weekly and daily consumption, and with an possible energy consumption saving, both daily an weekly. The outcome Sankey diagrams on this can be found in: on the next page.
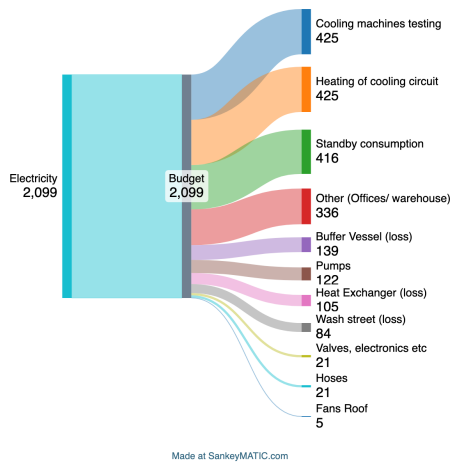
Table 3.12: Overview of components, energy consumption, and savings in the testing facility

Type	Name	P (day$_{winter}$)	P (week$_{winter}$)	P (day$_{spring}$)	P (week$_{spring}$)
Cooling machine	Averaged	3.926e2	1.542e3	3.926e2	1.542e3
Fans	Roof	5.000	25.00	5.000	25.00
Heat Exchanger	Roof	87.24	342.5	29.91	127.1
Heat Exchanger	Washing St.	84.14	420.7	54.40	272.0
Heating element	In BV20	3.926e2	1.542e3	3.926e2	1.542e3
Hoses (1%)	All	20.15	102.6	20.15	102.6
Pump	Filter	26.60	132.0	1.600	11.20
Pump	P0118 (1)	34.80	174.0	34.80	174.0
Pump	P0118 (2)	34.80	174.0	34.80	174.0
Pump	P090-16C	35.20	176.0	35.20	176.0
Silo	BV20	1.394e2	9.755e2	44.69	312.8
Valves/etc (1%)	Etc.	20.15	102.6	20.15	102.6
Standby consump.	No production	4.163e2	2.914e3	4.163e2	2.914e3
Other	Offices/etc	3.359e2	1.679e3	3.359e2	1.679e3
Totals		2.016e3	1.026e4	1.834e3	9.231e3

It can be seen that a small difference is noticable in the energy consumption in winter compared to spring, this is due to energy loss in winter. The energy recovery is a loss inn the current procedure. The weekly average energy use in the first 17 weeks is: 1.026×10^4kWh, and daily this is 2.016×10^3 kWh. This difference is not just 5 or 7 times one another, but differs due to the silo losing energy during the weekend, and the washing street not.

3.8. Conclusion

It can be concluded, that for the inspected components, controllers, for the floor heating, and insulation for the vessel, result into an annual energy saving of €951,- and €3575,- respectively. The investment costs for a controller are €350, which gives a payback time of 0,37 year (5 months). For the vessel insulation, a former invoice is used with indexing, which states €11460,-, and a payback time of 3.2 years (39 months). For the testing method, it is shown that the current use is far from efficient. Instead, the current procedure causes losses in the heat exchangers in the roof section of the facility. After extensive testing, with different testing setups and by implementing a possible solution it is demonstrated that with correct use of the heat exchangers, and the temperature and flow within these, more than 100 % of the energy exhausted by the machines can be recovered. Which, resulted in stagnation of the machine's production, since it was unable to produce enough cold, compared to the heat recovered in the system. Something that until now was only possible with small machines, in periods with warm ambient temperatures. In the most optimistic situation, when 100 % is recovered and more due to former losses that are solved, the total heat demand (94.52 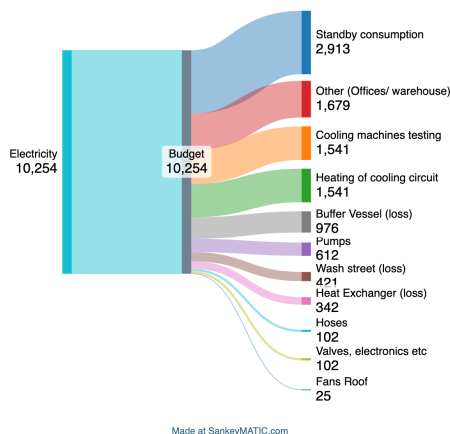MWh) could be saved. Taking 50 % as possible outcome this saves €10399,-. The investment in a proper sail costs €8980,-, resulting in a total cost of €13680 including two controllers and 4 higher capacity fans (each $\pm$ €100, from old machines), and a 1.3 year (16 months) of payback time.

(a) The total energy consumption of Coolworld Waalwijk, including standby, other production processes and subdivided energy consumption processes in the testing facility for a day in winter.

(b) The total energy consumption of Coolworld Waalwijk, including standby, other production processes and subdivided energy consumption processes in the testing facility for a day in spring

(a) The total energy consumption of Coolworld Waalwijk, including standby, other production processes and subdivided energy consumption processes in the testing facility for a week in winter.
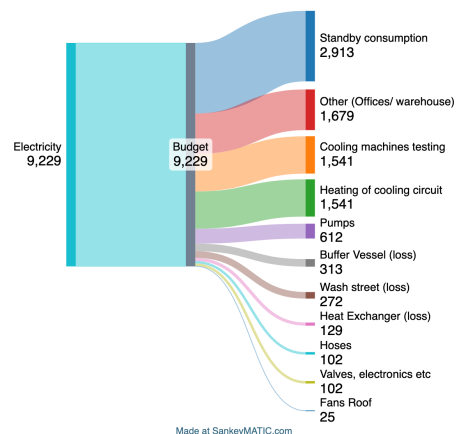

(b) The total energy consumption of Coolworld Waalwijk, including standby, other production processes and subdivided energy consumption processes in the testing facility for a week in spring

<div style="text-align: right; font-size: 3em;">4</div>

Analyses of a PV/Thermal system, with Coolworld as a case study

This part of the study will further elaborate on a model and experimental approach to determine the energy generation that could cover a part of the current energy needs at Coolworld Waalwijk more sustainably. This chapter will specifically go into depth about a solar energy study on three different possible systems. The chapter opens with background information in section 4.1. Second, the different systems are explained in section 4.2, section 4.3 and section 4.4. After this, the model software is described in section 4.5, considering data loads and parameters. Then, a validation of the model is made with a testing setup of PVT panels in section 4.7. At last an economical feasibility is made of the different options, based on a Levelised Cost of Energy (LCoE) in section 4.8.

4.1. Background

It is of interest to make a comparison between solar heat collection and electrical energy generation for testing facilities for cooling machines to find out what energy solution fits best, and to what extend at Coolworld Waalwijk. Former plans for the implementation of PV modules at Coolworld exist but have not been continued. The warehouse of Coolworld is a big 3200 m^2 (40x80) building that can be used, but there have been notions of this roof not being strong enough.

4.2. Option 1: PV System

This section will elaborate on which PV panel will be the most sufficient to generate as much energy as possible to provide high energy levels at the testing facility of Coolworld.

4.2.1. Electrical efficiency

The impact of ambient temperatures and solar irradiation on different types of solar panel's efficiency is crucial for optimising performance. Generally, solar panels experience a decrease in efficiency as temperatures rise. This temperature dependence is described by the temperature coefficient, representing the percentage decrease in power for each degree Celsius increase in temperature [31]. A more in depth description on this can be found in section J.1

The electrical energy output from the PV cells can be calculated as:

$$E_{\text{elec}} = \eta_{\text{elec}} \cdot A_{\text{PV}} \cdot G \tag{4.1}$$

where η_{elec} is the electrical conversion efficiency of the PV cells, A_{PV} is the area covered by the PV cells, and G is the solar irradiance.

In the below picture one can see the efficiency change over temperature, for different panel types.

Power Vs Temperature chart notes:
- STC = Standard test conditions - 25°C
- NOCT = Nominal operating cell temperature - 45°C

<div style="text-align: center;">36</div>
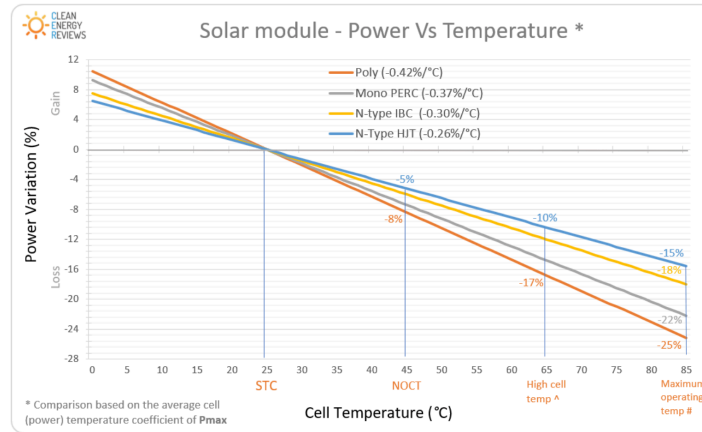
Figure 4.1: Different solar panel types, and their efficiency differences, over temperature (source: [31])

- (□) High cell temp = Typical cell temperature during hot summer weather - 65°C
- (#) Maximum operating temp = Maximum panel operating temperature during extremely high temperatures mounted on a dark-coloured rooftop - 85°C

For this study only the Mono-Crystalline will be studied any further since this is most common in the Netherlands. In the Dutch climate, where temperature variations are moderate, the impact of temperature on solar panel efficiency is manageable. However, it is fairly unknown what active cooling of these panels could do to their efficiency, when they are brought to temperatures below the STC 25 °C. To do so, the panels need to be attached to a heat exchanger.

4.3. Option 2: Thermal heat collector systems

Small background information on the working principle of a solar collector can be found in section J.2.

4.3.1. Thermal efficiency

The thermal efficiency of a collector is based on its collection, minus its losses which is shown in Figure J.2.
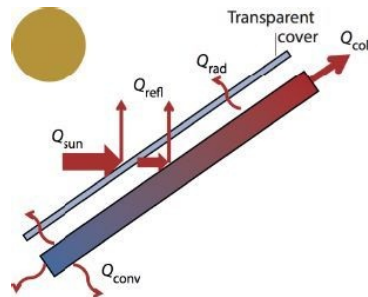
Figure 4.2: Solar collector collection and losses, source: [3]

In equation form this can be written as in Equation J.1, below.

$$Q_{\text{col}} = Q_{\text{sun}} - Q_{\text{refl}} - Q_{\text{conv}} - Q_{\text{rad}} \tag{4.2}$$

In which the losses are based on the equations from Appendix A. Some are rewritten, see the following equations. The solar radiation absorbed by the collector is also found below, in equation:

$$Q_{\text{sun}} = I \cdot A \tag{4.3}$$

where I is the solar irradiance (W/m^2), and A is the area of the solar collector (m^2). The **reflected** solar radiation is:

$$Q_{\text{refl}} = \rho \cdot Q_{\text{sun}} \tag{4.4}$$

where ρ is the reflectivity of the collector surface (dimensionless). The convective and radiation heat losses are the same as the ones in Appendix A but with T_s as the surface temperature.
Total heat generation can then be derived as:

$$Q_{col} = A \cdot I \cdot (1 - \rho) - h_c \cdot A \cdot (T_s - T_a) - \epsilon \cdot \sigma \cdot A \cdot (T_s^4 - T_a^4) \tag{4.5}$$

Which is the same as taking all losses from the actual solar irradiance that are lost in the collector. If each loss cannot be determined separately, η_{th} can be found with the following equation,

$$\eta_{\text{th}} = \eta_{\text{opt},0^\circ} - a_1 \frac{T_m - T_a}{DNI} - a_2 \frac{(T_m - T_a)^2}{DNI} \tag{4.6}$$

With the parameters $\eta_{\text{opt},0^\circ}$, a_1 and a_2 specified by testing. More information on this can be found in Appendix O

- η_{coll} = the collector efficiency
- $\eta_{\text{opt},0^\circ}$ = the zero loss eff. of the collector
- a_1 = 1st order heat loss coefficient, $\frac{W}{K \cdot m^2}$
- a_2 = 2nd order heat loss coefficient, $\frac{W}{K^2 \cdot m^2}$
- DNI = Direct Normal Irradiance, $\frac{W}{m^2}$

- T_a = Ambient temperature, °C
- $T_m = \frac{T_{in} + T_{out}}{2}$, Working temperature, °C
- T_{in} = inlet temp. to heat exchanger, °C
- T_{out} = outlet temp. to heat exchanger, °C

More on these can be found in section 4.6. For the T_{in} of the solar collector, a temperature, based on T_a and the energy produced by the cooling machines with corresponding ΔT of the chilled vessel, is is tried to define.

4.3.2. Storage
The setup of a solar collector includes a heat storage, collector array, a pump and the possibility to make use of an extra secondary heat supply as is described in Figure 4.3.
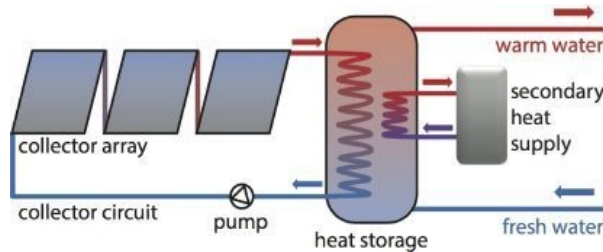
Figure 4.3: Solar collector setup, source: [3]

It is possible to store more heat than needed at Coolworld, and the working fluid will be the current existing glycol water. In this proposition, without heat-exchanger between it, this is an active direct loop including a pump. Important for the overall setup is the capacity of heat storage, which affects the costs, reliability, and performance. At Coolworld Waalwijk, currently, a 20 m³ vessel is a possible liquid storage that can be used. This vessel will therefore be implemented in the calculation. The usable energy storage can be calculated with Equation 4.7

$$Q_{\text{stored}} = V \cdot \rho \cdot C_p \cdot \Delta T \tag{4.7}$$

Here, V stands for the tank's volume, ρ represents the fluid's density in [kg/m³], C_p denotes the specific heat capacity of water in [J/(kgK)], and ΔT is the interval of operating temperature. There are no further boundary conditions since this cold liquid currently exists in the setup, and boiling point lies higher than water an freezing lower.

4.4. Option 3: Photovoltaic/Thermal (PVT) System

Photovoltaic/Thermal (PVT) performances with both heat and electrical production suggests that this is an optimal form of solar energy usage. More details on the different types can be found in subsection J.2.3

4.4.1. Electrical and thermal efficiency

The electrical output is the same as for the PV system in section 4.2.

Heat Absorption: by the collector that is not converted into electricity is:

$$Q_{\text{abs}} = A_{\text{coll}} \cdot G - E_{\text{elec}} \tag{4.8}$$

where η_{th} is the thermal efficiency of the collector, and A_{coll} is the collector area.

Thermal Energy Output: collected by the panel can be determined by:

$$Q_{\text{th}} = \eta_{\text{th}} \cdot (A_{\text{coll}} \cdot G - E_{\text{elec}}) \tag{4.9}$$

Total Energy Output: is the sum of the electrical and thermal energy, given by:

$$E_{\text{total}} = E_{\text{elec}} + Q_{\text{th}} \tag{4.10}$$

Further details on how these generations are calculated can be found section 4.5

System Efficiency Relation:

The efficiencies of the PV cells and the thermal system are related by the fact that any energy not converted into electricity can potentially be recovered as thermal energy. The performance of the PV cells is inversely related to their temperature: as temperature increases, electrical efficiency decreases, but thermal recovery can increase. Therefor the balance is, see Equation 4.11

$$A_{\text{coll}} \cdot G = E_{\text{elec}} + Q_{\text{th}} + Q_{\text{loss}} \tag{4.11}$$

The model chosen for PVT is the existing model on the Dutch market, which consists of a separate heat exchanger on the backside of the PV panel.

4.5. Numerical model: PVT, PV and thermal collector solar energy prediction

A model is built with software program MATLAB with the help of the PVMD Toolbox to predict energy generation for one whole year in Waalwijk.

4.5.1. Meteorological solar data

The solar irradiation is defined in Waalwijk. The effectiveness of all three systems is heavily influenced by ambient meteorological conditions. For an optimal PV solar thermal and PVT system design, knowledge of the sun's position at any given time is crucial. A MATLAB computational model, as cited in [3], transforms ecliptic coordinates into horizontal ones. Acompanied with local weather conditions, thermal and electrical generation can be predicted. This data is obtained from the nearest weather station of the Royal Netherlands Meteorological Institute (KNMI) in Gilze-Rijen, Noord Brabant Koninklijk Nederlands Meteorologisch Instituut (KNMI) [32]. An hourly resolution is used in the model. Appendix K elaborates on the details for the sun path calculator, which determines solar azimuth and altitude.

Climate Data

Hourly historical data is retrieved since 1991 for Gilze-Rijen and a yearly average is taken of it. Some notes on this that need to be taken into account are:

Note:

- $T_{ambient}$: average ambient temperature measured at 1.5 m above the ground.

- T_{ground}: average ground temperature at 10 cm above the ground.
- Wind: average wind speed at 10 m above the ground.
- Cloud: cloud coverage in eighths of the visible sky area where 0 is clear-sky and 8 is a completely obscured sky.
- Pressure: air pressure at the measurement station in Pascal.
- Rainfall: rainfall at the measurement station in mm/hr.

4.5.2. Azimuth and tilt angles optimisation for solar irradiance

An example building with typical structure is used to visiualise the solar radiation based on an example of the Course PV Systems of the SET programme.

In the data dataset a distinction is made between Global Horizontal Irradiance (GHI) including, Direct Normal Irradiance (DNI), and Diffuse Horizontal Irradiance (DHI). To calculate the total irradiance G_m on a PV module, the sun's altitude a_s and azimuth A_s play a pivotal role, based on the location Waalwijk. These solar coordinates are essential for evaluating the albedo effect on solar panels. The zenith angle is computed as $90° - a_s$, which helps to separate DNI and DHI from GHI, this has only been done for calculations on 2024 data, since this only provided GHI. Then the following equations can be made.

$$\text{GHI} = \text{DNI} \cdot \cos(90° - a_s) + \text{DHI} \tag{4.12}$$

$$\text{DNI} = \frac{\text{GHI} - \text{DHI}}{\cos(90° - a_s)} \tag{4.13}$$

$$\text{DHI} = \text{GHI} - \text{DNI} \cdot \cos(90° - a_s) \tag{4.14}$$

The determination of the Sky View Factor (SVF), indicative of the proportion of sky visible to the PV panels is shown below (calculated with the svfCalculator script). This ratio is computed for panels throughout the year,

$$\text{SVF} = \frac{1 + \cos(\theta_{\text{module}})}{2} \tag{4.15}$$

enabling it to determine the diffused irradiation component via:

$$G_{m,\text{diff}} = \text{SVF} \cdot \text{DHI} \tag{4.16}$$

Further, the irradiation reflected onto the panels is evaluated by:

$$G_{m,\text{ref}} = \alpha \cdot \text{GHI} \cdot \frac{1 - \cos(\theta_m)}{2} \tag{4.17}$$

With the albedo, α, assumed to be 0.15 [33]. At last, the direct irradiation component is calculated, based on the Shading Factor (SF). The SF is depending on skylines and position of the sun. The roof of Coolworld is positioned 9m above sea-level without any interruptions, so SF is stated as 1

Following the shading analysis, for a module with azimuth A_{module} and tilt angle θ_{module}, the angle of incidence (AOI) for direct irradiance is, as can be seen in Equation 4.18:

$$\text{AOI} = \cos^{-1}[\sin(\theta_{\text{module}}) \cos(a_s) \cos(A_{\text{module}} - A_s) + \cos(\theta_{\text{module}}) \sin(a_s)] \tag{4.18}$$

With, α_s as the azimuth angle this the direct radiation is calculated as follows:

$$G_{m,\text{dir}} = \text{SF} \cdot \cos(\text{AOI}) \cdot \text{DNI} \tag{4.19}$$

Combining all components yields the total irradiance

$$G_{\text{m}} = G_{m\text{dir}} + G_{m\text{dif}} + G_{m\text{ref}} \tag{4.20}$$

To optimise the PV panel's placement, a cumulative of irradiation is defined for both landscape and portrait orientations. Which will be shown in subsection 5.1.2

4.5.3. Load analysis
A load profile of Coolworld Waalwijk will be used, to define a system for all three system options. The load profile is based on the hourly data that is collected from the metering institute for high capacity energy consumption: Fudura™ [34] for the year 2023.

4.5.4. PV system
The module efficiency η_m is given by the product of the cell efficiency η_c, the transparency of the PV module glass τ_c, the absorptivity of the solar cell α_c, and the packing factor δ_c, [35]

$$\eta_m = \eta_c \cdot \tau_c \cdot \alpha_c \cdot \delta_c \quad (2) \tag{4.21}$$

where τ_c is the transparency for the PV module glass, which is assumed to be 0.95. α_c is the absorptivity, which can be calculated with

$$\alpha_c = (1 - \text{Refl})(1 - \text{eff\_STC}) \tag{4.22}$$

and δ_c is the packing factor; their values are taken as 0.90, 0.95, and 0.90, respectively [36]. A table with different heat transfer coefficients for PV back panel in different circumstances is made by Ceylan et al. [35]. Calculation of these is comparable to those in Appendix A. The calculation is an approach and mainly air velocity (measured between 0 to 5 [m/s]) made a difference to the number, in contrast to $T_{ambient}$ (10 - 40 °C) the following table with heat transfer coefficients is used based on this study:

Table 4.1: Effect of the rear-panel air velocity on the heat transfer coefficient.

Air velocity (m/s)	Average h (W/m^{2}K)
2	7.4
3	9.0
4	10.5
5	11.9

This table is based on measurements on poly-crystalline PV panels, but these are considered almost similar in thermal performances to mono-crystalline. Such as the panels used in this study. It must be said, that this is forced convection only, and not natural, which will also depend on the inclination angle, but this is not considered in this study. The temperature in a module is normally based on Steady State conditions (SS) without wind conditions taken into account, as can be seen in Equation 4.23. This temperature model is based on (Normal Operating Cell Temperature (NOCT). Since the model produced will partly be based on wind interferences, especially when calculating for PVT, it is decided to include this in the PV study as well.

$$T_M = T_a + \frac{T_{NOCT} - 20°}{800} G_M. \tag{4.23}$$

With wind included in the equation, the mounting configuration module temperature definition is used from Smets, Jäger, et al. [3]. This is to Installed Nominal Operating Cell Temperature (INOCT) which describes the cell temperature of an installed array under NOCT conditions. In rack mount position, as in this case, based on results from Fuentes [37], the INOCT is:

$$INOCT = NOCT - 3°C \tag{4.24}$$

The temperature coefficient can be obtained by, see Equation 4.25. For V, I and P this can be found in subsection K.0.1

$$\eta(T_M, G_{STC}) = \eta(STC) + \left(\frac{\partial \eta}{\partial T}\right)_{STC} (T_M - 25°C). \tag{4.25}$$

But for the panel these are given. It can be seen in Figure 1.2a, that a slight difference in the increase in I_{sc} is outweighed by the decrease in V_{oc}, and so the reduction in efficiency, this can be seen in Figure J.1b. At last the temperature is influenced by forced conventional heat. Which can be calculated with the Re number and v_{air} as well as the radiative heat loss. Both in NOCT and based on Appendix A.

For the panel investigated in this study, the DMECGDM 405M10-54HBBB/-V(405 Wp) is used. [**dmecg**] The efficiency of the this cell 20.91 %, and its temperature dependent coefficients are:

Table 4.2: Temperature coefficients for PV module parameters.

Temperature Coefficients	
Temperature coefficient I_{SC}	$+0.0448\%/°C$
Temperature coefficient V_{OC}	$-0.246\%/°C$
Temperature coefficient P_{MAX}	$-0.330\%/°C$

4.5.5. System sizing

For Coolworld Waalwijk needs a coverage of 70 % is considered. For this, simplified losses for transportation are taken into account, and the load mentioned above. Ultimately with the above-mentioned efficiencies and irradiance the yearly power generated per panel can be defined and a sizing can be done (N_{PV}) using the formula presented below:

$$N_{PV} = \frac{\text{TEDCW} \cdot C \cdot \text{SF}}{100 \cdot P_{annual} \cdot \eta_{MPP} \cdot \eta_{aux} \cdot \eta_{inv}} \tag{4.26}$$

Definitions:

- TEDCW: Total Energy Demand CW in kWh
- C: coverage = 70 %
- SF: Sizing factor: 1.05, for losses due to mis-alignments.
- P_{annual}: Annual energy yield of the panel

- η_{el}: Electrical Efficiency at Maximum Power Point: 99.8 %
- η_{aux}: Efficiency of auxiliary components: 97 %
- η_{inv}: Conversion efficiency of the inverter: 95.6%

Validation: Dutch PV Portal 3.0

The Dutch PV Portal is a publicly accessible resource developed to offer insights into solar energy in the Netherlands, built by colleagues from the PVMD department at the TU Delft and coupled with weather data of the KNMI. A PV system design is used, as comparison to the built model.

4.5.6. Solar thermal collector

For the solar thermal part of this study basics from the book of Smets, Jäger, et al. [3] are used for overall approaches, definitions and calculations as mentioned in section 4.3. Accompanied with these and the actual solar heat production, described in Equation 4.27, the actual production is calculated, and a corresponding number of panels is determined.

$$\dot{Q} = m \cdot C_p \cdot (T_{out} - T_{in}) \tag{4.27}$$

Where Q is the amount of heat absorbed, m the body's mass (flow), and C_p the heat capacity. At last are T_{in} and T_{out} temperature differences between the in and outlet temperature of the collector.

Validation: nPro

The validation of the calculation is made with a calculation tool that is developed by nPro. This is calibrated to the Solar Collector Energy Output Calculator (ScenoCalc) from Solar Keymark, which is responsible for certificates for solar collector systems in Europe. nPro is an online tool an accessible for free for academic use. It supports comprehensive evaluations of solar collector performance under various conditions. It facilitates the comparison of different solar collectors, independent of the testing method used—whether Steady State or Quasi Dynamic as specified in EN 12975, which will be further defined below.

4.5.7. PVT system

A PVT system can be built in different setup possibilities, which can be found in subsection J.2.3. The panel for this study is the unglazed panel of Alius, also called a Wind, Infrared and Sensitive Collector.

The Volthera EVO, which in more detail can be found in section 4.6. Integrating photovoltaic (PV) systems with thermal collectors impacts the temperature of fluid in the collector which results in a difference in electrical efficiency. Additionally, the extra PV layer increases reflection losses, which results in a lower thermal efficiency. So, the electrical generation is influencing the thermal efficiency and the other way around. So a combination of the above mentioned η_{th} and η_{el} is used.
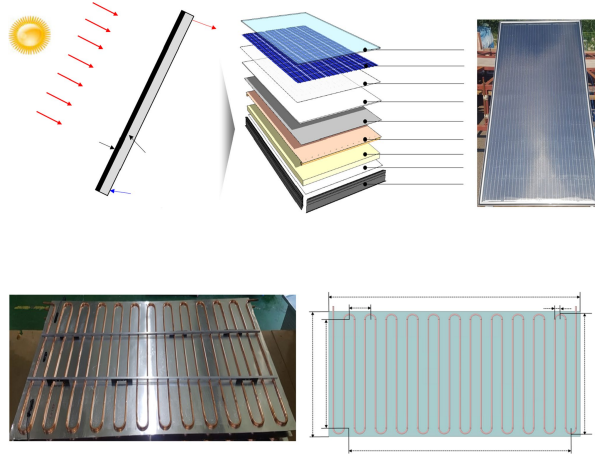

Figure 4.4: A schematic drawing of a PVT module with an insulated back surface (source: [3])

two equations, 4.28 and 4.29

$$\eta_{\text{el}} \equiv \frac{V_{\text{MPP}} \cdot I_{\text{MPP}}}{G \cdot A_{\text{PV}}} \tag{4.28}$$

$$\eta_{\text{th}} \equiv \frac{\dot{m} \cdot c_p \cdot (T_{\text{out}} - T_{\text{in}})}{G \cdot A_{\text{PV}}} \tag{4.29}$$

The electrical efficiency of a PV panel ca be calculated with the following equation:

$$\eta_c = \eta_o \left[1 - \beta(T_c - 25)\right] \tag{4.30}$$

in with β is based on the panels characteristics, which differ for their materials. they are the temperature coefficients as stated in Table J.1. With β:

$$\beta = \frac{\gamma}{100} \tag{4.31}$$

Since this PVT model consists of 2 standalone systems, it is assumed that there is no transmissivity through the PV panel, considering it having all layers and an back reflector.
But the setup as above comes with complications that influence the efficiencies. Therefor some assumptions/ complications are named such as:

- A PV laminate is not as homogeneous as thermal collector, it consists of PV cells, top grid and spacing between cells (τ_a as transmisivity.
- Mixing in the tubes bending parts can lead to additional heat resistance, therefore the serpentine like tubes is assumed straight.

τ_a is suggested to be 0.74 after testing in [12]. This is done since for example the top grid reflects sunlight which does not reflect back the cell in. τ_a Can be calculated with,

$$\tau_a = (1 - refl.) * (1 - \eta_{el}); \tag{4.32}$$

In which $refl$ is the reflectivity of the PV panel Thermal efficiency is calculated from the effective transmission-absorption factor $\tau_{a,eff}$, as can be found below:

$$\tau_{a,eff} = \tau_a - \tau \cdot \eta_{el} \tag{4.33}$$

Next the thermal efficiency is defined as:

$$\eta_{\text{th}} = \frac{P}{GA} = F_R(\tau_a - \tau_{\eta_e}) - F_R U_{\text{loss}} T_{\text{red}} \tag{4.34}$$

In this is F_R the removal factor, and U_{loss} the heat loss coefficient of the panel and T_{red} is:

$$T_{\text{red}} = \frac{(T_{\text{in}} - T_a)}{G} \tag{4.35}$$

4.6. Validation: PVT Test

Dedicated system sizing tools in providing information for PVT systems are limited. Therefore a validation is made, with a real testing setup. This setup is formerly used in TUV tests, and donated by Alius Volthera, a PVT manufacturer from Eersel, The Netherlands.

4.6.1. Test methods; based on ISO9806-2017

The setup aimed to investigate the influence of cold temperature liquid on the efficiency of the PV panels and in comparing the energy and heat production that is claimed possible with the numerical model. Assisted to the insights garnered from the MATLAB model, the experimental setup was built to replicate real-world conditions accurately, as well as, predict what the actual energy revenue could be when scaling up this small set to a bigger version, to possibly implement at Coolworld Waalwijk. While temperature and flow control is integrated, the irradiance level is based on solar input from an extra PV panel, that figures as a calibration model, since the test setup is built at Coolworld Waalwijk.

4.6.2. Guide to Standard ISO 9806:2017

The "Guide to Standard ISO 9806:2017" serves as a resource for manufacturers, testing laboratories (Steady State Testing SST), certification bodies, and regulatory agencies involved in the evaluation of solar thermal collectors, including PVT panels for thermal performance determination. This guide is used as information for testing, but it has not been fully applied since the testing conditions and instruments were based on current components as well as environmental conditions which could not be manipulated as in specific testing laboratories. The testing is done in Quasi Dynamic Testing (QDT) testing environment. Therefore an official certification is not applied to the results, but the underlying background is considered as a baseline for methods.

A strategy can be found in Appendix P which describes the different approaches between a SST and QDT procedure. Together with this are the Standard Reporting Conditions (SRC) that are used.

4.6.3. Solar energy - Solar thermal collectors - Test methods (ISO 9806:2017

In the actual ISO for testing solar thermal collectors, the "Collectors co-generating thermal and electrical power" is the PVT that is used in this study. Other test such as internal pressure and statgantion temperature are described in this, but only thermal performances test will be test, with conditions and its effects on efficiency, involving the cooling of the internal water circuit to below $0°$C and monitoring the effects of cyclic temperature changes.

4.7. PVT Test setup: Thermal performance, based on ISO9806-2017

The assessment of heat and electrical power delivered by the PVT panels is based on the ISO9806-2017 report. At least 1 m^2 of unit area should be considered. In this test three panels and an additional calibration panel are used.

4.7.1. Mounting and location

As specified by the manufacturer the panels are placed 2.5m above the ground (Figure 4.5), not nearby buildings (reflected radiation), or machines (thermal radiation), with as much air flow as possible. The Sunbeam Nova gives the model a 12 °angle. Thermal reflection is minimised by placing them further away form the test facility or any other objects. Air can freely move around it.The positioning can be found in Figure 2.2.

(a) Positioning on a lunch spot, at 2.5m above the ground.

(b) Topview of the thermal collectors installed, the Alius EVO

(c) Topview of the PV panels installed. top left is panel 1, front, 2, top right 3 and top middle 4.

Figure 4.5: Pictures of the PVT panels installation spot.

4.7.2. Instrumentation

Instead of solar radiation measurements such as pyranometers a calibration panel as the standard zero-measurement is used. Thermal radiation from long ware irradiance is also not in the scope of this study and therefor not included.

Temperature

For temperature the inlet and outlet (probe, out of direct sunlight) of the fluid and the ambient temperature (climate data) is measured. For the three panels, the $PV1_{in}$, $PV2_{in}$, $PV3_{in}$ and $PV3_{out}$ are positioned. Besides this additional temperature measurements are be done, to provide information on the PV panel temperature part. The temperature on the backside of the panel and ambient are measured with the Testo922 and 410-1, as displayed in below's Figure 4.6. All other sensors can be found in subsection F.0.1.

(a) Testo 922 temperature probe for temperature

(b) Testo 922 temperature probe for temperature

**(c)** Testo 410-1 temperature probe for temperature

Figure 4.6: Testo measurement tools.

Flow and airspeed

For the flow rate inside the piping the flow meter from Endress % Hauser is used, as described in subsection F.0.1. Flow is 0.291833333 kg/s, with small adjustments at times. Furthermore is the Testo 410, is used for checking climate data ambient air wind speeds and T_a. The fluid inside this cycle is the same as in vessel BV06, which is continuously filtered and can be adjusted with valves. Flow rate is suggested (by the manufacturer) to be close to the region between laminar and turbulent flow. In *ISO9806-2017* can be read that this could lead to instability of the internal heat transfer coefficient, and that therefore it may be necessary to raise the flow rate.

4.7.3. Test setup

A schematic overview of the testing setup is made in Figure 4.7a and Figure 4.7b. A heat exchangers including a three way valve to give the possibility to preheat the liquid is attached in the system to be able to control liquid temperature towards the test setup.
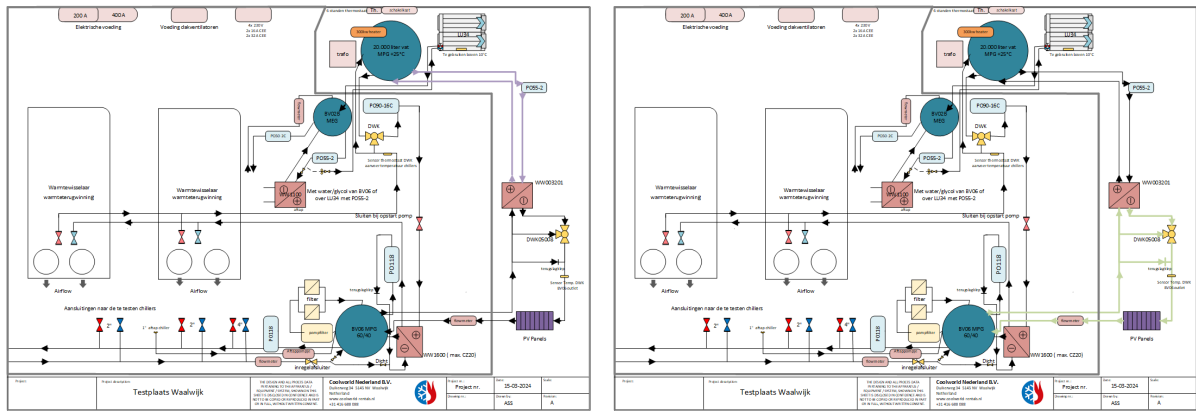
(a) Warm water circuit to preheat cold liquid before the PVT system

(b) Cold water circuit directly attached to the cold liquid vessel BV06

Figure 4.7: Both circuits within the PVT test setup

The new circuits that have been placed are as follows, see Table 4.3

Name (Coolworld)	Color	Description
CC08	Lilac	The heating water-glycol (MPG +25 °C) circuit, from the BV20 vessel for PVT
CC09	Light Green	The cold water-glycol filter (MPG until -10 °C) circuit, from the BV06

Table 4.3: Names of circuits in the setup of the testing facility

Test characteristics: ISO9806

The characteristics, for QDT testing (Appendix N) are:

- Hemispherical solar irradiance, PV4 Panel calibrated
- Diffuse solar irradiance (PV4 Panel), based on GHI
- Angle of incidence, tilted 12 °

- Air speed (climate data)
- T_a
- T_{in}
- T_{out}
- Flow rate of the heat transfer fluid

PV Panel

The researched PV panel is **DMEGC DM405M10-54HBB/-V**.[38] Details can be found in subsection 4.5.4. The inverter is the Hoymiles HM 2000, with DTU modem.[39]

4.7.4. Thermal collector

The thermal collector is the Alius Volthera EVO. Thermal performances were unknown, but TüV testing reports provided. In between the are rubber hoses used, with low conductivity ($\lambda = 0.29\ (W/m.K)$ [40], that withstand temperatures between -20 and +80 °C.

4.7.5. Thermal performance collector: ISO9806

The thermal performance of the collector is the main characteristic of the panel. No direct thermal efficiency is provided by the manufacturer Alius. Though, the thermal performance testing reports are shared, as can be found in Appendix O. Tests are done by the TüV Rheinland, named: *Test report: DE23HT1U 001; Volthera EVO + DM405M10-54HBB + Sunbeam Portrait*, [41]. With this an approach is made in different circumstances.

4.7.6. Thermal efficiency profile

The thermal efficiency will be defined in graph as function of the reduced temperature. This is done to built a lineair relation. [12], as stated in

Different on this equation, is that the efficiency is determined by the relation to GHI. Itis also tried to define it with the electrical power of the calibration panel PV4 over its electric efficiency, since effective radiation is unknown.

4.7.7. PVT Panel system

The PVT panel used in this research is that of Alius Volthera, not many dimensions are defined. The datasheet concerning the panel can be found in Appendix L.

4.7.8. Test procedure

For this test, the rest cold effects to both the thermal and electrical efficiency are tested. Besides, freezing of the panels will be tested, and therefore in humid weather with different flows and inlet temperatures.

4.8. Levelised Cost of Electricty

More specific is the Levelised Cost of Electricity (LCoE) [42], which can become very complex in defining the cost per kWh of electricity produced by a power generation plant. Equation 4.36 shows a simplified version.

$$LCOE = \frac{\sum_{t=1}^{n} \frac{I_t + M_t + F_t}{(1+r)^t}}{\sum_{t=1}^{n} \frac{E_t}{(1+r)^t}}.$$

(4.36)

The calculation of the LCoE accounts for all expenses and yields throughout the system's projected lifetime, labelled as n years. Each year t contributes to this cumulative assessment, with I_t signifying that year's investment costs, M_t denoting operational and maintenance costs for that year, and F_t, which is negligible for PV, but not for PVT and Solar Thermal systems (due to electrical pumps), representing fuel costs. The term E_t quantifies the annual electrical output. At last, r serves as the discount rate, which defines a factor to discount future costs, enabling the expression of future financial obligations in today's monetary terms. For simplicity purposes only all energy generated is used in kWh, and a Levelised Cost of Heat (LCoH) is not considered. Finally the LCoE for the three options must be compared to that of conventional energy resources to see if an investment is realistic.

$$LCoE_{PV/Collector/PVT} \leq LCoE_{conventional}$$

(4.37)

4.9. Conclusion

Part of the results of this chapter's objectives is carried out in section 1.3, namely the study conducted on reusing rest cold. Besides, the high energy demand as stated in the former chapter and chapter 1, is the baseline in defining a more sustainable alternative to buying this from the grid. A research study is done on different solar system types to cover part of the demanded energy load, which is partly heat demand. In this methodology, a numerical model is compiled which determines the possible energy generation for a stand-alone PV, solar collector and PVT system, in order to cover the high energy demand at Coolworld Waalwijk. A comparison will be made with the outcome, based on the load pattern throughout the year. A validation on each of these outcomes is done by the use of a secondary calculation model, and with an experimental test setup which is connected to Coolworld Waalwijk's testing facility with rest cold.

# Analyses of a PV/Thermal system, with Coolworld as a case study

The results in this chapter elaborate on the used parameters and corresponding outcomes, which refers to the methods used in the former chapter. Firstly, a load and possible generation can be found in section 5.1. For each of the numerical models the outcome with these conditions throughout the year can be found in section 5.2 for PV, section 5.3 for solar collectors and section 5.4 for the PVT model. For each system, a system size is created, based on the corresponding energy/ heat demand, and validated. Concluding with an economic feasibility comparison.

## 5.1. Numerical model: PVT, PV and thermal collector outcome

A PV, solar collector and PVT-type system will be used in defining the system sizing for the energy consumption of Coolworld Waalwijk. To do so, the first paragraph describes Coolworld's load.

5.1.1. Load analysis

For Coolworld Waalwijk a load profile has been constructed in MATLAB from the data that was collected from Fudura ™, this can be found below in hours (Figure 5.1a) and months (Figure 5.1b)
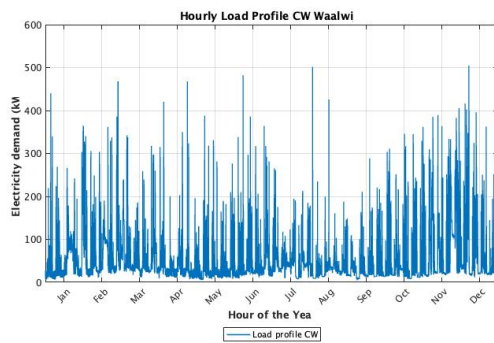
(a) Load profile Coolworld Waalwijk per hour
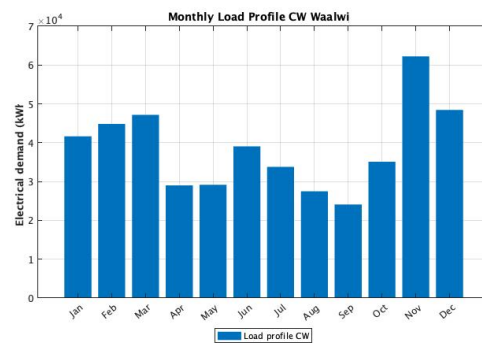
(b) Load profile Coolworld Waalwijk per month

Figure 5.1: Load profile Coolworld Waalwijk per hour and month

From this, an approach to the heat load is determined. based on the heat consumption in subsection 3.4.2. Since the heat demand at Coolworld Waalwijk is not constant, a different heat load is made. Firstly the baseload, energy consumption per day, (checked with days of zero testing 752 kWh) see section 3.7 is extracted from the total energy consumption. Then the average does not include days without testing. Based on this a load profile of 40% of the new total energy profile is made, which is

calculated to be around 28.79%, which is the actual energy consumption of the heater in the vessel from subsection 3.4.2. As can be seen in Figure 5.2a and Figure 5.2b
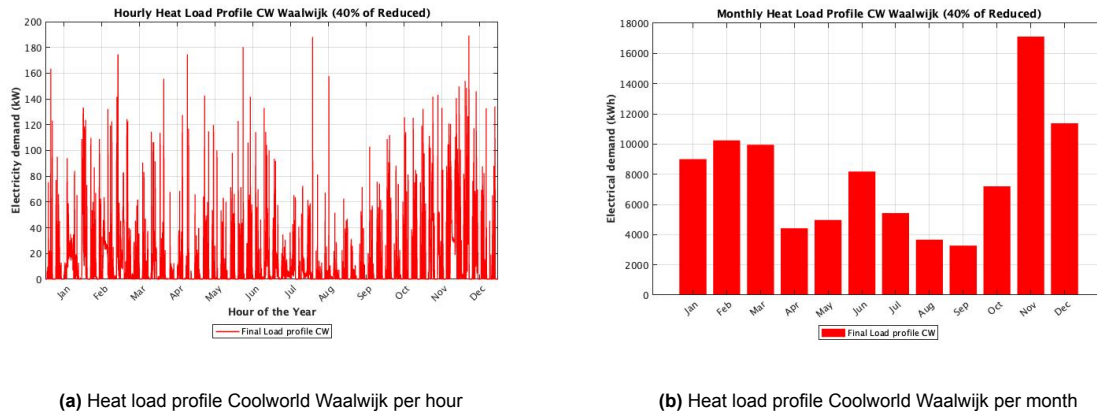

(a) Heat load profile Coolworld Waalwijk per hour

(b) Heat load profile Coolworld Waalwijk per month

Figure 5.2: Heat load profile Coolworld Waalwijk per hour and month

With this load (94.52 MWh) a system for solar thermal and PVT will be built. It s visible that the energy consumption is much higher in winter periods, this is due to two reasons: First, there is more demand in winter, due to demand for cooling ice rinks, and second, in summer more energy can be extracted from the ambient temperature, in the current testing setup, besides, as shown in section 3.5, more energy is lost in the testing facility during winter.

5.1.2. Solar irradiance

A distinction is made between a South and East-West irradiance per year setup. In the Sky View Factor determination is shown that the optimal would be between the range of 21 to 52 °, visible in Figure 5.3b. This is in line with the mounting position of panels in the Netherlands which is around 36°, [3], and this can give an extra efficiency of around 4-5 %. Besides, with the help of the exercise mentioned in subsection 4.5.4, in defining this radiation, for both the South and East-West (EW) an irradiation profile is sketched. This can be seen in Figure 5.3a
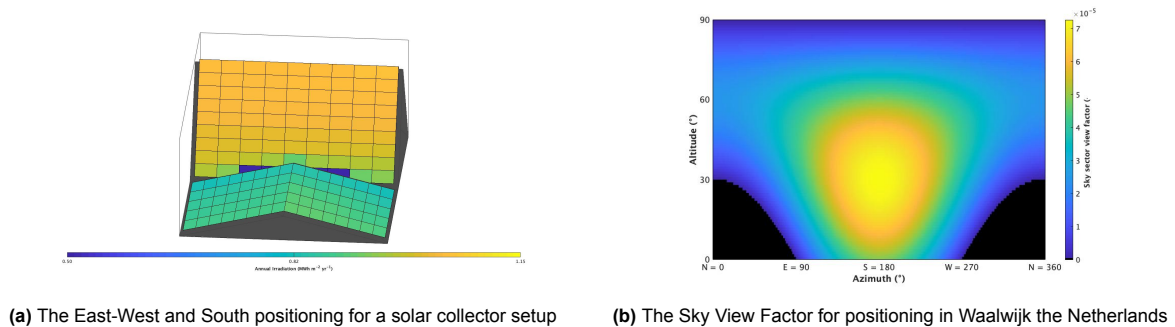

(a) The East-West and South positioning for a solar collector setup

(b) The Sky View Factor for positioning in Waalwijk the Netherlands

Figure 5.3: Annual irradiation and Sky View Factor

Irradiation for EW is smaller than for the southern directed panels. Then a more stable energy generation throughout the day can be achieved. But since Coolworld Waalwijk practises during working hours in the 'middle' of the day, a southern direction would be more convenient. Further calculations are therefore decided to be with a southern direction. Differences between portrait and landscape are neglectable. For both in a 30 °angle, the irradiation per month and day were calculated as can be seen in Figure 5.4a and Figure 5.4b
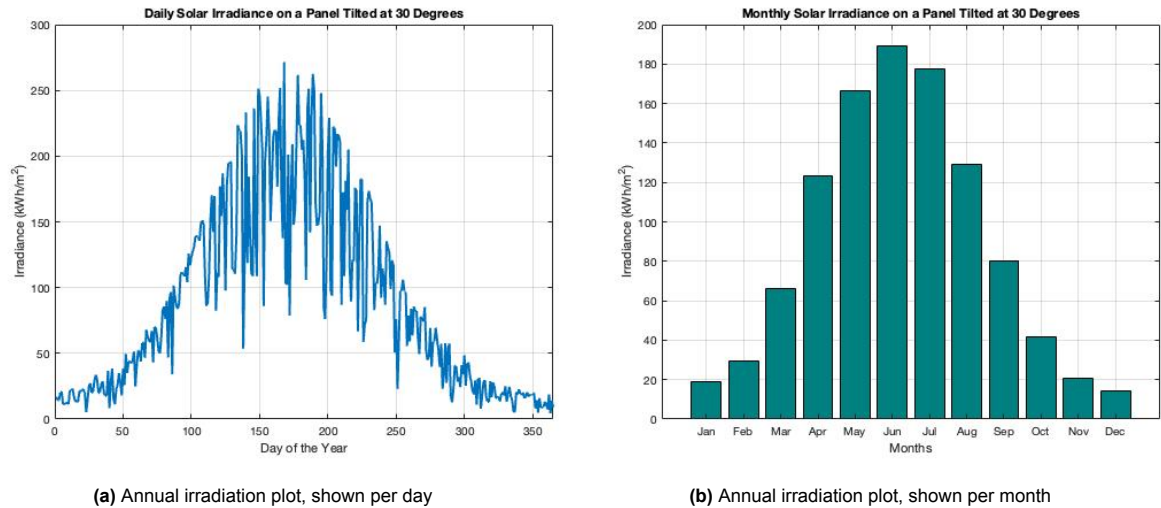
(a) Annual irradiation plot, shown per day

(b) Annual irradiation plot, shown per month

Figure 5.4: Annual irradiation plot for both a month and per day

5.2. Option 1: PV system

In the model, a temperature calculation for the PV panel (T_{module}) is integrated. With this, it is possible to calculate the temperature throughout the day based on the solar irradiance. This is done for a south-facing module. The results are shown in Figure 5.5a, based on the ambient temperature, and heat development in the PV panels with seasonal variation. In Figure 5.5b, the monthly average temperatures are displayed, but these include night measurements as well. To check whether the calculations seem correct, a distinction is made between total averaged temperatures in blue, and temperatures between 10am and 4pm (green) and 11am and 2 pm (brown). Later named temperature profiles are higher, which corresponds to higher temperatures during these hours so the calculation of the temperatures seems accurate.
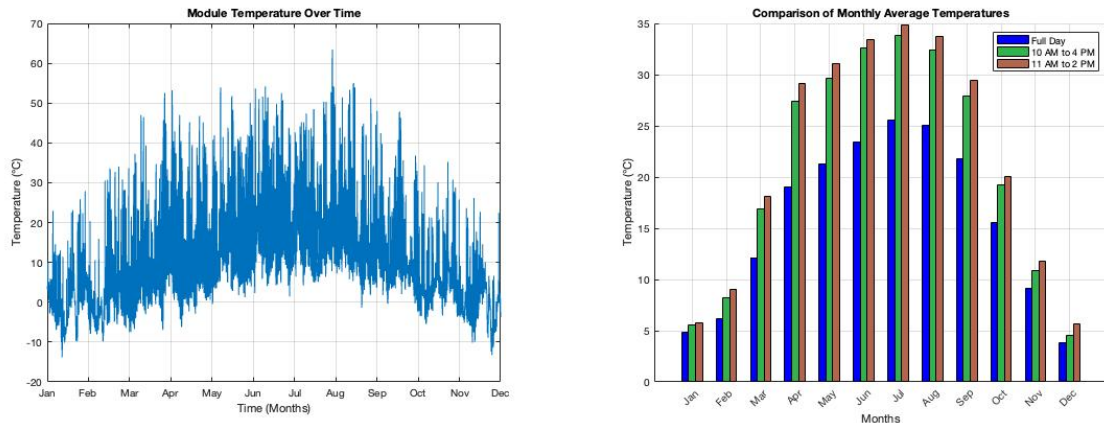
(a) Temperature profile for the module, which shows low temperatures during summer as well, during the night.

(b) The T_{module} for solar panels between 11am and 2pm, 10am and 4pm and the average for the whole day shown per month.

Figure 5.5: Annual T_{module} specified per hour and with monthly averages distinguished for different moments during the day

It can be seen that the average temperatures are not extremely high, which is due to the mild climate in Waalwijk.

5.2.1. System sizing

With this, a total energy yield of 374.3 kWh per year per panel is calculated. With 70 % coverage of the load, an mppt efficiency of 99.8 %, inverter efficiency of 95.6%, [43], other auxiliary efficiencies of 97 % and a sizing factor (SF) of 1.05, a total of 955 panels is needed. For this, a system is built with 28

SolarEdge 40K inverters, each having 97 panels per string. With this a DC and AC yield, with suggested power cable lengths, and a Real Power output could be determined, shown in the Figure 5.6a below, with the monthly grid exchanged energy between Coolworld and the grid in Figure 5.6b.
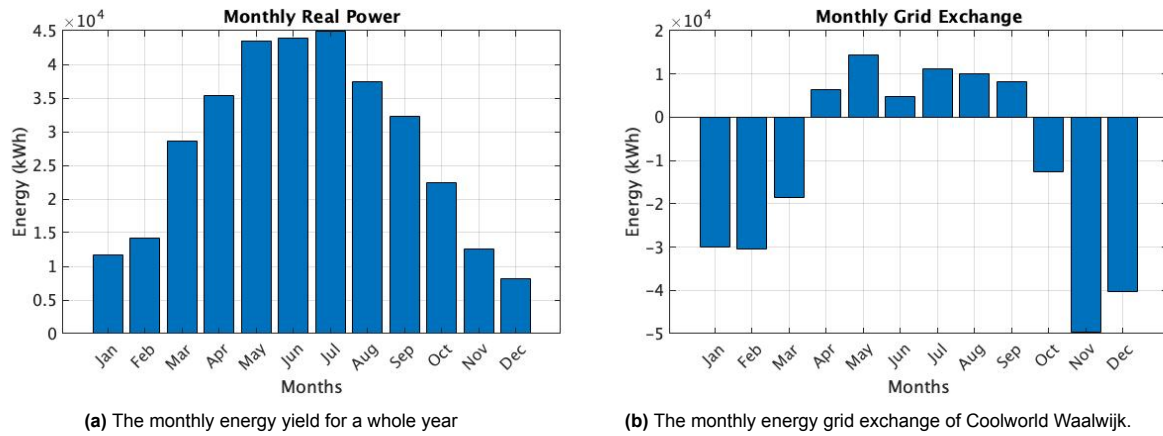

(a) The monthly energy yield for a whole year

(b) The monthly energy grid exchange of Coolworld Waalwijk.

Figure 5.6: The real power produced by the PV panels, and extracted from the load as grid exchange

With this system a total energy output of 339.1 MWh is possible to produce on yearly basis including cable, mismatch and other losses. This is a bit over-designed considering that this is 72.6 % of the energy demand. There is overproduction in summer, due to the lower energy demand, but higher energy generation, and not enough production in winter to cover demand, as can both be seen in Figure 5.6b

5.2.2. Validation: Dutch PV Portal 3.0
A validation of the calculation is made by using the Dutch Solar Portal, based on 1.63 m^2 panels with an output of 327 Wp and efficiency of 20% a number of 975 panels is calculated for the same 70 % coverage of the total load. This does differ 14%, although it must be said that the numerical design is slightly over-designed. It is unknown if the validation tool includes thermal influences on the panels.

5.3. Option 2: Solar thermal collector
For the solar thermal collector calculation, the Maxi collector from the manufacturer HR Solar (also producer of PVT panels) is used. [44] The potential heat yield per year with solar irradiation is 749.4 kWh/ m^2. Then for one panel, the heat yield is 1875 kWh, sizing of 2.507 m^2. This is based on a thermal efficiency of 67 %. The total heat load is defined as 94.52 MWh (section 5.1). This suggests a total number of 51 collectors, but since demand and generation are not aligned during the whole year this is not suggested correctly.

Next, the thermal efficiency is tried to approach with cold fluid inlet to the system. An estimation of the T_{in} is tried to make. When taking Coolworld Waalwijk's heat demand from subsection 5.1.1, this heat is needed for the cooling process consistency, so every kWh in this is $\pm$ one kWh in produced cold. With this a ΔT profile can be sketched, assuming more heat is needed than cold produced and a constant flow ($\dot{m}$ of 0.296 kg/s, Cp = 3.72 kJ/kg.K is used). Then a reduced temperature profile T_{active} is sketched (Figure 5.7a. Since the flow is much higher (17 l/min in the collector, versus 90 l/min in the cooling circuit) in the cooling circuit, and with losses accumulated (30 %), the actual profile is $\Delta T * \frac{17}{90} * 0.7$. This profile is considered usable since losses occur during transportation in the collector's circuit. The max T_{active} is -23.05 °C. The average cooling temperature (only during working hours) is than $\pm$ 3.68 °C, but, this is without a warming circuit in between and when 6 out of 24 hours of testing per day. The assumed inlet temperature profile is then made with $T_{in} = T_a - T_{active}$, shown in Figure 5.7b:
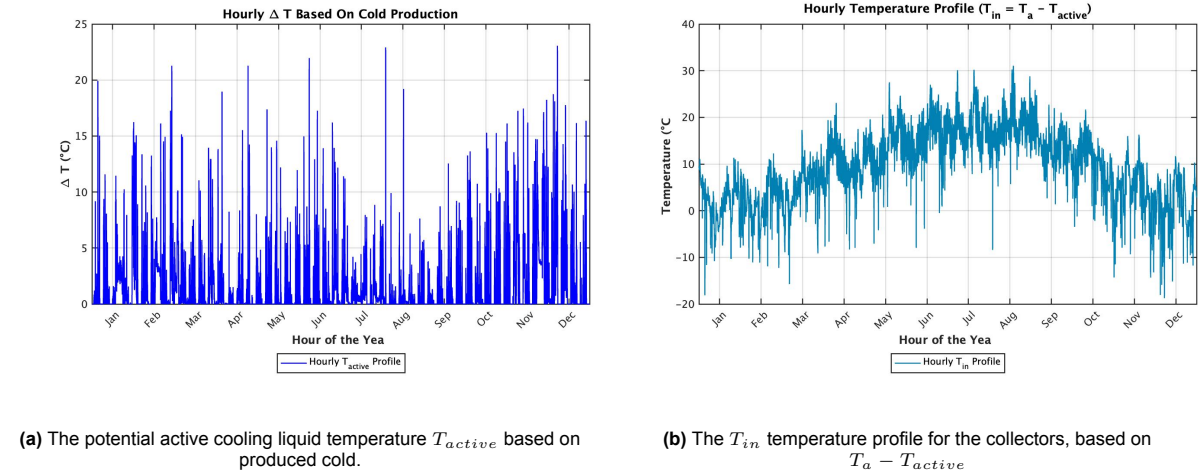
(a) The potential active cooling liquid temperature T_{active} based on produced cold.

(b) The T_{in} temperature profile for the collectors, based on $T_a - T_{active}$

Figure 5.7: The real power produced by the PV panels, and extracted from the load as grid exchange

Next, the outlet temperature will be determined for the panel, with which a T_{mean} can be generated. This is on average 10.02 °C, which is lowe than the average T_a of 13.7 °C. With the modules characteristic parameters for energy loss, an approach can be made for the actual losses in it and corresponding thermal win. Based on the Equation 4.6. Which gives an extra yield of 119 kWh per panel and efficiency of 9.4 %.

5.3.1. System sizing

75 Panels produce too much heat in summer, as displayed in Figure 5.8a.A maximum over production of 25 % is incorporated, which occurs in Augustus (23.3 %,) as can be seen in Figure 5.8b. A total of 28 solar collectors is a good fit, which covers a total heat yield of, 35.24 MWh. When incorporating the extra yield due to cold liquid application, 18 panels is enough to cover 35.7 MWh yield, which saves the installation of 2 solar collectors. So another 58.82 MWh for heat demand is needed from another source and in the winter months a different solution is necessary. Besides an extra PV system is needed of 806 panels and corresponding 9 inverters to cover the set 70% load coverage.
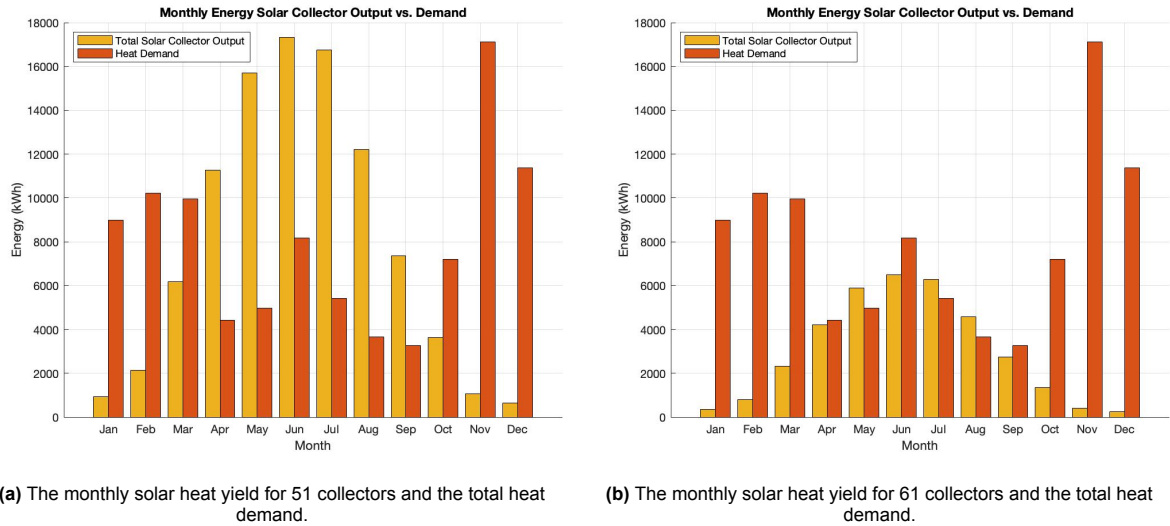

(a) The monthly solar heat yield for 51 collectors and the total heat demand.

(b) The monthly solar heat yield for 61 collectors and the total heat demand.

Figure 5.8: The monthly solar heat generation and demand for Coolworld Waalwijk.

Storage

For storage, the daily average $Q_{consumption}$ is 259 kWh and Q_{loss} for a tank is 4.502 kWh (per day, 100mm insulation, from subsection 3.4.2). This makes 264.16 kWh on average. Considering 10 °C as ΔT, which means that until 15 °the glycol can be used starting at 25, the storage size of 24.4 m³ is

needed. The current vessel allows a storage of 25 m^3 which is still enough. Warmer temperatures can be achieved, when functioning as a thermal battery.

5.3.2. Validation: nPro

The validation tool defines an energy yield of 726 kWh/m^2, which is close tot the 749.4 kWh as calculated. This is when considering a T_{mean} of 30 °C. With this a capacity of 56.8 (57) collectors is suggested to cover 35.9 MWh of the demand, which is also very much in line with the suggested amount of 28 collectors as calculated considering their size (2.507m^2 for the Maxi panel from HR Energy over 1.63m^2 from the tool)

5.4. Option 3: PVT system

Based on the abovementioned models for both a solar collector and a PV system, with the absorption factor and the electrical efficiency of the PV panel (20.81 %) a PVT panel design can be used for calculating the amount of panels needed. Considering the transmittance τ_a of PV being 0.74, as tested by Zondag et al. [13], the transmissivity τ of glass cover being 92 %, the effective absorption factors, incorporating the electrical efficiency, gives the $\tau_{a,eff}$ is 0.547. This gives a reflectivity loss of 0.0644 respectively with a new PV efficiency of 14.5 %. With the 67 % thermal efficiency conversion from section 5.3. With this the new calculations are made. Firstly the amount of panels needed to tackle the heat demand is calculated, since over generation would be of no interest. The thermal load from subsection 5.1.1 is used (94.52 MWh) and the new thermal energy yield is 60.6 kWh/ m^2, which suggests the installation of 51 panels, this gives the energy profiles of Figure 5.9a

(a) The total heat demand, and thermal and electrical yield of a PVT setup.

(b) A new sketched electrical demand in blue and heat demand in purple, after extracting the PVT generated energy
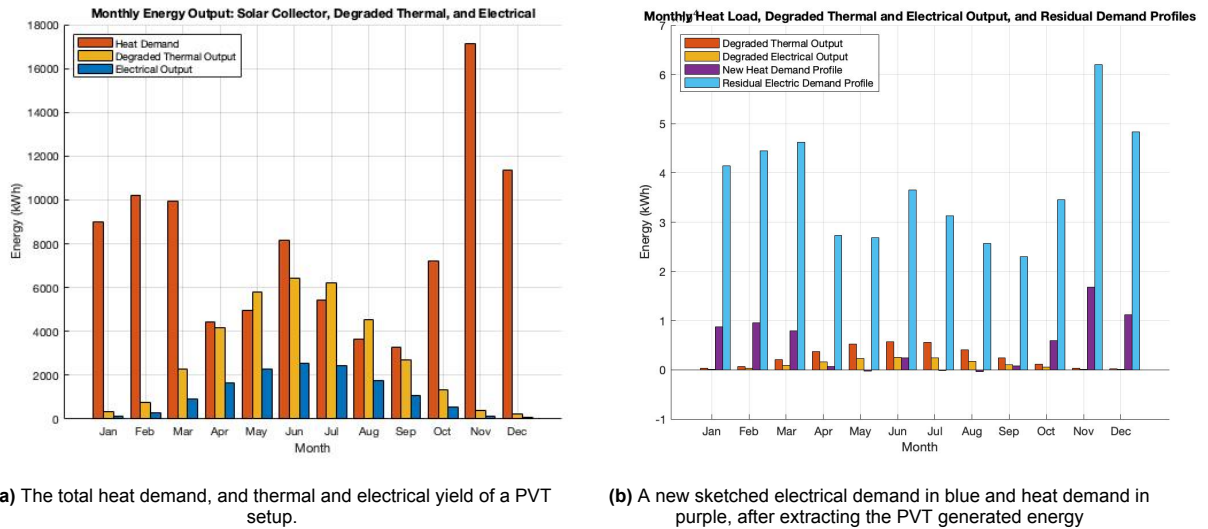
Figure 5.9: The PVT generated energy, and the energy extracted from both the het and Electrical load

Then, when extracting the heat generated by the solar collectors (35.22 MWh) from the heat demand, and incorporating the electric yield of the corresponding PV panels (13.31 MWh) integrated in the PVT panels, with their new efficiency, a PV system can be designed for the residual load, of which a 70 % coverage will be considered. The new load profile and the corresponding PV generation for it are visible in Figure 5.9b. The calculation led to another 827 PV panels being installed.

5.5. PVT Test setup

To compare the tests done, a calibration for the electrical energy yield is needed. For thermal efficiency this can only be done in between panels, or based on the reports share information on their efficiency exist of this panel,

5.5.1. Electrical performance PV panel

One PV panel is used as a calibration panel, since no pyranometer (to measure irradiance) is available. The total averaged differences in power generation between the panels and the zero measurement panel PV4 are:

- P_{PV1} compared to P_{PV4} is: +0.3379
- P_{PV2} compared to P_{PV4} is: +1.517
- P_{PV4} compared to P_{PV4} is: -0.2909

With this, efficiency provisions with active cooling panels can be made. From the above-mentioned numbers, a percentage is taken during the day, since these numbers are measured at highest irradiation point. Therefore between 09:00 and 17:00 a calibration curve is made, with its peak at 13:00, so that a valid difference for each time during the day could be made. Now, electrical efficiencies could be defined between the panels. Since efficiencies for PV panel 1, 2 and 3 can be considered relatively similar, only for panel 1, (with the coldest liquid inlet) efficiency is showcased. The efficiency for P_{PV1} is calculated with:

$$\Delta\eta_{PV1} = \frac{P_{PV1} - P_{PV4} - \Delta\text{Calibration}}{P_{PV4}} \tag{5.1}$$

for $PV2$ this is the same, and for $PV3$ the calibration will be added to the difference, since this is negative. The second plot of the following test days showcases the electrical efficiency gain/ loss ($\Delta\eta_{PV1}$) in blue and total energy generation P_{out} per quarter.

## 5.5.2. Thermal performance collector: ISO9806

By examining the calculations and the efficiency changes due to different environmental conditions from Appendix Q, based on the calculations from Appendix O the following can be said:

- With the biggest $\Delta T = T_m - T_a$ of for example 9 °C, the highest efficiency is reached of 55 %
- Per °C significant, 7.22 % difference with 2.4 m/s windspeed and 0.0562 kg/s flow.
- Wind plays a significant role in this transfer
- For windspeed 1.9 m/s and half the ΔT efficiency is just 31.3 %.

Based on this a hypothesis is made, that with even higher $\Delta T = T_m - T_a$ the efficiency can increase further. The thermal heat production (Q_{prod}), is calculated with Equation O.1. Each third plot shows the Q_{prod}. The thermal efficiency can be calculated in multiple ways. One is with the extracted power calculation done with Equation O.2. But, real-time measurements including wind gave big distortions, therefor the simplified version Equation 4.6, including the third term: $-a_3u'(\vartheta_m - \vartheta_a)$ is used.
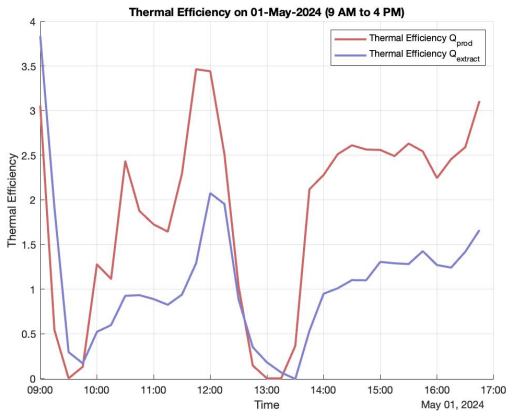
(a) T_{mean} of the flow and $T_{ambient}$
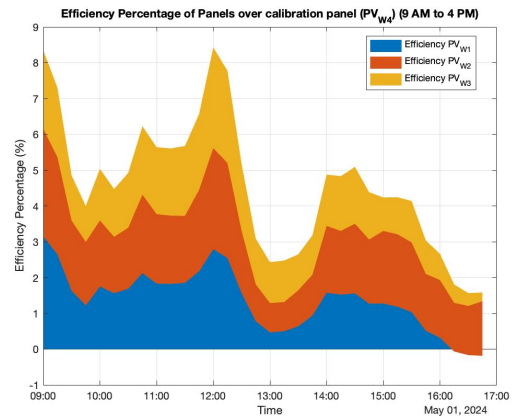
(b) The $\Delta\eta_{el}$ in blue, orange and yellow for PV1, PV2 and PV3 repectively.

Figure 5.10: Measurement comparisons

To check whether the thermal efficiency calculation alligns with one another, both methods are used and they do differ from eachother as Figure 5.10a Shows. This can be related to wind influences. Besides that, a comparison is made for all three panels, to see what their $\Delta \eta_{el}$. In Figure 5.10b it can be seen that efficiency for all the panels is comparable, which indicates a valid calibration, also when propositioned in a different order. It is also visible that temperature changes in the fluid have high variations.

5.5.3. Test procedure

Multiple test days, preferably in hot weather to see differences in energy production more clearly, are done. Also, days with high cold production are likely to be efficient and examined. The T_a ambient temperature was translated from hourly to quarterly climate data and is therefore built as steps as can be seen in the first plot for the following dates, together with the T_{mean} of the first PVT panel. At last, each fourth plot is the thermal efficiency η_{th}, over the reduced temperature T_{red}, which showcases the normalised performance characteristics which make comparison of the testing days easier.

Testing day 1: 11-04

This day cold liquid was also immediately recovered with a sail to the heat exchangers. It was a hazy day, with very low irradiance (124 W on average). However, a prolonged flow of cold was established (T_{mean} = 5.31°C). Average electrical efficiency η_{el} increase for $PV1$ is 0.616%. Figure 5.11a shows the mean temperature (T_{mean}) of the flow in $PV1$ and the ambient temperature in which the obvious cold inlet is visible, the correlation to its peak (lowest temperature) is visible when comparing with the high heat output from Figure 5.12a. Furthermore Figure 5.11b shows the efficiency and actual power generated. The power output was rather low, still higher efficiencies have been found in all three panels. Effectively 0.6 to 0.7 %. At last a η_{th} over reduced temperature $T_{reduced}$ is made, but the outcome is unexpected high, which could be related to high heat generation with the ambient air instead of irradiation, which is more related to windspeeds. The thermal efficiency is also much higher than expected with Equation 4.6.
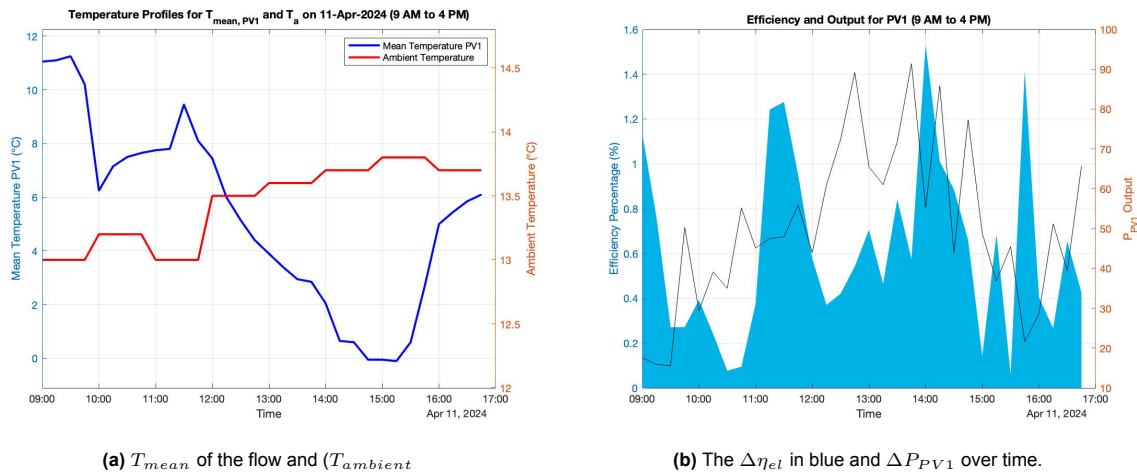

(a) T_{mean} of the flow and ($T_{ambient}$

(b) The $\Delta \eta_{el}$ in blue and ΔP_{PV1} over time.

Figure 5.11: Measurements on 11-04-2024

(a) η_{th}) and heat production Q_{prod}
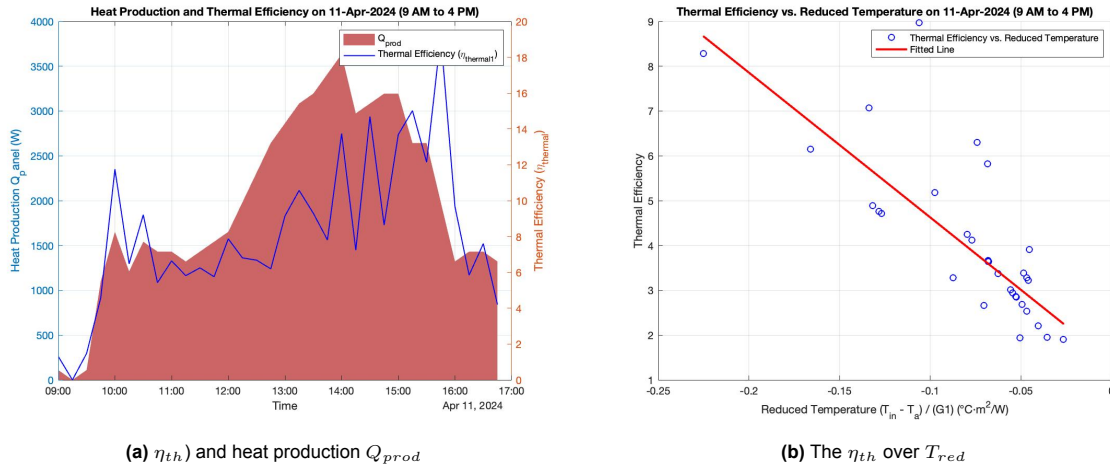

(b) The η_{th} over T_{red}

Figure 5.12: Measurements on 11-04-2024

Testing day 2: 01-05

On this day there was finally, a constant solar irradiation (658 on average), as can be seen in Figure 5.13b. Average electrical efficiency η_{el} is 1.356% for PV1, and 1.763 and 1.389 for PV2 and PV3 respectively. This was also the first day with T_a around 25 °STC. In the second plot, a direct relation is visible, to the PV efficiency increase, correlated to the same form (upside down) for the cold liquid in the collector. Same can be said for Q_{panel} which behaves the same, the exact correlation is also visible in PV2 and PV3 and manual measurements support this. Therefore it can be said that the actual efficiency increase is very much due to the cold application. Also it was measured that the calibrated panel, was on average 10 °C warmer, up to 48.7 °C measured 14:30. When looking at the graph this indicates a ΔT of 10.9 °C and ΔP_{PV1} of 1.53 %, indicating a 0.14 $\frac{\%}{K}$, which is half of the described temperature coefficient from subsection 4.5.4. Beside this, was the flow was adjusted to 8 l/min instead of the normal 17 l/min at 13:00, therefor the sudden drop occurs in the measurements and the rise in temperature from water that stood still in the warm hoses. This lead to heat collection at a certain point. The thermal efficiency shows that with higher flow rate more heat is transfered.
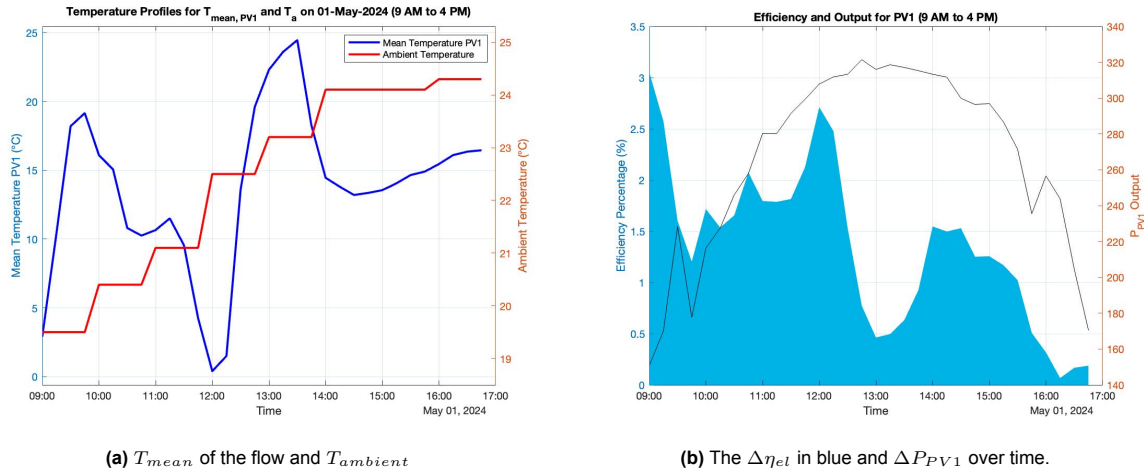

(a) T_{mean} of the flow and $T_{ambient}$

(b) The $\Delta\eta_{el}$ in blue and ΔP_{PV1} over time.

Figure 5.13: Measurements on 01-05-2024

(a) η_{th}) and heat production Q_{prod}
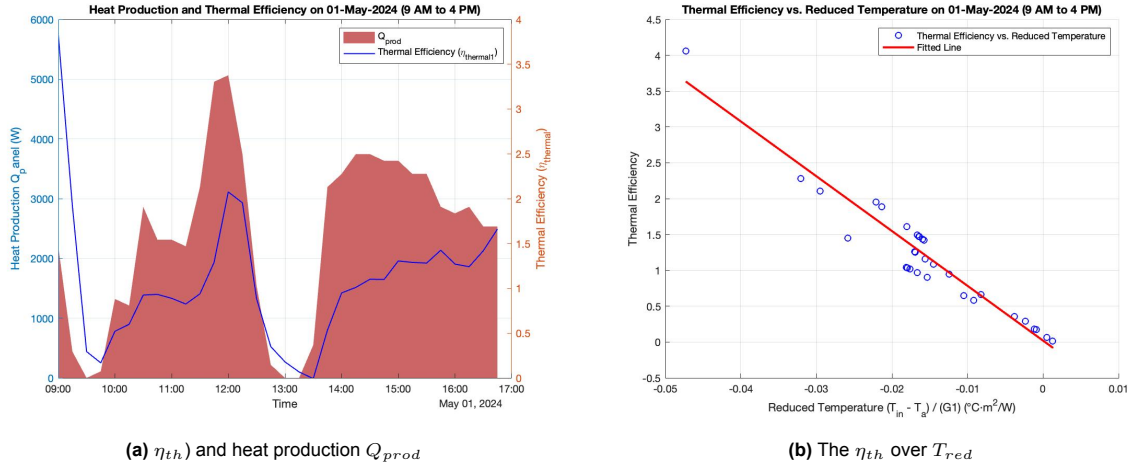

(b) The η_{th} over T_{red}

Figure 5.14: Measurements on 01-05-2024

Testing day 3: 05-05

For comparison, it was decided to also include a day, without applied rest cold. Therefore a day in the weekend is chosen, and with high solar irradiation (569 on average) as can be seen in Figure 5.15b. The average electrical efficiency η_{el} is for PV1 is 0.615% which is much lower compared to a sunny day when cold is applicated. The temperature profile clearly shows that no cold is applied in Figure 5.15a. It should actually be noted that the ambient temperature was lower then the collectors fluid temperature. But, still the fluid temperature increased. This indicates that the panel is higher in temperature, and transfers its heat to the liquid. This did lead to a negative thermal efficiency with low irradiance in the morning, and in the fourth plot it can be seen that the reduced temperature to efficiency indicates this, being a positive number.
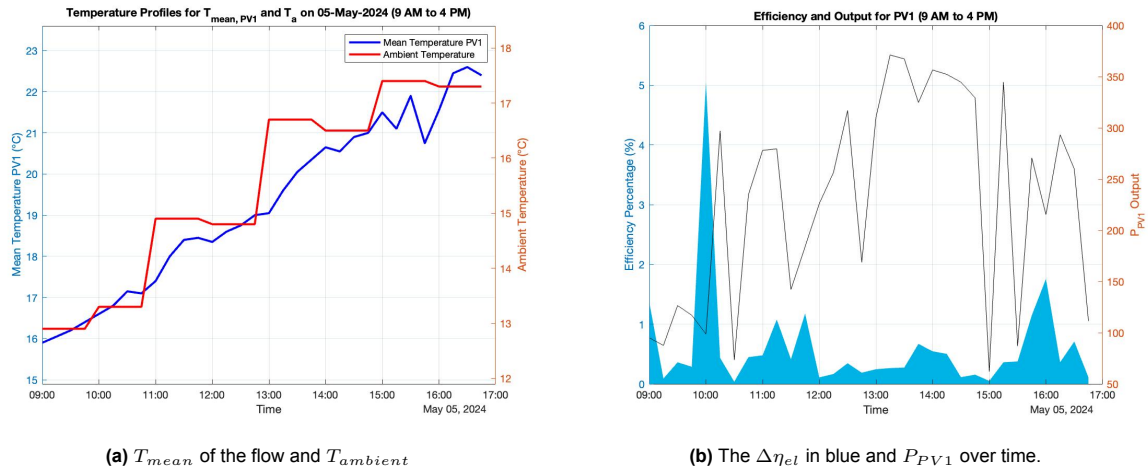

(a) T_{mean} of the flow and $T_{ambient}$

(b) The $\Delta\eta_{el}$ in blue and P_{PV1} over time.

Figure 5.15: Measurements on 05-05-2024

(a) η_{th} and heat production Q_{prod}

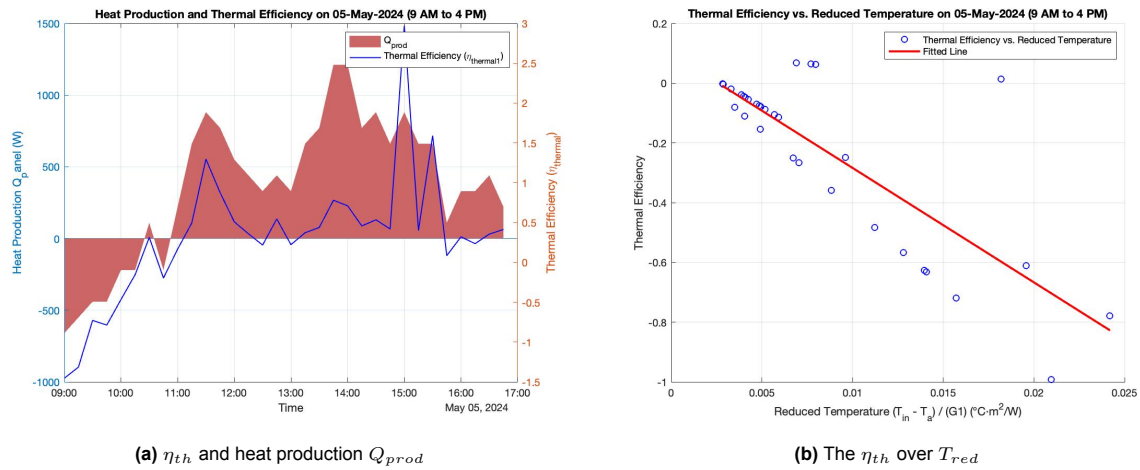
(b) The η_{th} over T_{red}

Figure 5.16: Measurements on 05-05-2024

With the outcome of this experiment, it can be said that the former calculation of the numerical model was not stated correctly. The thermal efficiency of the heat collectors is much higher with cold application, suggesting it to reach 93% when partly used with cold liquid. The electrical efficiency also rises a few decimal percentages, as already suspected, but mainly the solar thermal part does include much more heat collection. A new system sizing is therefore, based on again the reduced heat and 70 % coverage electrical load, with 12 PVT panels, and 797 PV panels.

5.6. Economical aspects

Both payback time and an LCoE are constructed for each system this is derived as follows, with approaches made. For this especially investment costs are of high influence as well as the discount rate and price for energy. The economic analysis consists of the following variables and outcome.

5.6.1. PV

The numbers for a LCoE of a PV system are:

Table 5.1: Units and numbers for a standalone PV system

Component	Quantity or Details	Unit Price (€)	Total Cost (€)
PV Panels	955 panels	€110	€105,050
Inverters	Initial	€3,850	€38,500
Cables	6000 meters	€2	€12,000
Mounting Materials	955	€25	€23,875
Optimizers	955	€35	€33,425
Installation	-	-	€50,000
Total Initial Investment	-	-	€262,850

Then all other the parameters are:

Table 5.2: LCoE parameters for PVT and PV combined system

Parameter	Description	Values
I_t	Initial and replacement investment costs in year t	€262,850 for year 1, €38,500 for year 15
M_t	Annual operational and maintenance costs (1% It)	€26,285 per year
F_t	Fuel costs (not applicable to PV systems)	€0
E_t	Annual electrical output with €0.17/ kWh	339,100 kWh
r	Discount rate	5%
n	Total number of years of system's projected lifespan	25 years

Which concludes in: 0.07541 €/kWh and a payback period of 11 years.

5.6.2. Solar collector

For the solar collector an LCoE is made with the following investment costs, the PV costs are scaled to the former table

Table 5.3: Units and numbers for a combined PV and solar collector system

Component	Quantity or Details	Unit Price (€)	Total Cost (€)
PV Panels	808 panels	€110	€88,880
Mounting Materials PV	955	€25	€23,875
Inverters	Initial	€3,850	€34,650
Cables	5000 meters	€2	€10,000
Optimizers	808	€35	€28,280
Solar Collectors	18	€675	€12,150
Heat Transfer Fluids	300 liters	€2 per liter	€600
Piping	750 meters	€5	€3,750
Storage Tank (already in house	-	-	-
Pumps and Controllers	-	-	€5,000
Mounting Materials Solar	18	€35	€630
Installation	-	-	€70,000
Total Initial Investment	-	-	€277,815

All the other parameters are then as followed:

Table 5.4: LCoE parameters for solar collector and PV combined system

Parameter	Description	Values
I_t	Initial investment costs	€288,915
M_t	Annual operational and maintenance costs	€28,166 per year
F_t	Fuel costs (pump)	€3500
E_t	Annual thermal + electrical energy output	337,100 kWh
r	Discount rate	5%
n	Total number of years of system's projected lifespan	25 years

With a total of 0.08050 €/kWh the payback period is 13 years.

5.6.3. PVT

For PVT the investment costs are:

Table 5.5: Units and numbers for a PVt and PV combined system

Component	Quantity or Details	Unit Price (€)	Total Cost (€)
PV Panels	797 panels	€110	€87,560
Mounting Materials PV	797	€25	€19,925
Inverters	Initial	€3,850	€34,650
Cables	5000 meters	€2	€10,000
Optimizers	797	€35	€27,895
PVT Collectors	12	€845	€10,140
Heat Transfer Fluids	240 liters	€2 per liter	€480
Piping	650 meters	€5	€3,250
Storage Tank (already in house	-	-	-
Pumps and Controllers	-	-	€5,000
Mounting Materials Solar	12	€35	€420
Installation	-	-	€70,000
Total Initial Investment	-	-	€234,704

Which then gives;

Table 5.6: LCoE parameters for PVT and PV combined system

Parameter	Description	Values
I_t	Initial investment costs	€234,704
M_t	Annual operational and maintenance costs	€23,470 per year
F_t	Fuel costs (if any backup systems)	€2,400 per year
E_t	Annual energy output (electric + thermal)	341,500 kWh
r	Discount rate	5%
n	Total number of years of system's projected lifespan	25 years

and an LCoE of 0.07108 €/kWh and payback period of 9 years. When comparing all these, with the LCoE for energy from the grid, being 0.1700 €/kWh since feed-in prices are lower than cost price (0.22€/kWh)

5.7. Conclusion

Three different stand-alone solutions presented, each of these incorporating losses that occur. This showed that the load of Coolworld is difficult to cover with solar heat collectors since the highest demand is in winter when not much heat can be generated with a flat plate collector. Therefore, for both solar collectors (26 panels) and PVT systems (12 panels) an extra set of PV panels, 808 and 797 respectively is advised to install, for a 70 % coverage. The heat generation is then based on 1 third of the total head demand (92.54 MWh). Furthermore, a PV systems standalone setup would consist of 955 panels.

Besides, the PVT experimental system setup showed that much more heat can be recovered. This is due to the heat extraction from environmental air. Namely, on a hazy day, with an average of 124 W irradiation, still 0.7 % electrical efficiency increase could be achieved, and a remarkable 13.1 kWh per day with one panel, and $T_{ambient}$ around 14 °C. Furthermore, it was measured that the calibrated panel, was on average 10 °C warmer, up to 48.7 °C measured at 14:30, see Figure 5.13b, compared to the PV1 panel. A ΔT of 10.9 °and ΔP_{PV1} of 1.53% was found, meaning a 0.140 $\frac{\%}{K}$ temperature coefficient, which is half the factor from subsection 4.5.4.The last testing day shows that even negative thermal efficiency could lead to a positive electrical performance increase.

At last, an LCoE is built for all the different system setups, showcasing that a PVT setup is most interesting due to the increased PV and thermal performances, this also suggests a longer lifespan for the PV panels, due to the cooling of them. The payback time of this investment is considered 9 years, with total cost of €234,704 and an energy price of €0.17 for feed-in.

6

Discussion

6.1. Investigating the energy structure of Coolworld Waalwijk's testing facility

Within this research conducted at the Coolworld Waalwijk facility, many things were unknown, or not easy to access. The first holdup in this was the large amount of data and folders that exist at Sharepoint, which is the shared data folder system of Coolworld. Due to the lack of information, many assumptions had to be made, such as the dimensions of the floor heating system. It is unknown how the structure is below the concrete. Besides, the actual materials used are not known and are therefore either approached or assumed. The same can be said for the vessel calculations. Besides design factors, also many environmental conditions and actual flow within the systems are approached. These are big factors on the calculations but cannot be established. Smaller deviations can occur due to a lack of knowledge of the actual glycol-water mixture ratio. For the validation of this vessel, material characteristics are also assumed. The outcome of the calculations is within a reasonable margin compared to this. Actual measurements were not possible, since the temperature probe was positioned above the fill level of the tank. After the tank is filled a better approach can be made.

The same must be said for calculations on the testing facility's testing method. The actual flow in the heat exchangers in the roof section is unknown. No flow meter is installed, but, when considering the nominal power of the pump in the system and relating that to the power of the other installed pumps, an approach can be made. In this approach, one should take note that an average pump power is used. This is due to the change of tested cooling systems. Some chillers have much higher flow rates than others. The cooling circuit pump can be adjusted, and so can the associated pump for heat exchange to the buffer vessel, and heat exchangers in the roof circuit. These are connected wirelessly and their capacity can be equated. The pump of the warming circuit (P090-16C) cannot be adjusted. Related to this, it cannot be checked whether the big WW1600 heat exchanger's efficiency is still on point, or that it has been defiled (exchanger between cooling machine circuit and warm water vessel, see Figure 1.3). The bottom of the vessel indicates that a lot of dirt exists in the system. Also in this system, are the heat exchangers in the roof, which therefore could be contaminated as well, but this is indefinable. Since the actual flow is not determined in the warm liquid circuit, assumptions for the heat recovery had to be made, assuming a close to the nominal power output of the pump. Besides, it is unsure when the heat exchangers in the roof are actively used, since there is no known record of the pump's running periods. Therefore the overall heat exchange for longer days has been filtered to working hours, but the exact moments of testing are not always known. The outcome of these is rather high, but it has been a cold (9 °C) humid day on the 22th of April, when high heat loss occurred, see Figure 3.8a. When known, a more detailed loss can be determined of the heat exchangers warming the environmental air as also Figure 3.4 showcases. Besides, since there are two exchangers in the roof, in series connected, actual heat won in the first, could lead to losing this potential win in the second exchanger, if environmental air is colder than the inlet temperature of water to the second exchanger.

This leads to the next point of discussion, namely the lack of time for extensive testing. At the facility

a high workload exists, which resulted in a scarce number of test moments. Besides, more meetings on how to test, what to test and what to do with the outcome would surely improve the outcome, but more importantly the concerns and awareness of the current situation and the misunderstanding in the current test procedure. Two measurements showed remarkable outcomes up to 100 % energy recovery and more, heat than cold produced, but validation on this, and the exact energy efficiency could not be determined. Besides, the actual power delivered within the cooling machine is based on one AC circuit output, which therefore shows a lower power consumption in Figure 3.11. Additionally, it is suggested that more heat recovery is possible, since more heat trapped in the enclosure wants to escape, as can be seen in Figure 3.12a. At last, it should be noted, that these tests were done extensively, for a longer period of time, to define the actual heat recovery. The new method and its description will have to be tailored for normal testing procedures, and logistics should be optimised to it.

This research has specifically been carried out on the testing facility, but since an undefinable energy loss occurs during weekends and holidays, this research should be extended to the whole company. The source of this energy consumption has not been found during this research and should therefore be prioritised in future research.

Since a plan of action is missing in the search for sustainability measurements within Coolworld Waalwijk, and for testing facilities for cooling machines in general, a strategy is built on how to do research. This strategy is not based on literature but on knowledge gained by the author during events and projects. This strategy describes a possible method for ensuring high energy recovery from rest heat and cold, to a workable warm product. More strategies can be made on for example the implementation of renewable solutions, and a more in-depth study on the energy consumption outside of the testing facility, which is out of the scope of this research.

6.2. Numerical model for solar energy generation

in defining the system sizing of a PV, solar thermal or combined PVT system three different standalone, and a combined system are provided, with a solution that fits Coolworld Waalwijk's energy consumption. Most energy consumed is based on electrical energy, but gas consumption is not included in this study. This is only being used in heating the warehouse.

It was suspected that the solar energy generation would be at its highest in the middle of the summer but after comparing the outcome of the model to different years of solar generation, it turned out that per year this is a big difference. So the graph of energy generation with more generation in April and May is not as strange as thought, especially considering the temperature increase in summer. No high peaks are visible in the T_{module} graph, but the overall temperature is higher.
The electrical load profile could easily be loaded in the numerical model, but for heat this is different. Losses in actual heat consumption cannot be incorporated since definite numbers of for example the heating element's efficiency and losses occurring within the facility are unknown. Besides that, a measurement for heat consumption is done several times, showcasing different numbers, so the actual heat load is based on a standby energy demand, the energy consumed on production days, and patterns that illustrate heat consumption, together with an average of the actual measurements on the vessel. Based on that a heat load profile is built.

The PV module temperature is tried to approach when irradiation on the panels emerges. This temperature profile was checked but could not be fully validated. The measurements seem valid concerning a rise in temperature in sun hours, nevertheless, is this an approach, not being checked. Alongside is the determination of efficiencies from inverters, cables and sizing based on former studies and datasheets with averaged numbers, in standard testing conditions.

To determine a suitable solar heat system in solar thermal collector form, more details on energy losses could be incorporated, since the thermal efficiency is based on multiple factors. In this calculation an assumed constant thermal efficiency is used, since this is an empirical approach. If the comprehensive total heat loss formula is used, as stated in Equation O.2, then, radiation losses with sky temperature T_{sky} and windspeed dependency can be accumulated. Now, the panel is assumed fully insulated on

the backside and is Equation 4.29 used instead of determining the solar collector's performances as done by TüV Rheinland. This certificate is based on the Solar Keymark thermal performance certificate that is composed by testing. With this efficiency, and the annual heat generation possible in the Netherlands, alongside the heat demand at Coolworld Waalwijk, it can be said that solar heat generation can unfortunately only cover a small part of the energy demand. The validation of this was intended to do with the Solar Keymark calculation tool, the ScenoCalc, but this did not seem to work. Instead the nPro tool that is calibrated to the ScenoCalc is used. This study is based on a flat plate panel, the comparison to an evacuated collector or concentrating collector is not made in numerical model form.

During this study it has been tried to find what cold inlet temperature would do to the solar thermal efficiency. A baseline for the temperature is built from the heat demand, and then a factor of this, can be rewritten to a produced cold liquid ΔT. This is not a valid number but an approach. Besides the number has been checked with the Solar Keymark datasheet and seems to correspond in thermal efficiency

For a PVT numerical model, the assumptions were made in building this model based on a sheet and tube type of module. this type has most parallels with the Flat Plate panel and a normal PV panel and the lowest losses. When defining system sizing, it turned out that the actual thermal efficiency and PV efficiency reduced drastically when embedding the combination of the two and a suggested transmittance of 0.74. But, no study has been done on this number. It is from literature, from 2002 [13], but this number is suggested higher from current research and could therefor improve the overall performances. Besides this a validation for PVT was tried to make with an online tool, but no sophisticated tool was found. nPro does do calculations but only for energy generation maximisation.

6.3. PVT test setup

The first and foremost important topic in this study is that Dutch weather is unpredictable. Especially considering the short period in which the testing is performed. The months March and April had very bad climate conditions. This brought difficulty in both making a calibration measurement, defining differences in between the panels, and for actual cold liquid application testing, since temperatures stayed rather low. But, more importantly, radiation was very unstable, resulting in different solar generation profiles in between the panels. Since this test is Quasi Dynamic, the measurements are done with climate weather conditions. This is not a bad thing in the first place, but without knowing actual radiation due to the lack of a pyranometer, it is difficult in determining efficiencies. Besides this, average windspeed is at all times an approach, since this fluctuates a lot and differs much more from time to time, no constructive log was possible with the instruments used, as can be seen in Figure 4.6. At last, after 14:30, a minor shade of a lantern passes both PV1 and PV2.

The testing setup has been a gift from Alius Volthera, for which many thanks, but unfortunately. Since the panels had been tested before, they were not calibrated, and differences were noticeable without being able to define them. Rest material of stickers and glue was visible on the PV part. Besides, it was impossible to set a stable flow. At first, this had to be done with T-shaped valves, which give only 90 °of enclosure angle of the valve. Together with this, it turned out that with a flow above 14 l/min, a heat loss occurs in PV2 which could , instead of win. Second, the pump in the system was an overkill, resulting in a flow of 0.293 kg/s instead of the prescribed 0.02 kg/s. On the side of that, the filters, also attached to the same circuit, provided constant differences in the flow. At last, the flow was most of the time higher than recommended. Partly due to the pump, but also, since the distance to the system more than 50 meters, which resulted in high thermal losses in the transportation, through a long black coloured hose positioned in the sun.

Apart from the panels themselves, is the Hoymiles inverter not recommendable for further research. Besides the friendly helpdesk, is power measured per quarter with the inverter. Not on averages, but by specific measuring moments every quarter. Therefor the solar generation outcome profile is with a lot of peaks, and differences in between panels when clouds pass. Besides, only the past 15 days of data collection is possible, which was found out later. Passing clouds, also resulted in a generation of 113.1 %, which could be due to more diffusive radiation when cloudy, but this is not validated.

When calculating the values from the panels, and defining the differences between them, the differences in solar generation increase until the highest radiation point (middle of the day), and decrease after this point throughout the day. Same for the irradiation profile, this curve of efficiency differences should by exponential, but this is not possible to define easily. A linear difference throughout the day is used instead in between the panels. Moreover, is T_a and the wind speed taken from clime data, since no logging was possible for both of these.

The data set of the temperature sensors sometimes shifted 5 minutes, and gave odd time steps such as 14:44:59. This made the actual data set preparation, very time-consuming, but more importantly, this could result in impurities. Another impurity that had to be approached was the solar irradiance during 2024. DHI and DNI were both not provided in this therefor the assumption is made for the DHI being 20 % of the GHI. With this the thermal performances could be approached for the solar collector of the test setup.

The tests are done with a much higher flow, five times the prescribed, with which the thermal heat transfer coefficients as stated in Appendix Q were formed. When using the TUV testing flow, a more logical outcome was found for $\eta_{thermal}$. Besides, in these calculations, some parameters were not possible to include, which made the calculation not completely valid. All measurements show a negative reduced temperature, which is because of the cold liquid applied to the panels.

Manual measurements support the measurements done, but actual temperature logs the solar cells lacks. The manual ones were performed occasionally, and not enough sensors were available to consequently measure each panel. Besides, temperature differs from the panel at the backside in the middle compared to the side. On top of that, is a small air gap in between the PV panel's backside and the thermal collector, which results in much less heat transfer than with direct

At last, an inexplicable finding is that during testing, with a flow that is above 14 l/min, there seems almost no heat transfer ocurring in the second PVT panel when on 11-04 around 13:45 an adjustment from 6.62 l/min to 14.32 l/min was done. This, is so that more cold is reaching the panels, and less loss in between the facility and the panels. The phenomena could be due to the ISO9806 suggested heat transfer instability as mentioned in Figure 4.7.2.

The new outcome for both solar and electrical generation of the PVT panels is based on assumptions. Measurements for March April and May can not represent the whole year, therefor a baseline is chosen for performance increments. Although normally the highest production is on these months since less heat generation in the PV panels, these past months have been cold, and perfect solar irradiation profiles were not able to use in this study.

At last is the LCoE not incorporating longer possible lifespan of PV panels due to active cooling and prevent from high heat generation within the panel. Besides, the lifespan of a solar collector is comparable, but that of a PVT hybrid collector is unknown, especially in the WISC form. Many assumptions for cables and other components had to be made.

7

Conclusion

7.1. Investigating the energy structure of Coolworld Waalwijk's testing facility

This research is set up to gain insight into the energy-intensive processes and losses within the testing facility of Coolworld Waalwijk. To do so, firstly a constructive overview of the different existing circuits in the system setup is created to ensure that future research and help by experts can be realised. With this, it is more convenient to overlook the facility and its components. The examination of the facility's various circuits shows the complex ways in which cooling, heating, and filtering processes are interconnected. An overview of all the components within the facility is made and calculations on potential energy-intensive production, as well as stand-alone component energy losses, are done.

For the losses of energy-consuming components in the facility that potentially leak energy, an approach is made. Besides, a validation checked whether this approach is in line with expectations. To reduce heat loss in the washing street floor heating, controllers should be installed. So that with T_a temperatures above 1 °C the warm liquid is not unnecessarily warming up the environment, which could result in an energy loss of 84.14 kWh on an average winter day with T_a 5°C and an average windspeed of 3.7 m/s, and 54 kWh when T_a is 10°C, both when the pump is turned on 8 hours a day.

With the same environmental conditions the heat loss for the BV20 silo is determined, which is positioned outside, without any insulation precautions. On an average winter day (5 °C) the energy loss is 139 kWh per 24 hours and 44.7 kWh in spring (15 °C). Insulating the vessel with 100 mm Rockwool™ and plating would reduce this amount significantly to 9.65 kWh per day in winter and 4.82 kWh in spring. This results in a potential saving of €3575,- per year. Which

The current machine testing procedure and capabilities of the installed heat exchangers in the roof section for heat recovery are unknown. Currently, the machines are misaligned with the heat exchangers, and a sail is used on one side of the cooling machine's exhausts. The data log showed that with this setup, during testing, no heat was recovered, but in the long run lost. Partly due to preheating the liquid, to prevent the piping structure from 'raining' when this gets too cold. Because of this, warm liquid is cooled down in winter months by the environmental air. On the other hand, is the three-way valve not calibrated, which leads to an undesirable increase in heat loss. Tests with different setups with only aligning and, alignment with a sail on one side does not include full heat recovery possibilities. Only when a full enclosure of the exhausted air can be assured, as much heat can get recovered, as cold cold is produced, showing a heat recovery of over 100 %. This is possible due to other heat-producing processes that run during testing inside the machines, such as pumps. Formerly, only with small machines, with ambient temperatures above 25 °C this was possible. This test was done with 10 °C ambient temperature and one of the biggest machines (600 kW). It should be noted, that with this machine the power delivered by its fans, exceeded the possible power of the fans in the heat exchangers in the roof, therefore these should reviewed in both power alignments, since now in winter cold environmental air is dragged over the exchangers. A big enclosing sail would be sufficient, but

other options are discussed in chapter 8. To support other testing facilities for cooling machines in this process of research, installation of tools, and data logging calculations, an Energy Management Strategy is built for this procedure. Which can be found in Appendix I.

At last, a more careful look should carried out on the standby energy consumption. Past data logs show that at weekends without production 416 kWh of energy is consumed, and during holidays, additional systems start-up throughout the day, which results in more extra consumption. An example is the heating element in the vessel, which start up every morning at 6am. Except for weekends, but including holidays. The outcome of the above study and the implementation of energy-saving solutions cost €350,- €11460 and €13680,- for the controllers, vessel and recovery sail + controllers respectively. Resulting in a payback time of 5, 39 and 16 months respectively.

7.2. Independent Energy Supply: PV/ Thermal

Besides energy-saving solutions, also, a renewable energy alternative is also investigated. At Coolworld, the demand for heat and electrical energy are both of considerable size. Therefore three different energy system setups are deliberated. Based on both the electrical demand and the reduced heat demand, made by an approach for the heat consumption. For this a numerical model is built, with the following outcome per system type.

For a PV stand-alone energy generation, the model concludes that the approach of 955 panels of 405 Wp each and an efficiency of 20.91%, a 72.6% coverage of the total load (467 MWh) can be achieved when incorporating all the corresponding losses, such as inverter, cable and mppt. With this size a total of 372,9 MWp is produced per year, creating a positive grid exchange, considering 100% possible. However, this production is not enough for winter production months. The total cost of this investment is €262,850 with a payback time of 11 years.

This problem is worse when considering a stand-alone solar collector energy system. Mainly because less heat can be produced from solar radiation in a flat plate collector in winter, but demand is also higher then in summer. An implementation of 28 panels can cover one-third of the total heat demand (94.52 MWh), with a maximum over-production of 25 % per month (in August). The extra yield due to rest cold application is 9.4 %, but a standalone solar collector design would, when using flat plate panels only, never be sufficient. This is partly due to the efficiency of the panel, but mainly since the annual heat generation possible in the Netherlands, alongside the heat demand at Coolworld Waalwijk, does not line out. This makes heat recovery an even more interesting type of energy reuse since solar heat can only account for a small part of the total heat demand. For the residual energy demand, if 100% feed-in is possible, a total of 808 PV panels is needed for the residual energy consumption with a total cost of €277,815, and payback time of 13 years.

7.3. PVT Test setup

With the installed PVT setup, more exact numbers on actual thermal and electrical efficiency are found. It turned out that heat recovery was much higher than expected. On a day with hazy weather (124 W/ m^2), it was possible to reach up to 13.2 kWh of heat generation in the first collector, with a mean temperature of 5.31 °C and ambient temperature of 13.4 °C. This low temperature resulted in a very high thermal efficiency, but, it also provided an effective 0.626 % increase in electrical efficiency compared to the calibration panel. Comparing this with a sunny day, efficiency can extend to over 2.7 %. The biggest gain is measured with a $\Delta\eta_{el}$ of 1.53 °C with a temperature difference of 10.9 °C, indicating a 0.140 %/K temperature coefficient, which is about half the indicated coefficient of the manufacturer. At last, it is found that even negative thermal efficiency could lead to a rise in electrical efficiency, stating that the PV panels on top, still actively transfer heat with the thermal collector.

When installing a PVT hybrid setup as such, the heat generation is taken as the cap. So, with losses incorporated due to the hybrid setup PV combination, but with gains due to active cooling, a total of 12 PVT panels together with 797 PV panels will be able to reach a 70 % coverage, and maximum over-production of 25 % for heat generation. This setup would have a total cost of €234,704 and a payback time of 9 years.

With this research, new insights have become available in Coolworld Waalwijk's energy consumption. Most important is current practices, which are energy-intensive, and redesigning these would be the most efficient. Their short payback time represents this. Based on these findings, a strategy is built to implement such solutions in other testing facilities for cooling machines. However, an investment in a PV stand-alone system would be interesting to cover the energy consumption of other practices. If redesigning the test facility would bring logistical problems, the implementation of 12 PVT panels would be sufficient to cover one-third of the total heat demand, but seasonal heat storage would be worth an investment due to big differences. A total energy consumption of 476 MWh is significant, but so are the potential savings. The facility as the one at Coolworld has a rather rare residual flow, in the form of cold liquid and it would be a waste if no new goal would be given to it. Let this be the start of a blue-coloured Coolworld, with a green edge.

8
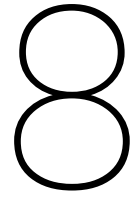
Recommendations

Since this paper is a strategy design based on the current existing testing facility as the one of Cool-world in Waalwijk, it has been chosen to deliver multiple recommendations and therefore a specific paragraph has been added to this paper. The first recommendations will be on the testing facility, advice will be given to Coolworld, for which an overview of suggestions can be found in **??**. The second part will also include future research recommendations.

Test Facility

Within the study on the different components it has become clear, that an updated overview of the current facility is highly recommended. Regular checks and adjustments of these circuits are suggested, to avoid energy losses such as incorrect usage of installed material. Especially when future research will be carried out, or when experts will come by to give advice on solutions. With this, the first recommended solution is the installation of controllers. In the floor heating at the washing street, the system should only turn on when the ground temperature will tend to get below 1 °C. Otherwise the energy will be lost in environmental air. Together with this, controllers should be implemented in the roof exchanger system, to see if the fluid temperature is not higher than ambient air, to prevent warming up the surroundings. Valves in between the two exchangers should be positioned to ensure one exchanger's outlet, does not result in energy loss in the other. Alongside this, the uninsulated vessel needs insulation to avoid further energy losses. Its has been shown that with current practices a 24 m^3 is big enough, but when considering more testing at the same time, an investment in a bigger size could be beneficial. Take note that if more rest heat can get recovered as tested, and when a solar collector water system exists, an extra tank could be interesting, to ensure that temperatures as low as possible can flow through the exchangers in the roof. Together with this, when investing in a new vessel, a more efficient heat pump could replace the current heater in the vessel.

Alongside components that could use energy saving solutions, the current testing method should be reviewed. The current positioning of the machines together with the placement of the sail on one side, does not recovery much energy when comparing this with a fully enclosed extractor. Then the air is pushed through the heat exchangers, which on their part need higher capacity fans installed, to ensure all heat will be sucked through, and no bulging will appear in the installed sails. Besides this, it might be interesting to start testing at customers, by having a look at the online DaikinOnSite environment. Multiple characteristics can be read from a distance. Which then, could save testing time in the facility. Also, the type of test and testing time in general should be reviewed. It might not be compulsory to test until a -10 °C is reached in the system.

Placement of a filter in the warm liquid circuit, for permanent or temporary use is recommended since the outlet down the big vessel indicates a lot of contamination, which therefore could also be in both heat exchangers connected to this circuit.

8.1. Energy consumption

The outcome of this study is a strategy on heat and cold recovery, but an advice to use this paper's outcome in building a strategy creating sustainable solutions to both the components in the testing facility for cooling machines, and the implementation of a standalone renewable energy source for all other facilities. Besides this, a study on its own should be done on what energy is used during weekend and holidays, outside the testing facility, to reduce the 416 kWh standby energy consumption. This goes hand in hand with employee awareness, the organisation of meetings to think of solutions within the company could be beneficial for both parties. Encourage to adopt eco-friendly practices in daily operations. This could include turning off equipment when not in use.

The current energy is bought is no renewable energy. However, the energy intensive production of Coolworld is at most during the day. Especially in the middle of the day. With a dynamic contract this could even be interesting pricewise, as well as for the production itself, since less heat from other sources is needed when testing can be done during the hottest part of the day.

In this study, no actual heat displacement to the warehouse is considered. But, for the testing facility's heat, this would be an interesting goal. Especially since the current heat development in the facility is too high, and in the warehouse gas driven heaters are costly. Another solution could be, testing on the side of a place that actually needs cooling. When future testing facilities are constructed, it could be highly interesting to station these nearby cold-demanding productions, so that immediate reuse of the cold could be possible, such as data centres, industrial metal processes etc. Current nearby cold-demanding companies are:

- Huiskes Metal Recycling: cooling down high-temperature processes.
- Oerlemans Foods: cooled vegetables, which could be an interesting company to sell rest cold to.
- Ocuengineering Metal Manufacturer: cooling down high-temperature processes.
- Netcranes: For the production of cranes which are energy and heat-intensive.

Future plans: Investigate on energy-saving solutions outside of Coolworld
Now that the urge for reuse of waste energy streams rises, Coolworld could differentiate itself by showing what solutions they could give to customers. A pilot could be set up to see what residual energy flows could be used besides the production of the cooling systems. Currently, all systems are air-cooled, which makes it difficult to win back the same amount of energy compared to an energy system that's closed with water cooling. But if more air could be collected, for example by using movable containers where a machine to be tested can be loaded in, with heat exchangers on the roof and fans to extract the heat form the cooling machines immediately, more heat can possibly be trapped and reused. Which could result in a 100 % recovery, as tested in the roof heat exchangers. This could then be reused in local heating systems. These containers can be used at the testing facility as well as with costumers. This could make rental cooling machine more efficient, since both energy streams are possible to use.

8.2. Analysis of a PV Thermal system for Coolworld Waalijk.

Based on the numerical model an outcome with different standalone possibilities are sketched. Nevertheless, it is highly recommended to not focus on on solar techniques only. For example, evacuated solar thermal heat generation is not yet very common in the Dutch energy market. But, this is on the rise, and specifically with the current rest cold in combination with possible high-temperature heat storage, if the vessel would be sufficiently insulated, these panels can give high efficiencies. Therefore, advice from an independent sustainability advisory group is suggested. Especially since these are also able to think along with subsidies the implementation of other sustainability measurements as stated before.

As the results for the solar collector and PVT system show, there is more energy and heat demand in the winter months, accompanied by the lowest generation possible. This is in summer the other way around, wich suggests that a seasonal storage would be interesting to investigate further.

8.3. PVT Test setup

This panel/ heat exchanger combination, was surely not build to exchange as much heat as possible from the PV part to the heat exchanger part. Namely in between the two, a small (air) gap exists. Therefore the possible outcome in exchange could be upgraded by using a better-conducting material such as aluminium in between the two of them, or another type of heat exchanger, such as the sheet and tube, with PV hybrid could be considered. Instead of having as much heat transfer as possible with the environment, a whole different energy transfer could be arranged by applying cold liquid in the collectors' circuit, resulting in possibly higher electrical gains.

Besides this a more constructive testing setup up with more sensors and data logs options applied, in order to understand behaviour within the solar panels and the solar collector would be an interesting follow up to this study. Especially when another type of collector could be experimentally tested such as the sheet and tube PVT panel. On the side of that, a more temperature-dependent PV panel could be used in order to see what the active cooling would do to it. In this study, unfortunately, a major part of the cold was lost during transportation to the panels.

References

[1] Max Roser. Why did renewables become so cheap so fast? 2020. URL: `https://ourworldindata.org/cheap-renewables-growth`.

[2] CBS. 46 percent more solar energy production in 2022. 2023. URL: `https://www.cbs.nl/en-gb/news/2023/24/46-percent-more-solar-energy-production-in-2022`.

[3] A. Smets, K. Jäger, et al. Solar Energy. 1th ed. Delft: Cambridge UIT, 2016.

[4] Alternative Energy Tutorials. Temperature Coefficient of a PV Cell. 2023. URL: `https://www.alternative-energy-tutorials.com/photovoltaics/temperature-coefficient.html`.

[5] EngineerToolbox. Ethylene Glycol Heat-Transfer Fluid Properties. 2003. URL: `https://www.engineeringtoolbox.com/ethylene-glycol-d_146.html`.

[6] M. H. Noor Akashah et al. "Utilization of Cold Energy from LNG Regasification Process: A Review of Current Trends". In: Processes 11.2 (2023), p. 517. DOI: `10.3390/pr11020517`. URL: `https://doi.org/10.3390/pr11020517`.

[7] International Standardisation Organisation ISO. "Solar energy — Solar thermal collectors — Test methods". In: 9806-2017.2 (2017), pp. 1–90.

[8] International Standard. "GUIDE TO STANDARD ISO 9806:2017". In: 9806-2017.1.0 (2017), pp. 1–66.

[9] European Committee for Standardization. "Solar collectors - General requirements". In: 12975:2022.1.0 (2017), pp. 1–66.

[10] Quality Assurance in Solar Heating and Cooling Technology (QAiST). "A guide to the standard EN 12975". In: 12975-1.1.0 (2017), pp. 1–80.

[11] Ben cheikh el hocine H. et al. "Model Validation of an Empirical Photovoltaic Thermal (PV/T) Collector". In: The paper title may require capitalization according to the conference's style guidelines. Unité de Recherche Appliquée en Energies Renouvelables, URER, Centre de Développement des Energies Renouvelables, CDER, Laboratory Modeling Renewable Energy Devices, and Nanometric, Department of Electronic, University Constantine 1. Ghardaia, Algeria and Constantine, 25000, Algeria, 2015.

[12] H. A. Zondag et al. "The Thermal and Electrical Yield of a PV-Thermal Collector". In: Solar Energy 72.2 (2002). PII: S0038-092X(01)00094-9, pp. 113–128.

[13] H.A. Zondag et al. "The yield of different combined PV-thermal collector designs". In: (2003). Accepted 6 March 2003.

[14] S.A. Kalogirou and Y. Tripanagnostopoulos. "Hybrid PV/T solar systems for domestic hot water and electricity production". In: (2006). Available online 22 March 2006.

[15] R. Santbergen et al. "Detailed analysis of the energy yield of systems with covered sheet-and-tube PVT collectors". In: (2010). Available online 21 March 2010.

[16] R. Santbergen, C. C. M. Rindt, and R. J. C. Zolingen van. "Improvement of the performance of PVT collectors". In: (2008). Ed. by G. G. M. Stoffels, T. H. van der Meer, and A. A. van Steenhoven, Article TSE 2.

[17] K. Touafek, M. Haddadi, and A. Malek. "Modeling and Experimental Validation of a New Hybrid Photovoltaic Thermal Collector". In: IEEE Transactions on Energy Conversion 26.1 (Mar. 2011).

[18] Gabriel Colț. Performance Evaluation of a PV Panel by Rear Surface Water Active Cooling. PhD student, Electrical Engineering Faculty, University "Politehnica" of Bucharest. Bucharest, Romania, 2016.

[19] Marzieh Lotfi et al. "Cooling of PV Modules by Water, Ethylene-Glycol and Their Combination; Energy and Environmental Evaluation". In: Journal of Solar Energy Research 7.2 (2022). Journal homepage: jser.ut.ac.ir, pp. 1047–1055. URL: `http://jser.ut.ac.ir`.

[20] M. Hasanuzzaman et al. "Global advancement of cooling technologies for PV systems: A review". In: Solar Energy 137 (2016). Available at ScienceDirect, pp. 25–45. URL: `www.elsevier.com/locate/solener`.

[21] IEA. The Future of Cooling. 2018. URL: `https://www.iea.org/reports/the-future-of-cooling`.

[22] Future Market Insight. Industrial Cooling Systems Market. 2022. URL: `https://www.futuremarketinsights.com/reports/industrial-cooling-systems-market`.

[23] RVO. Energiebesparingsplicht vanaf 2023. 2023. URL: `https://www.rvo.nl/onderwerpen/energiebesparingsplicht-2023`.

[24] Nieuwstroom. Stroomverbruik. 2024. URL: `https://portal.nieuwestroom.nl/nl_NL/mijn-verbruik/stroom/`.

[25] A. F. Mills and C.F.M. Coimbra. Basic Heat and Mass Transfer. 3th ed. San Diego, CA: Temporal Publishing, 2015.

[26] VDI-Verlag GmbH. VDI-Warmeatlas. Dd 17. Table 8-3-1: Properties of Mixture Water/Glycol. Düsseldorf: VDI-Verlag GmbH, 1991.

[27] Torr Engineering. Refrigeration Cycle. 2020. URL: `https://www.torr-engineering.com/the-refrigeration-cycle/`.

[28] Coolworld. Accessed: 2024-04-14. Coolworld. URL: `http://www.https://www.coolworld-rentals.com/`.

[29] Arnold Franck. "Karakterisatie van afgiftesystemen". In: 3.1 (2013).

[30] Engineering Toolbox. Convective Heat Transfer. `https://www.engineeringtoolbox.com/convective-heat-transfer-d_430.html`. Accessed: 2024-05-02. 2024.

[31] Jason Svarc. Most efficient solar panels 2024. 2024. URL: `https://www.cleanenergyreviews.info/blog/most-efficient-solar-panels`.

[32] Koninklijk Nederlands Meteorologisch Instituut (KNMI). Daggegevens van het weer in Nederland. `https://www.knmi.nl/nederland-nu/klimatologie/daggegevens`. 2024.

[33] Amerisolar. Measuring the Albedo Effect. `https://www.amerisolarsolar.com/measuring-albedo-effect`. Accessed: [insert access date here]. 2019.

[34] Fudura. Energie inzicht met Mijn Fudura. `https://www.fudura.nl/energie-inzicht-met-mijn-fudura`. Accessed: [insert access date here]. 2024.

[35] İlhan Ceylan et al. "Determination of the heat transfer coefficient of PV panels". In: Energy 175 (2019), pp. 978–985.

[36] Swapnil Dubey, S.C. Solanki, and Arvind Tiwari. "Energy and exergy analysis of PV/T air collectors connected in series". In: Energy and Buildings 41 (8 2009), pp. 863–870. DOI: `10.1016/j.enbuild.2009.03.010`.

[37] Martin K. Fuentes. A Simplified Thermal Model for Flat-Plate Photovoltaic Arrays. SANDIA REPORT SAND85-0330 UC-63. Unlimited Release. Albuquerque, New Mexico 87185 and Livermore, California 94550: Sandia National Laboratories, May 1987.

[38] DMEGC Solar. DM405M10-54HBB/-V. `https://www.dmegc.com/solar/dm405m10-54hbb-v`. Accessed: 2024-05-19. 2024.

[39] Hoymiles Power Electronics Inc. Data Transfer Unit User Manual: Technical Data. Accessed: 2024-05-19. Hoymiles Power Electronics Inc. Hangzhou, China, Jan. 2022, p. 33.

[40] Joost de Vree. Warmtegeleiding van enkele materialen. 2024. URL: `https://www.joostdevree.nl/shtmls/warmtegeleiding_meer.shtml`.

[41] Technischer Überwachungsverein TÜV. "Test report no.:DE23HT1U001, VoltheraEVO+DM405M10-54HBB + Sunbeam Portrait". In: 1 (2023), pp. 1–9.

[42] Moses Jeremiah Barasa Kabeyi and Oludolapo Akanni Olanrewaju. "The levelized cost of energy and modifications for use in electricity generation planning". In: TMREES23-Fr, EURACA (Feb. 2023). Conference held 06-08 February 2023, Metz-Grand Est, France. DOI: `10.1016/j.egyr.2023.06.036`. URL: `https://doi.org/10.1016/j.egyr.2023.06.036`.

[43] Three Phase Inverter Datasheet: SE25K, SE33.3K, SE40K. Solar Edge. 2024. URL: `http://www.solaredge.com`.

[44] HR Solar. Maxis collector. `https://www.hrsolar.nl/zonneboilers/zonnecollectoren/maxis-collector`. Accessed: 2024-05-19. 2024.

[45] Alptug Yataganbaba, Ali Kilicarslan, and Irfan Kurtbas. "Exergy analysis of R1234yf and R1234ze as R134a replacements in a two evaporator vapour compression refrigeration system". In: 60 (2015), pp. 26–37. DOI: `INSERT_DOI_HERE`. URL: `http://www.sciencedirect.com/science/article/pii/S0140700715002760`.

[46] Mohamed Sharaf, Mohamed S. Yousef, and Ahmed S. Huzzayin. "Review of cooling techniques used to enhance the efficiency of photovoltaic power systems". In: 29 (2022), pp. 26131–26159. DOI: `10.1007/s11356-022-18719-9`.

[47] Manuel Lammle, Maria Herrando, and Glen Ryan. Basic concepts of PVT collector technologies. SHC Task 60/Report D5. Contributors: Laetitia Brottier, Matteo Chiappa, and others. IEA Solar Heating and Cooling Programme, May 2020. DOI: `10.18777/ieashc-task60-2020-0002`. URL: `https://task60.iea-shc.org/Data/Sites/1/publications/SHC-Task60-ReportD5.pdf`.

[48] Ruobing Liang et al. "Performance evaluation of sheet-and-tube hybrid photovoltaic/thermal (PVT) collectors connected in series". In: Procedia Engineering 205 (2017). 10th International Symposium on Heating, Ventilation and Air Conditioning, ISHVAC2017, 19-22 October 2017, Jinan, China, pp. 461–468. URL: `https://www.sciencedirect.com/science/article/pii/S1877705817302460`.

[49] Pennsylvania State University. 3.1 Overview of Flat Plate Collectors. John and Willie Leone Family Department of Energy and Mineral Engineering. Accessed 2023.

[50] S.Md. Iqbal Chandan Sumon Dey. "Numerical modeling and performance assessment of elongated compound parabolic concentrator based LCPVT system". In: Renewable Energy 167 (2021), pp. 199–216. DOI: `https://doi.org/10.1016/j.renene.2020.11.076`.

A
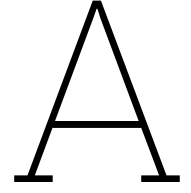
Energy Definitions

All the main energy definitions that are used in this paper that describe Heat Transfer energy, are named in the following section. These definitions are mainly based on studies on Mills and Coimbra [25] and Smets, Jäger, et al. [3].

A.0.1. Heat

Firstly in all the heat calculations, there is a distinction between 2 types of heat. Namely *Sensible Heat*, which does not include a phase change but the difference between two bodies' temperature, see Equation A.1 and *Latent Heat*, which is calculated on a phase change, for example when ice melts. When the temperature is equivalent to the melting point temperature, the temperature will not increase, but ice will melt first. So from a solid to liquid phase. See Equation A.2

$$Q = m \cdot C_p \cdot (T_2 - T_1) \tag{A.1}$$

Where Q is the amount of heat absorbed in [J], m the body's mass in [kg], and C_p the heat capacity in [J/(K*kg)]. At last, are T_1 and T_2 temperature differences between the two materials

$$Q = m \cdot L \tag{A.2}$$

In which L is the specific latent heat. In this study, latent heat does occur at phase changes for example in and around hoses and heat exchangers that freeze, or liquefaction of water vapour into liquid around hoses or heat exchangers. Since these are not directly measurable, not all of them will be taken into account. Sensible heat will be prioritised.

Heat transfer can be divided into three types of heat, namely conduction, convection and radiation. All three basic principles will be elaborated below.

A.0.2. Thermal conduction

Firstly, thermal conduction refers to heat movement within a material caused by a difference in temperature. This could occur in vessels and hoses which are enclosed by a material, but which are exposed to the surrounding temperature which is different to the medium inside of it. This process of heat transfer can be quantified using Fourier's law of thermal conduction,

$$\frac{dQ_{\text{cond}}}{dt} = -k \cdot A \cdot \frac{dT}{dx}, \tag{A.3}$$

wherein $\frac{dQ}{dt}$ denotes the rate of heat transfer in watts (W), k represents the material's ability to conduct heat, known as thermal conductivity, with units W/(m K), A is the surface area over which heat is passing, measured in square meters [m^2], and $\frac{dT}{dx}$ symbolises the rate of temperature change per unit distance in the direction of heat flow, denoted in [K/m]. Assuming that the material in between the two is homogeneous, the temperature rate of change, $\frac{dT}{dx}$, is constant across the wall thickness. Therefore, it can be simplified to the term $\frac{\Delta T}{\Delta x}$, where Δx indicates the wall's thickness.

A.0.3. Convection

Second, heat conduction through fluid movement, known as convection, serves as an alternative heat transfer pathway. It can be categorised into two types:

- **Forced Convection**: This occurs when an external force prompts the fluid to move.
- **Natural Convection**: Arises from the movement induced by variations in fluid density, which are themselves the result of temperature differences within the fluid.

Regardless of the convection type, the heat transfer equation that connects a higher temperature region, T_1, with a lower temperature region, T_2, adheres to the principle formulated by Newton's law:

$$\frac{dQ_{\text{conv}}}{dt} = -h \cdot A \cdot (T_1 - T_2) \tag{A.4}$$

In this context, $\frac{dQ_{\text{conv}}}{dt}$ represents the convective heat transfer rate, h stands for the convective heat transfer coefficient, with units of W/m^{2}K, A is the contact surface area, and $\Delta T = T_1 - T_2$ denotes the temperature differential. The coefficient h is a complex function dependent on the fluid's velocity, surface characteristics, and the liquid's habitual flow movement, whether this is laminar or turbulent.

Heat Transfer Coefficient: h
In this paper, this heat transfer coefficient needs to be calculated more often, therefor it has been decided to write the steps down in this part:

1. The First step is finding the coefficient is finding the Reynolds number with the following Equation A.9. This is determined by:
$$Re = \frac{\rho \cdot u \cdot L}{\mu} \tag{A.5}$$
   where ρ is the fluid density in kg/m³, u is the fluid velocity in m/s, L is the characteristic length in meters, and μ is the dynamic viscosity in Pa·s, together with the surface geometry (smooth or differently, by a friction factor) With this number one can determine if the flow is laminar or turbulent.
2. Second, the Nusselt number Nusselt number for the system needs to be determined with the following Equation A.6
$$Nu = C \cdot Re^m \cdot Pr^n \tag{A.6}$$
   with Pr as the Prandtl number, known for materials, C, m, and n as material-specific constants related to the specific geometry and flow conditions.
3. Third, by obtaining fluid properties like thermal conductivity k at the mean temperature of the surface and fluid, one can compute h using the Nusselt number:
$$h = \frac{Nu \cdot k}{L} \tag{A.7}$$
   where k is the thermal conductivity of the fluid in W/(m·K).

A.0.4. Radiation

Third is the radiative heat transfer. This mode of heat transfer is the propagation of heat through electromagnetic waves, which travel at the speed of light. Bodies emit this form of energy based on their temperature, with the emission process involving the de-excitation of electrons to a lower energy state, accompanied by the release of photons. The emission of energy from a blackbody (foundational model in thermodynamics and absorbs all incident light, ideal emitter) is quantified by the Stefan-Boltzmann law:

$$Q_{\text{rad}} = \epsilon \cdot \sigma \cdot A \cdot (T_{\text{surface}}^4 - T_{\text{surroundings}}^4) \tag{A.8}$$

Here, Q_{rad} is the radiative heat transfer. ϵ Is the emissivity of the material, without any unit. σ represents the Stefan-Boltzmann constant, with a value of approximately $5.670374419 \times 10^{-8}$ W/m^{2}K^4 and A the surface area.

A.1. Washing street

A more detailed calculation of the floor heating from subsection 2.6.1. First a heat convection coefficient of the PE-RT plastic tubes needs to be calculated. This is done by determining the Reynolds number first in the tubes, which is shown in the following Equation A.9

$$Re_D = \frac{V_{flow} * D_{in}}{(v_{glycol-water})})$$ (A.9)

In which the V_{flow} is the flow speed of the glycol-water inside the tubes, D_{in} is the inner diameter of the tubes and $v_{glycol-water}$ can be found in the Table 3.3 above. This gives a Reynolds number of: 5618.5.

$$f = (0.790 * 1n(Re_D) - 1.64)^{-2}; 10^4 < Re_D < 5 * 10^6$$ (A.10)

This corresponds with a friction factor f = 0.037, that is given in Equation A.10, from 4.42 in [25]. Then the Nusselt Number Nu_D, as stated in equation 4.45 from [25] gives Equation A.11:

$$Nu_D = \frac{\left(\frac{f}{8}\right)(Re_D - 1000)Pr}{1 + 12.7\sqrt{\frac{f}{8}}\left(Pr^{2/3} - 1\right)} \quad \text{for } 3000 < Re_D < 10^6$$ (A.11)

With Prandtl $Pr > 0.5$, This gives a Nu_D of, 49.05. As follows the heat transfer coefficient for the tube is determined by:

$$h_{c,\text{tube}} = \frac{Nu_D k_{\text{glycol-water}}}{D_{in}}$$ (A.12)

Which is: 1465 [W/(m²K)]. Now with different Shape Factors S as stated in [25] table 3.2, the different heat resistances (R) can be determined for the pipes in the concrete shell. Which is as follows. First for the tubes buried in concrete

$$r = \frac{D_{\text{outer}}}{2} = 1.0 \text{ cm} = 0.01 \text{ m}$$ (A.13)

$$S_{concrete} = \frac{2\pi L}{\ln\left(\frac{2h}{r}\right)} = \frac{2\pi L}{\ln\left(\frac{2 \times 0.3}{0.01}\right)} = 1.53L$$ (A.14)

$$R_{concrete}L = \frac{L}{S_{concrete}k_{concrete}} = \frac{L}{1.53L \times 2.0} = 0.326 \text{ m.K/W}$$ (A.15)

for the tube itself it is the following:

$$S_{tube} = \frac{2\pi L}{\ln\left(\frac{r_{\text{out}}}{r_{\text{in}}}\right)} = \ln\left(\frac{D_{\text{out}}}{D_{\text{in}}}\right) = \ln\left(\frac{2.0}{1.6}\right) = 28.16L$$ (A.16)

$$R_{tube}L = \frac{L}{S_{tube}k_{\text{PE-RT}}} = \frac{28.16L \times 0.40}{L} = 0.0888 \text{ m.K/W}$$ (A.17)

The convective resistance through the tubing due to the glycol flow is:

$$R_{\text{conv}} = \frac{1}{h_{c,tube}A} = \frac{1}{h_{c,buis}T_D D_{\text{in}}L}$$ (A.18)

$$R_{\text{conv}}L = \frac{1}{1465 \cdot \pi \cdot 0.16} = 0.136 \text{ m.K/W}$$ (A.19)

So the total resistance is:

$$R_{\text{tot}}L = R_{concrete}L + R_{tube}L + R_{\text{conv}}L = 0.416 \text{ m.K/W}$$ (A.20)

First without radiation it is.

$$\dot{Q} = q_{\text{total}}sL = \frac{(T_a - T_s)}{R_{\text{tot}}}$$ (A.21)

with

$$q_{\text{total}} = h_{c,air}(T_s - T_a) \tag{A.22}$$

Which gives

$$T_s = \frac{T_{\text{glycol}} + h_{\text{c,air}} s R_{\text{tot}} L * T_a}{h_{\text{c,air}} s (R_{\text{tot}} L + 1)} \tag{A.23}$$

Then, per tube a total heat flux can be made with the following, the T_s is here unknown and needed to determine. The q_{total} is only based on convectional heat transfer by the ambient air, Then the surface temperature can be calculated, with which a heat loss can be determined.

A.2. Buffer vessel

The overall calculation for the outdoor buffer vessel is: *Steady State conditions*
The calculation for heart loss is based on Steady State conditions, with **convective**, **conductive** and **radiation** heatloss. First the total thermal resistance for the vessel is built with the calculations similar as from subsection 2.6.1. The Re_D Reynolds number for a cylinder is:

$$Re_D = \frac{VD}{\nu} \tag{A.24}$$

where V is the air velocity, D is the characteristic length, and ν is the kinematic viscosity of the fluid, based on air conditions. Which gives (when $4 \times 10^5 < Re_D < 5 \times 10^6$), average Nusselt number, Nu_D, of:

$$Nu_D = \frac{0.3 + 0.62 \cdot Re_D^{1/2} \cdot Pr^{1/3}}{\left(1 + \left(\frac{0.4}{Pr}\right)^{2/3}\right)^{1/4} \cdot \left(1 + \left(\frac{Re_D}{282000}\right)^{5/8}\right)^{4/5}} \tag{A.25}$$

from the convectional resistance in the vessel, the conductional resistance in the steel wall by using by using Shape Factors S and the convectional resistance in the outer part. temperature due to conduction is determined, $T_{surface}$, as named above and determine the R_{tot}. This is done for a cylinder, and a determined h_{avg}
Next, given the Reynolds number range:

$$4 \times 10^5 < Re_D < 5 \times 10^6$$

where Nu_D is the Nusselt number, Re_D is the Reynolds number, and Pr is the Prandtl number. This correlation is known as 4.71c in [25].

$$h_{\text{avg}} = \frac{Nu_D \cdot k_{\text{air}}}{D} \tag{A.26}$$

.
Internally this is considered the thermal conductivity for the glycol, which is 0.478, but during working hours, there is convectional heat loss due to circulating glycol-water. When in still the thermal resistance R_{tot} is then the following, starting with the area sizing:

$$A_{cyl} = \pi \times 2.4\,\text{m} \times 2.6\,\text{m} \tag{A.27}$$

$$A_{hemi} = 2\pi \times (2.4\,\text{m})^2 \tag{A.28}$$

$$A_{total} = A_{cyl} + 2 \times A_{hemi} \tag{A.29}$$

Assuming a convective heat transfer coefficient inside the vessel (h_{in}). which is than the same as the thermal conductivity at the wall.:

$$R_1 = \frac{1}{k_{glycol-water} \times A_{total}} 2 \tag{A.30}$$

next the conduction through the steel wall is:
with S_{steel} is the following:

For the cylindrical part:

$$R_{2,\text{cyl}} = \frac{2\pi \times 2.6\,\text{m} \times \ln\left(\frac{r_2}{1.2\,\text{m}}\right)}{45\,\text{W/mK}} \tag{A.31}$$

For the spherical ends:

$$R_{2,\text{sphere}} = \frac{4\pi \times (1.2\,\text{m})}{1} \tag{A.32}$$

The total conduction resistance ($R_{2,\text{total}}$):

$$R_{2,\text{total}} = R_{2,\text{cyl}} + 2 \times R_{2,\text{sphere}} \tag{A.33}$$

The external convection (R_3): Assuming a convective heat transfer coefficient outside the vessel (h_{avg}) as calculated above:

$$R_3 = \frac{1}{h_{avg} \times A_{total}} \tag{A.34}$$

Then the total thermal resistance is

$$R_{total} = R_1 + R_2 + R_3 \tag{A.35}$$

Using the temperature difference between the inside and the ambient ($\Delta T = T_i - T_a$), Q can be calculated.

$$Q = \frac{\Delta T}{R_{total}} \tag{A.36}$$

<div align="right">

B

</div>

Refrigeration Cycle: R134a

A more detailed R134a cycle can be found below. The diagram in Figure B.1 shows heat transfer with a P-H graph and T-S diagram, which is different for each different refrigerant and is based on each process in the refrigeration cycle as aforementioned. This diagram shows the process steps for cooling. The R134a refrigeration cycle follows a sequence of steps where the refrigerant undergoes various phase transitions and thermal interactions as can be found in Yataganbaba, Kilicarslan, and Kurtbas [45]:

1: The refrigeration cycle initiates with the cold refrigerant (saturated vapour) being drawn into the compressor at **state 1**. Here, the refrigerant absorbs heat at a low temperature, causing it to change phase from liquid to gas or stay from liquid to liquid, and increase in pressure and temperature.

2: At **state 2**, the refrigerant, now under higher pressure and temperature due to mechanical energy applied by the compressor, is heated up further due to the compression.

3: Moving to **state 3**, the superheated refrigerant reaches the condenser, where it condenses into a liquid form, releasing the absorbed heat to the environment. Additionally the refrigerant, in its liquid form and at high pressure, then gets sub-cooled as it experiences a reduction in temperature.

4: At **state 4** and **state 8**, the sub-cooled liquid refrigerant is expanded in the expansion valves to a lower evaporation pressure.

5: In the evaporators, at **state 5** and **state 9**, the refrigerant starts evaporating at a temperature not typically associated with boiling, absorbing heat in the process.

6: The refrigerant completes the transition from **state 5** and **state 9** to **state 6** and **state 10** through the evaporation process.

7: Electronic Pressure Regulators (EPRs) are installed after the evaporators in a multi-evaporator system to maintain constant pressure, ensuring equal pressure at the inlet of the mixing chamber for each evaporator. In this example, two evaporators are utilised, conforming to different cooling needs, with each connected in parallel and equipped with their expansion valve.

8: After mixing in the mixing chamber **state 6** and **state 10**, the cycle is completed as the refrigerant re-enters the compressor at **state 1**.

B.1. Component specific information

B.1.1. Hoses

A small approach to energy losses in hoses is given with the following equation by determining the heat flux. This is the heat flow per running meter, based on **??**

$$q = \frac{Q}{L} \tag{B.1}$$
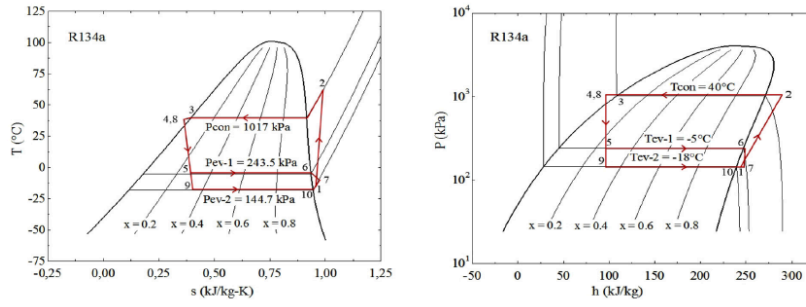
Figure B.1: A Temperature-Entropy (T-s) and Pressure-Enthalpy (p-h) Diagram for R134a refrigerant, source: Yataganbaba, Kilicarslan, and Kurtbas [45]

So for standard dimensions of hoses, the flux per running meter could be defined by the following, this can be found in Equation B.2.

$$q_{\text{cond,cylinder}} = \frac{2\pi k(T_{\text{inside}} - T_{\text{outside}})}{\ln\left(\frac{r+t}{r}\right)} \tag{B.2}$$

With the same parameters as can be found above. For convectional heat loss, the internal convection due to the liquid flowing through the hoses is taken into account and based on **??**. This gives Equation B.3

$$q_{\text{conv,cylinder}} = \frac{2h\pi(r+t)(T_{\text{fluid}} - T_{\text{wall,inside}})}{\ln\left(\frac{r+t}{r}\right)} \tag{B.3}$$

The external convectional heat transfer is neglected since the hoses are inside the testing facility without many environmental influences. With this equation deposition of vapour directly into ice or the forming of ice-condensed liquid on the hoses has not been taken into account. So only for the material itself, under different circumstances, with a different flow and material as well as temperatures from the fluid inside and the ambient temperature around it is taken into consideration. The $T_{wall,inside}$ is considered as the ambient temperature.

B.1.2. Couplings

A big part of the circuits are couplings, more details on these can be found below. Bewlow a picture is shown in Figure B.2a of the flange connection. This permanent solution is based on the compression of two separate hose parts with a seal in between them. These are made for long-term use and are therefore not considered easy to replace, these couplings are all made out of metal partly due to the structural strength that is needed. Another coupling type that is used in the facility is that of the Bauer connection. This type is easy to mount and dismount, which is of high importance during testing and a picture of it can be found in Figure B.2b. Both parts used in the facility are not considered in this sustainability measurements research.

(a) Couplings: Flange Connection

(b) Couplings: Bauer Connection

Figure B.2: Pictures of two types of couplings used at the testing facility

B.1.3. Valves/ Taps/ Liquids/ Other

Further items mentioned are the following, as can be seen in Table B.1.

Table B.1: Other items in the test facility that are not included in this study

Component	Description	Not included in study because	Image
Filters	Filters the MPG glycol water in the cold circuit at the facility. These are in a separate circuit attached to the cold circuit vessel BV06, CC04. They are turned on 24/7	Since no possibility of energy reduction or leaving out of the system	
Three Way Valve	Mixes glycol water of the roof heat exchanger circuit, with the warm water of BV20, regulating temperature to the roof exchangers.	Is needed to regulate temperature in	
Taps	Taps are used in the facility to control fluids and when needed change mixtures or get rid of dirt	They don't consume much energy and are all checked with safety pals when end parts are attached to ensure nothing will get lost	
Valves	Are used to control flow motions or flow speeds	Most are manual, so do not consume much energy, although controlled versions should be considered, more on that in results	
Liquids	The liquids used in the cooling circuits are known since that have their individual performances and do not need investigation	For the mixture, it could be beneficial to determine performances, for pumping and so the used energy for it.	

C

Checklist Chillers

Coolworld Heatworld

Coolworld Nederland BV duikerweg 34 5145 NV Waalwijk	Testplaats NL

Verzoek Datum:	Unit Nummer:	Verhuur Order:

Werkomschrijving

Algemeen Onderhoud, Lektest	
Return Check	
Running Test	
F-gas Inspectie	

Omschrijving			Omschrijving	
1	Stroom/Carterverw. Int/Ext. Voeding Ok	A	26 Water/Glycol Pomp/Voed Ok	A
2	Waterfilter Schoon/Ok		27 Water/Glycol Stromingsschakelaar Ok	
3	Instellingen **Klant / Standaard**		28 Water/glycol Temp./Druk In (EWT)	
4	Bijzonderheden Alarm Historie/Wissen		29 Water/glycol Temp./Druk Uit (LWT)	
5	Setpunt/Mode Test	°C	30 Warmte Wisselaar Schoon	ΔP
6	Type/Serienr. Lekdetector	Tapzx1A	31 Condensor Schoon/Onbeschadigd	
7	Koelschema Beschikbaar		32 Frequentie Regelaar(s) Schoon/Ok	
8	Omgevingstemperatuur (OAT)	°C	33 Cond.Ventilator Motor Stroom	
9	Mano/Temperatuurmeters Ok		33 1 A 2 A 3 A 4 A	
10	Persdruk/Temp. Circuit 1	b °C	33 5 A 6 A 7 A 8 A	
11	Zuigdruk/Temp. Circuit 1	b °C	33 9 A 10 A Gem van 3Ph !	
12	Persdruk/Temp. Circuit 2	b °C	37 Stickers Coolworld Ok	
13	Zuigdruk/Temp. Circuit 2	b °C	38 Casco/Constructie Ok	
14	Vloeistoftemp. Circuit 1 / 2	°C °C	39 Verf/Uiterlijk Ok	
15	Compr. Motor Stroom Circuit 1	A	40 Staat Bedrading/Schakelkast(en) Ok	
16	Compr. Motor Stroom Circuit 2	A	41 Relais/Timers/Beveiligingen Ok	
17	Filterdroger(s) Ok		42 Controle Verlichting/display Ok	
18	Lagedrukveiligheid Ok/Getest		43 Schakelkast(en) Filters Schoon	
19	Hogedrukveiligheid Ok/Getest (5Jr)		44 Draai Uren Compr.	
20	Kijkgla(s)(zen) Vol/Droog		45 Start/Stop Compr.	
21	Magneet Spoel(en)/Ventiel(en) Ok		46	
22	Expansieventiel(en) OK / Opening	%	47 Werking Daikin on Site Ok	
23	Circuit/Compressor Olie Niveau Ok 1x/Jr		48 Datum Volgende NEN 3140 Keuring	
24	Olie verschildruk (>150 kPa Filter!)	b	49 Juiste Onderhouds Stickers Geplakt	
25	Olie Zuurtest Uitgevoerd 1x/Jr		50 Reparatiekaart Ingevuld	

Materiaal & Uren Registratie			Koudemiddel Registratie			

Materiaal code		Aantal	Koudemiddel	R134A	R407C	R410A	R32
			KG				
			GWP	1430	1774	2088	675
			T-CO2EQ				

Monteur	Datum	Aanvang	Einde	Gew.Voor:		Reden/Lekage:	
				Gew.Na:			
				Gevuld:		Ja	Nee
				Rekening Klant:			
				Werkzaamheden Gereed:			

D

Schematic components drawing

LEGEND:

Sink	Filter	Un-de-fined	Not e
Drain	Tap	Out-let inlet	In/ outlet
Valve	Flow meter	Cold Buffer	Heatex-changer
Coupling	Pump	Warm Buffer	TempM eter

E

Topview Drawing

Testplaats Waalwijk

Coolworld Nederland B.V.
Duikerweg 34 5145 NV Waalwijk
Netherland
www.coolworld-rentals.nl
+31 416 688 088

| Project nr.: | Project nr. |
| Drawing nr.: | |

| Date: | 23-01-2024 | Scale: |
| Drawn by: | ASS | Revision: A |

THE DESIGN AND ALL PROCES DATA
PERTAINING TO THE APPARATUS /
EQUIPMENT / SYSTEM, SHOWN ON THIS
SHEET IS DISCLOSED IN CONFIDENCE AND IS
NOT TO BE COPIED OR REPRODUCED IN PART
OR IN FULL, WITHOUT WRITTEN CONSENT.

Project description:

Project:

Labels and text in diagram:

- LU34
- Te gebruiken boven 10°C
- schakelkast
- Th.
- 6 standen thermostaat
- 300kw heater
- 20.000 liter vat MPG +25°C
- trafo
- Water spoeltank
- Afpers- en spoelpomp 10 bar
- Voordruk pomp HD reiniger
- HD reinigerpomp
- HD reiniger vat +70°C
- Aftap water
- WW1600 (max. CZ20)
- PO90-16C
- DWK
- Sensor thermostaat DWK aanvoer temperatuur chillers
- PO180
- BV02B MEG
- PO55-2
- flowmeter
- PO50-2C
- Met water/glycol van BV06 of over LU34 met PO55-2
- WW1100
- BV06 MPG 60/40
- terugslagklep
- filter
- pompfilter
- Aftappompje
- inregelafsluiter
- PO180
- flowmeter
- 4"
- 2"
- 1" aftap chiller
- 2"
- Warmtewisselaar warmteterugwinning
- Airflow
- Aansluitingen naar de te testen chillers
- 2"
- Voeding dakventilatoren
- Elektrische voeding
- 200 A
- 400 A
- 4x 230 V
- 2x 16A CEE
- 2x 32A CEE
- 4x 230 CEE
- 16A CEE
- 32A CEE
- 63A CEE
- 125A CEE
- Water spoelen 2" Female Bauer
- Elektrische voeding
- 63A – 400A

Energy Management: Strategy

F.0.1. Instrumentation

To measure the heat exchange between different components of the facility, several sensors need to be installed. A few to mention are temperature sensors, flow meters, power meters, dataloggers, anemometers and more. In the table below, the actual sensors are named with a few important characteristics. It has been decided to work as much as possible with instruments that are currently so to say 'in-house'. These are 'off-the-shelf' products that are normally used in repairing procedures.

Controllers and datalogs

To log data and sent it to the needed environment two types are considered. First there is the collection of data, which happens in a controller, second is the transformation of this to online environment. Table F.1
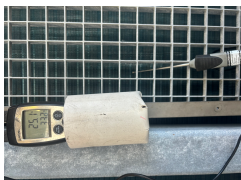
Table F.1: Different data log instruments

Brand	Name	Type	Description	Image
DIXELL	XR 570 C	Controller	Mainly used in refrigeration and air conditioning systems. It is specified as temperature and humidity control an at Coolworld it is mainly used as a measurement controller. In this setup, it is detached to a data log	
Coolworld	RM04010	Server	This is a specific module with a wireless connection to save data of different controllers and sent it to an online environment (XWeb) for real-time monitoring and analysis. This data can be downloaded	

Temperature Meters

For the determination of energy in flows, the temperature is needed. For this there are three different types that are considered. One is a permanent installation, the probe, second for temporary measurements such as the infrared and double mete. All of them are summed in Table F.2

Table F.2: Different thermometers that are used in the testing facility

Brand	Name	Type	Description	Image
Dixell	-	Probe	Temperature probes are attached to pipes and in environmental air to measure the temperature of heat and cold flows within various parts of the facility. These probes are placed either in air streams of heat exchangers or on piping with insulation tape.	
Hioki	-	Infrared	With this meter the adequacy and constructiveness of the data generated by temperature probes is checked. It is also used for immediate temperature measurements on site.	
Testo	922	Double K type	A Testo double input temperature difference sensor is used to determine two individual temperatures and measure the ΔT.	

Electrical Energy Meters

For the determination in energy AC clamps are used. for this, two types are considered. one is with a datalogg function, and the other is not. Both of them are summed in Table F.3

Table F.3: Different flow meters that are used in the testing facility

Brand	Name	Type	Description	Image
Hioki		AC clamp	Used for short term energy determination and checking on amperage The Fluke FC3000i, which includes data logging, is employed for long-term energy determination.	
Fluke	FC3000i	AC Clamp	Can be used for longer measuring processes like days and weeks. This clamp was able to measure over different cables at the same time. With wireless connectivity, a log could be shared with a mobile device.	

Flow Meters

A few different flow meters have been used during the testing. Each circuit has its flow meter installed. The following table (F.4) shows which flow meters are used within the testing facility. Air flow meters are also included in this scheme. But this of course has a tolerance that it could differ from the actual wind speed due to turbulence.

Table F.4: Different flow meters that are used in the testing facility

Brand	Name	Type	Description	Image
Endress & Hauser	Proline P 300	Electro- magnetic	Is used for the flow in a cold liquid circuit.	
Siemens	...	Pressure	Cooling machines flow	
Testo	410-1	Anemometer	Airflow cooling machines outlet	

Calculation Programs - Excel/MATLAB
For data processing, both MATLAB and Excel can be used. To have an easy implementation, at other facilities, it has been chosen to make an Excel layout in which data could be implemented to calculate different outputs for measurements

Visualisation Programs - Excel/ Python/ SankeyMATIC
Visualisation programs are used to give an overview of the current energy needs, and measurements and also complete energy flow overviews. Data measurements are produced in Excel and Python to create consistency in the layout. This is not a must but could be preferable, especially for papers, such as this one. The rest of the information on this strategy and the positioning of sensors can be found in section 3.6

G

ROCKASSIST

Rockassist (VDI 2055)
Online Thermal Calculation Tool

LICENSE HOLDER
Company Name	TU Delft
Contact	Lars Meeuwisse
Mobile	+31652112177
E-Mail	l.meeuwisse@student.tudelft.nl
Date	5/4/2024 9:04:16 PM
Page	1/4

PROJECT / CUSTOMER
Project Name
Contact
Tel.
E-Mail

NOTES

DESIGN CONDITIONS

TYPE OF CALCULATION ACCORDING TO VDI 2055
Detailed check: heat loss (q), T and CO2 savings

OBJECT
Object type	Vessel	
Filling Degree	100	%
Orientation	vertical	-
Vessel Diameter	2.400	m
Vessel Length	5.000	m
Operating temperature	25.0	°C

ECONOMIC DESIGN CONDITIONS
Energy Costs	0.10	€/kWh
Annual operation time	8,760	h/a
Lifetime of insulation	1	a

ECOLOGIC DESIGN CONDITIONS
Fuel type	Black coal	-
CO2-Factor	94.5	kgCO2/GJ
CO2 emission costs	100	€/t_CO2

AMBIENT CONDITIONS
Ambient Temperature		
- Personal protection	25.0	°C
- Heat loss, freezing, cooling	5.0	°C
Windspeed		
- Personal protection	0	m/s
- Heat loss, freezing, cooling	3.7	m/s

INSULATION SYSTEM
Cladding	Aluminium bright-rolled	
Emissivity of cladding	0.05	-
Support Constructions	Without support constructions	
Delta lambda per support construction	0.000	W/mK
Insulation fixings	None	
Delta lambda per pin	0	W/mK
Plant related thermal bridges	No	

RESULTS (FOR CHOSEN THICKNESS ONLY - MORE RESULTS ON THE NEXT PAGE)

Insulation thickness	Surface temp. at 25 °C ambient temp. and 0 m/s windspeed	Heat loss at 5.0 °C ambient temperature and 3.7 m/s windspeed		Annual savings compared to uninsulated situation			VDI 4610 Energy Efficiency Class
mm	°C	W/m	W/m²	t_CO2/a	Heat loss costs €/a	€/t_CO2	
100	25.0		7.9	36	10,513	3,577	E

Product name		s	lambda_B	theta_i	theta_a	f_VD	f_K	f_oF	f_A	f_s	f_ges
		mm	W/mK	°C	°C	-	-	-	-	-	-
ProRox MA 520 ALU		100	0.044	25.0	25.0	1.000	1.000	1.10	1.0	1.0	1.100

ATTENTION! You can find in total 3 messages on the last page.

s - Insulation thickness, Lambda_b – Opertional thermal conductivity, theta_i – Operating temperature, theta_a – Boundary layer temperature, F_VD – Compression of insulation, f_K – Effect of convection, F_oF – Effect of gaps (between the insulation), f_A – Ageing of insulation, F_s – Effect of radiation, f_ges – sum of all factors

LICENSE HOLDER

Company Name	TU Delft
Contact	Lars Meeuwisse
Mobile	+31652112177
E-Mail	l.meeuwisse@student.tudelft.nl
Date	5/4/2024 9:04:16 PM
Page	2/4

PROJECT / CUSTOMER

Project Name
Contact
Tel.
E-Mail

NOTES

Insulation thickness in mm
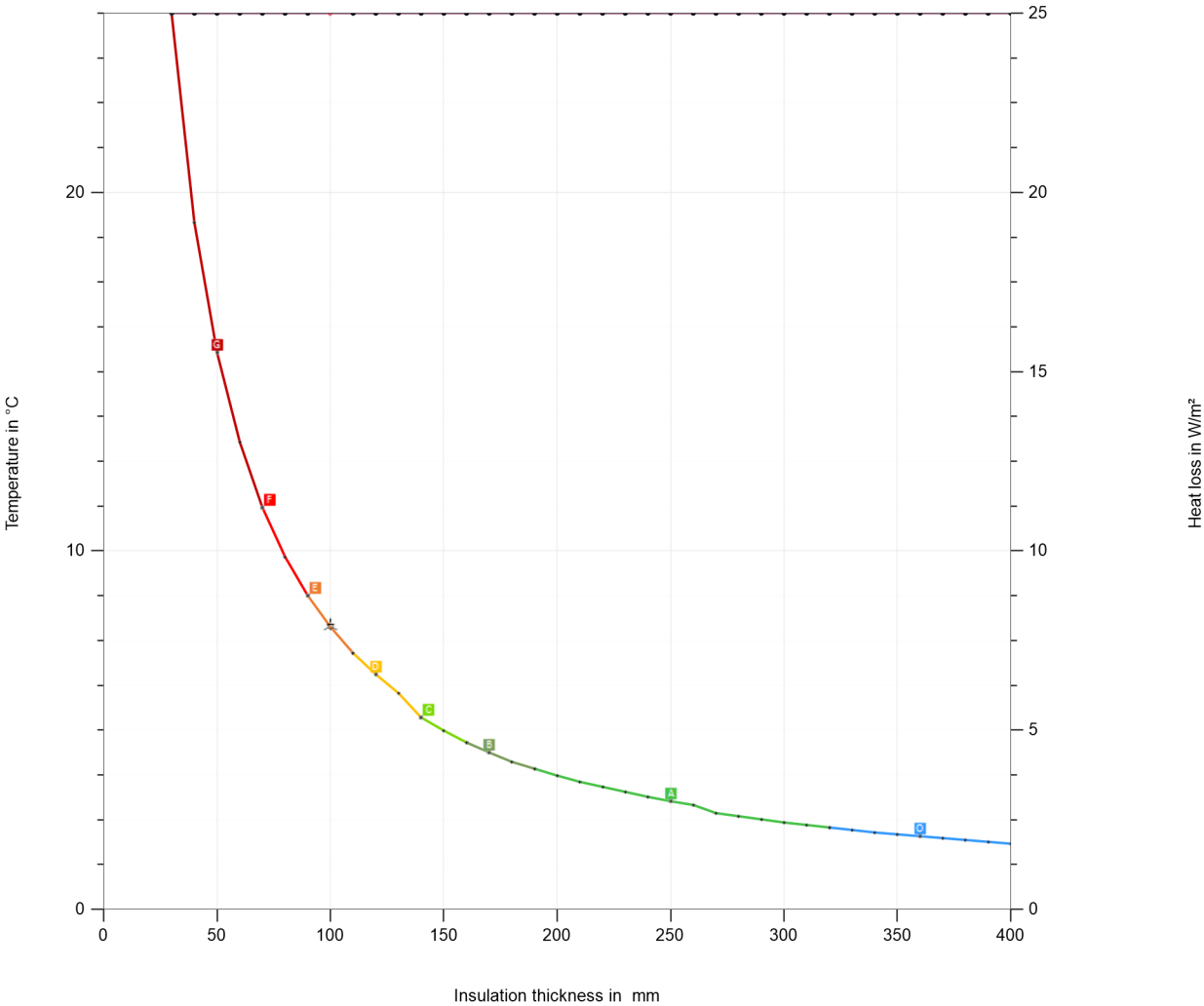
0 Surface Temperature
Heat loss

Rockassist (VDI 2055)
Online Thermal Calculation Tool

LICENSE HOLDER

Company Name   TU Delft
Contact   Lars Meeuwisse
Mobile   +31652112177
E-Mail   l.meeuwisse@student.tudelft.nl
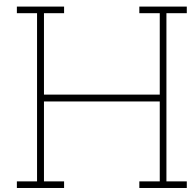Date   5/4/2024 9:04:16 PM
Page   3/4

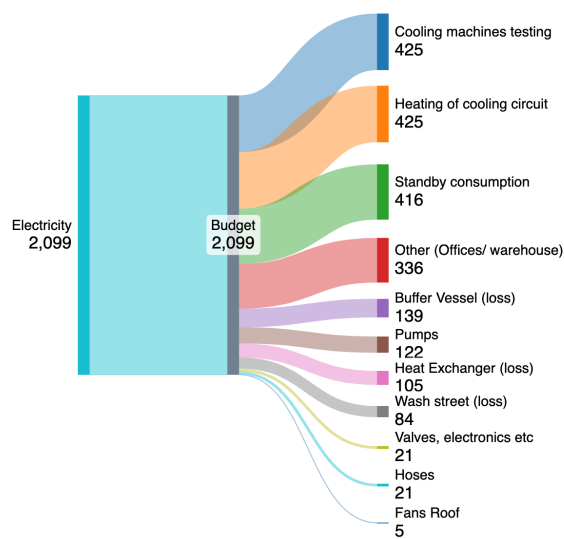**PROJECT / CUSTOMER**   **NOTES**

Project Name
Contact
Tel.
E-Mail

Insulation thickness mm	VDI 4610 EEC	Heat loss (q) W/m²	Heat loss W/m	Surface Temperature °C	CO2-Emission in tons/a t CO2/a	Heat loss costs €/a	CO2 emission costs €/t CO2	Convection -
0	G	297.4	2,242.2	25.0	36.9	10,859	3,694	laminar
30	G	25.0	192.9	25.0	3.4	988	336	laminar
40	G	19.2	149.3	25.0	2.6	773	263	laminar
50	G	15.5	121.9	25.0	2.2	637	217	laminar
60	G	13.0	103.2	25.0	1.8	543	185	laminar
70	F	11.2	89.5	25.0	1.6	474	161	laminar
80	F	9.8	79.1	25.0	1.4	421	143	laminar
90	E	8.8	70.9	25.0	1.3	380	129	laminar
100	E	7.9	64.3	25.0	1.2	346	118	laminar
110	D	7.2	58.9	25.0	1.1	318	108	laminar
120	D	6.6	54.3	25.0	1.0	295	100	laminar
130	D	6.0	50.5	25.0	0.9	275	93	laminar
140	C	5.3	45.0	25.0	0.8	246	84	laminar
150	C	5.0	42.3	25.0	0.8	232	79	laminar
160	B	4.7	39.8	25.0	0.7	219	75	laminar
170	B	4.4	37.7	25.0	0.7	208	71	laminar
180	B	4.1	35.7	25.0	0.7	198	67	laminar
190	A	3.9	34.0	25.0	0.6	189	64	laminar
200	A	3.7	32.5	25.0	0.6	181	62	laminar
210	A	3.6	31.1	25.0	0.6	174	59	laminar
220	A	3.4	29.8	25.0	0.6	167	57	laminar
230	A	3.3	28.6	25.0	0.5	161	55	laminar
240	A	3.1	27.5	25.0	0.5	155	53	laminar
250	A	3.0	26.5	25.0	0.5	150	51	laminar
260	A	2.9	25.6	25.0	0.5	145	49	laminar
270	A	2.7	23.6	25.0	0.5	134	46	laminar
280	A	2.6	22.9	25.0	0.4	131	44	laminar
290	A	2.5	22.2	25.0	0.4	127	43	laminar
300	A	2.4	21.5	25.0	0.4	123	42	laminar
310	A	2.4	21.0	25.0	0.4	121	41	laminar
320	opt	2.3	20.6	25.0	0.4	119	40	laminar
330	opt	2.2	20.3	25.0	0.4	117	40	laminar
340	opt	2.2	20.0	25.0	0.4	115	39	laminar
350	opt	2.1	19.6	25.0	0.4	113	39	laminar
360	opt	2.0	19.2	25.0	0.4	111	38	laminar
370	opt	2.0	18.8	25.0	0.4	109	37	laminar
380	opt	1.9	18.3	25.0	0.4	106	36	laminar
390	opt	1.9	17.9	25.0	0.4	104	36	laminar
400	opt	1.8	17.5	25.0	0.3	102	35	laminar

The convection type (laminar, turbulent or transitional) in the last column of the table is an indication for the wind situation near the surface of the cladding. It can be possible that increasing the thickness of insulation can cause a change from laminar to turbulent convection. This can be a reason for increasing surface temperature even if the insulation thickness is bigger than in the step before.

Rockassist (VDI 2055)
Online Thermal Calculation Tool

LICENSE HOLDER

Company Name	TU Delft
Contact	Lars Meeuwisse
Mobile	+31652112177
E-Mail	l.meeuwisse@student.tudelft.nl
Date	5/4/2024 9:04:16 PM
Page	4/4

PROJECT / CUSTOMER   **NOTES**

Project Name
Contact
Tel.
E-Mail

Message Type	Message
Warning	NOTE: You did not select a support construction for a vertical object. Please check the desing conditions.
Info	The required insulation thickness for tanks is calculated under worse case conditions. THis can especially for the tank bottom lead to extremely high heat losses. If this is the case please the heat loss should be calculated for the individual surfaces.
Info	For coolng of tanks its recommend increasing z* to avoid "unexpected" cooling of the medium by thermal bridges.

H

Sankey

(a) The total energy consumption of Coolworld Waalwijk, including standby, other production processes and subdivided energy consumption processes in the testing facility for a day in winter.

(b) The total energy consumption of Coolworld Waalwijk, including standby, other production processes and subdivided energy consumption processes in the testing facility for a day in spring

(a) The total energy consumption of Coolworld Waalwijk, including standby, other production processes and subdivided energy consumption processes in the testing facility for a week in winter.

(b) The total energy consumption of Coolworld Waalwijk, including standby, other production processes and subdivided energy consumption processes in the testing facility for a week in spring

Energy Balance Management Strategy

Energy losses and heat recovery in:

COOLING MACHINES - TESTING

Lars Meeuwisse

Coolworld Waalwijk

May the 20th, 2024

Table of Contents

Introduction

To give a better insight into the current energy use and where this energy goes, it has been decided to make an Energy Management Strategy for cooling machine testing facilities. With the help of this small booklet, it will be indicated how tools needed should be installed, which components the tools consist of, how they will be installed and how the measurement should take place.

The first paragraph gives small reasoning on what the targets are and how they will be tried to reach. Second, a methodology will be given with instrumentation and procedures. After this in the third paragraph, a case study is used to define what will be tested and how. After this, there is room for results. Results will be written down in an external Excel file, for calculation purposes. Next to this, a section is built with discussion points and remarks, as well as an FAQ.

This booklet is made with a case study. Namely the heat recovery of heat exchangers that are currently positioned in the testing facility for cooling machines at Coolworld Waalwijk. Other examples of tests that could be made are:

- Energy-consuming components such as buffer vessels
- Parts of the facility that are energy-consuming such as outdoor floor heating

For these another strategy can be used, this strategy is built to indicate what the methodology to achieve results could be and is purely indicational.

Target:

- Determine all objects in the testing facility
- Create an overview of the components
- Determine all circuits, to see how flows are flowing.
- Determine energy-intensive components, and determine their energy consumption
  - In this case the heat exchangers on the roof and their circuit
- Showcase the results
- Find energy-saving solutions
- (Built an energy consumption overview (Sankey)), not in this case study

Target:

Testing objectives in chronological order

Energy Definitions

Some energy definition examples are as follows with which calculations can be made. Energy, measured in different ways such as kWh or Joules in the Netherlands, is discussed with methods defined by Mills and Coimbra [28] and Smets, Jäger, et al. [3].

Heat

Heat is categorized into Sensible Heat (Equation 2.1), with no phase change, only temperature difference, and Latent Heat (Equation 2.2), associated with phase changes like melting.

Sensible Heat: $Q = m \cdot Cp \cdot (T2 - T1)$ where Q is heat absorbed (J), m is mass (kg), Cp is specific heat capacity (J/(kg·K)), and $T2 - T1$ is temperature difference.

Latent Heat: $Q = m \cdot L$, with L as specific latent heat.
Priority is given to sensible heat in calculations.

Thermal Conduction

Conduction involves heat movement within a material due to temperature differences, quantified by Fourier's law:

$$dQ cond dt = -k \cdot A \cdot dT dx,$$

where $dQ cond dt$ is the heat transfer rate (W), k is thermal conductivity (W/(m·K)), A is the surface area (m²), and $dT dx$ is the temperature gradient (K/m).

Thermal Convection

Convection transfers heat via fluid movement and is categorized into forced and natural types. The rate of heat transfer through convection, Qconv, is calculated by Newton's cooling law:

$$dQ \text{conv} dt = -h \cdot A \cdot (T1 - T2)$$

Heat transfer Coefficient (h)

Reynolds Number (Re): Indicates fluid flow type (laminar or turbulent).
$$Re = \rho \cdot u \cdot L \mu$$

Nusselt Number (Nu): Reflects the effectiveness of convective heat transfer.
$$Nu = C \cdot Rem \cdot Prn$$

Heat Transfer Coefficient (h): Derived from the Nusselt number and thermal conductivity.
$$h = Nu \cdot kL$$

Thermal Radiation

Heat is transferred through electromagnetic waves and is given by the Stefan-Boltzmann law:

$$Q_{rad} = \varepsilon \cdot \sigma \cdot A \cdot (T_{surface}^4 - T_{ambient}^4)$$

Where ε is the emissivity and σ is the Stefan-Boltzmann constant.

Method:

Plan of action:

Step	Action	Tools needed	Done?
1.	Create an overview of the components		☐
2.	Determine all circuits, to see how flows are flowing.		☐
3.	Make flow diagram	Drawing program	☐
4.	Determine energy-intensive components, and determine their energy consumption		☐
5.	Check the current testing procedure	Current testing description	☐
6.	Determine machines to check		☐
7.	Find tools/ instrumentation needed and order	See description	☐
8.	Place instruments in the facility		☐
9.	Determine temperature profile in piping/ exchangers/ silo etc.	Data log (XWEB)	☐
10.	Find the energy flow in piping/ exchanger/ silo etc.		☐
11.	Find out energy leakages, search for the biggest leaks		☐
12.	Make energy diagram	Excel/ MATLAB	☐
13.	Determine actual losses		☐
14.	Determine sustainable solutions to the leaks		☐

Determine all objects in the testing facility

Schematic overview

The first logical overview of all components needs to be made. The method to this is just by eye and following where which pipeline is going and to what next components this leads and discussing what this circuit is used for. This also includes all joints etcetera. This first version could simplify the declaration for possible energy leaks, which can come in handy for specific heat flow determinations. An example is shown below, this is a part of the Coolworld Waalwijk overview.
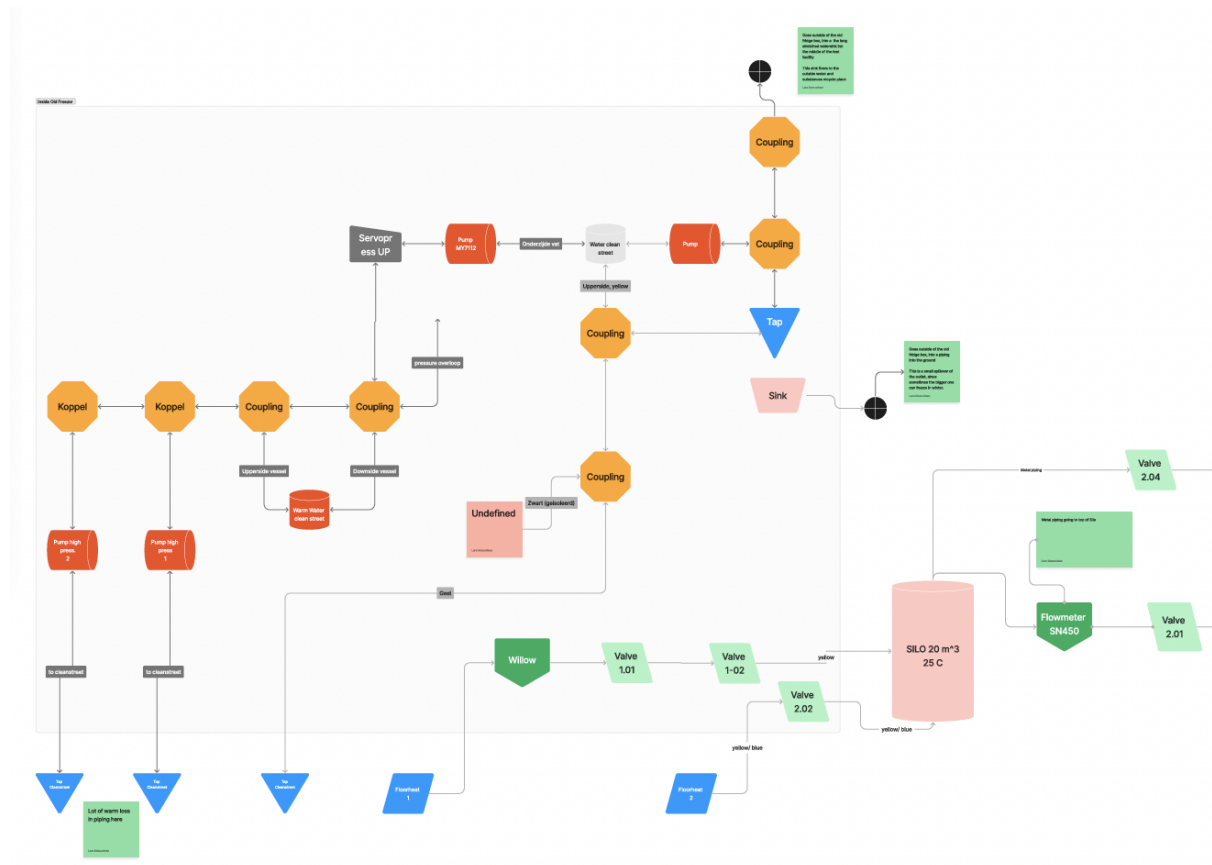
Instrumentation

This overview can be created with Figma. This is a free-of-charge educational programme and interchangeable use on multiple devices. This program lets you make a flow diagram with different adjustment possibilities and all sorts of components easily. A legend is coupled to the drawings.

Create an overview of the components

Topview overview

Second one needs to make a clear view of the setup as a whole, and easy to understand when teaching others about all types of components and the different heat and cold circuits that exist in the setup. That is possible with a Topview, as shown below:

Testplaats Waalwijk — Coolworld Nederland B.V., Duikerweg 34 5145 NV Waalwijk, Netherland, www.coolworld-rentals.nl, +31 416 688 088. Project nr., Date: 15-03-2024, Drawn by: ASS, Revision: A
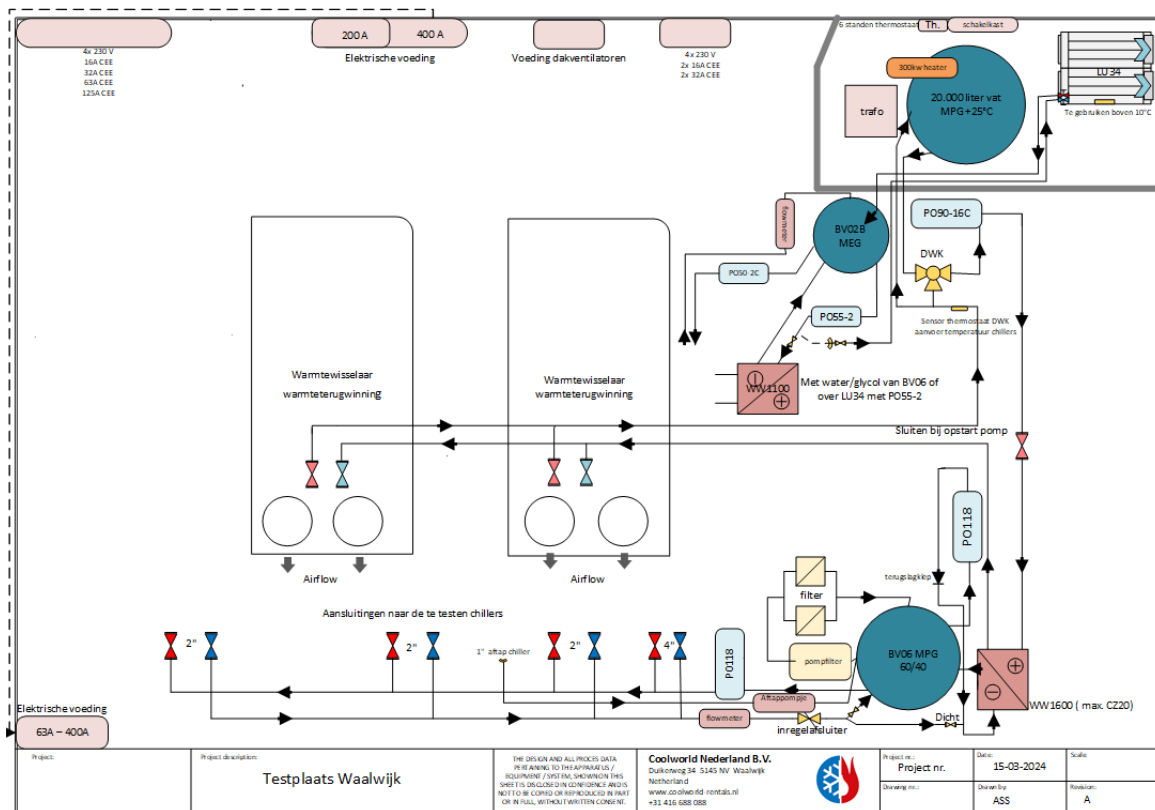
Instrumentation

The second drawing program is Microsoft (MS) Visio. With this, a more structured overview could be made with more possibilities. Results on this can be found in

Determine all circuits, to see how flows are.

Each circuit is an open or closed loop cycle with at least one pump, one buffer vessel, and a heat exchanger, cooling machine or other object. Every circuit has its working fluid and temperature and they are the core structure of the facility with which different measurements can be done. A basic structure of how each circuit flows, what its purpose is, what its working fluid is and what is connected by these should be of knowledge and therefore illustrated. An example is shown below of the cooling circuit for the machines.
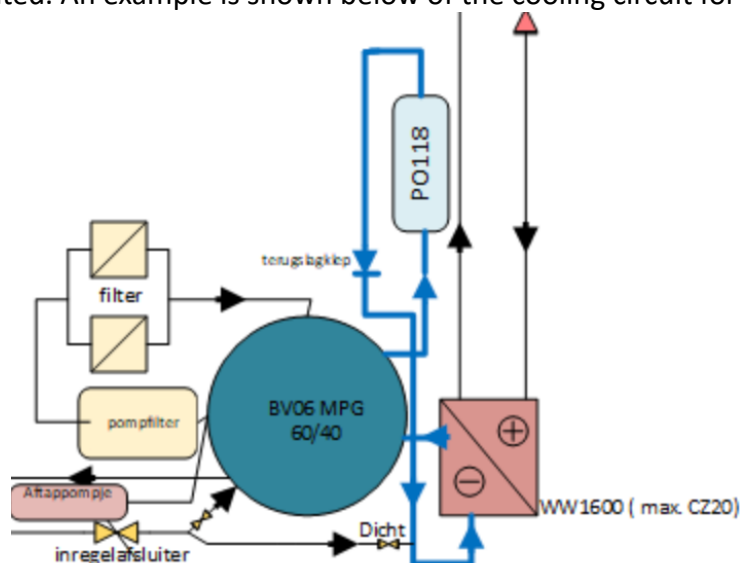
Determine energy-intensive components/ tests, and identify their energy consumption

All the circuits consist of multiple components which are at least the following. In the research attached to this booklet, the following split-up has been defined.

Components

Category	Description	Included in Study
Heat Exchangers	All exchangers are here taken into consideration, so both water to water as well as water to air	Yes
Silos	Vessels, tanks, and other liquid storage options	Yes
Hoses and Piping	Based on a business point of view, in which hoses are a big part of Coolworld's market, these are expected to be deliberately chosen	Yes
Pumps	Each circuit includes a pump which can build a consistent flow during operation	No
Couplings	Couplings are in two types, permanent and easy detachable/attachable	No
Valves/Taps/Liquids/ Other	All places where the flow can be adjusted with a tap	No

Each component is mentioned in the table above, a more specific example of Coolworld its 'Other' section can be found here, think of:

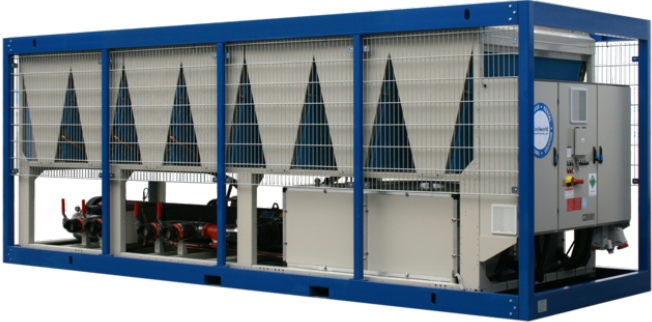| Component	Description	Not included in the study because
Filters	Filters the MPG glycol water in the cold circuit at the facility. These are in a separate circuit attached to the cold circuit vessel BV06, CC04. They are turned on 24/7	Since no possibility of energy reduction or leaving out of the system
Three Way Valve	Mixes the glycol water of the roof heat exchanger circuit, with the warm water of BV20, regulating the water that goes to the roof exchangers. It combines CC	Is to regulate the temperature in the circuits
Taps	Taps are used in the facility to control fluids and when needed change mixtures or get rid of dirt	They don't consume much energy and are all checked with safety pals when end parts are attached to ensure nothing will get lost
Valves	Are used to control flow motions or flow speeds	Most of them are manually used, so do not consume much energy, although controlled versions should be considered, more in the results
Liquids	The liquids used in the cooling circuits are known since they have the performances and do not need investigation, the heating circuits on the other hand, are a mixture of residuals	For the mixture, it could be beneficial to determine performances, for pumping and so the used energy for it

Testing Method

The current test procedure of Coolworld Waalwijk is shown below;

Coolworld Heatworld

Coolworld Nederland BV duikerweg 34 5145 NV Waalwijk	Testplaats NL	
Verzoek Datum:	Unit Nummer:	Verhuur Order:

Werkomschrijving	
Algemeen Onderhoud, Lektest	
Return Check	
Running Test	
F-gas Inspectie	

	Omschrijving				Omschrijving	
1	Stroom/Carterverw. Int/Ext. Voeding Ok		A	26	Water/Glycol Pomp/Voed Ok	A
2	Waterfilter Schoon/Ok			27	Water/Glycol Stromingsschakelaar Ok	
3	Instellingen **Klant / Standaard**			28	Water/glycol Temp./Druk In (EWT)	
4	Bijzonderheden Alarm Historie/Wissen			29	Water/glycol Temp./Druk Uit (LWT)	
5	Setpunt/Mode Test		°C	30	Warmte Wisselaar Schoon	ΔP
6	Type/Serienr. Lekdetector		Tapzx1A	31	Condensor Schoon/Onbeschadigd	
7	Koelschema Beschikbaar			32	Frequentie Regelaar(s) Schoon/Ok	
8	Omgevingstemperatuur (OAT)		°C	33	Cond.Ventilator Motor Stroom	
9	Mano/Temperatuurmeters Ok			33	1 A 2 A 3 A 4 A	
10	Persdruk/Temp. Circuit 1	b	°C	33	5 A 6 A 7 A 8 A	
11	Zuigdruk/Temp. Circuit 1	b	°C	33	9 A 10 A Gem van 3Ph !	
12	Persdruk/Temp. Circuit 2	b	°C	37	Stickers Coolworld Ok	
13	Zuigdruk/Temp. Circuit 2	b	°C	38	Casco/Constructie Ok	
14	Vloeistoftemp. Circuit 1 / 2	°C	°C	39	Verf/Uiterlijk Ok	
15	Compr. Motor Stroom Circuit 1		A	40	Staat Bedrading/Schakelkast(en) Ok	
16	Compr. Motor Stroom Circuit 2		A	41	Relais/Timers/Beveiligingen Ok	
17	Filterdroger(s) Ok			42	Controle Verlichting/display Ok	
18	Lagedrukveiligheid Ok/Getest			43	Schakelkast(en) Filters Schoon	
19	Hogedrukveiligheid Ok/Getest (5Jr)			44	Draai Uren Compr.	
20	Kijkgla(s)(zen) Vol/Droog			45	Start/Stop Compr.	
21	Magneet Spoel(en)/Ventiel(en) Ok			46		
22	Expansieventiel(en) OK / Opening		%	47	Werking Daikin on Site Ok	
23	Circuit/Compressor Olie Niveau Ok 1x/Jr			48	Datum Volgende NEN 3140 Keuring	
24	Olie verschildruk (>150 kPa Filter!)		b	49	Juiste Onderhouds Stickers Geplakt	
25	Olie Zuurtest Uitgevoerd 1x/Jr			50	Reparatiekaart Ingevuld	

Materiaal & Uren Registratie			Koudemiddel Registratie			
Materiaal code		Aantal	Koudemiddel	R134A	R407C	R410A	R32
			KG				
			GWP	1430	1774	2088	675
			T-CO2EQ				
Monteur	Datum	Aanvang	Einde	Gew.Voor:		Reden/Lekage:
				Gew.Na:		
				Gevuld:		Ja	Nee
				Rekening Klant:		
				Werkzaamheden Gereed:		

Find processes that are energy intensive and what could be done differently, at a different moment (at the customer?) or what could produce a lot of rest heat, which could be captured.

Machines to test

At first, it would be most interesting to find differences between different types of machines, and if this would fit in the current testing procedure. Otherwise, find all the components and test with possible options. Interesting are the oldest and newest machines for comparison. Include the biggest as well compared to a smaller one.

Machine type	Name	Age (yr)	Power (kW)	Refrigerant	Image
Old	CZ17	17	170	R410	
Big/ new	CZ80iH	<3	800	R134a	

Case Study: Heat Exchangers Roof Coolworld Waalwijk.

The main test for the facility of Coolworld Waalwijk is taken as a case study and shown below, the Heat Exchangers in the roof section will be tested on their performances.

Tools

At first, an investigation was done on sensors from outside of CW's warehouse products. That is how the energy measurements outside of CW can be ordered and done. Budget wise it is more appealing to make use of products that are so-called in-house and therefore easier to implement, cost-wise cheaper. Besides, from a sustainable point of view, can certain objects be reused after the termination of measurements?

It has therefore been decided to make a tool list for in-stock measurement tools. If some do need to be achieved differently this should be considered wisely if it is worth the investment, and if the ordered products can have a second purpose after testing. The installation will be a bit different from one another, but since the use of 'in-house' products has been decided to implement and these products are currently known, installation of these is the only method considered in this study.

Instrumentation

To determine the heat exchange between different in- and outlets, sensors, data logs, remote monitors and modems need to be installed. An overview of the components that could be used within Coolworld's operating fleet. The actual sensors are named with a few important characteristics. It has been decided to work as much as possible with instruments that are currently so to say 'in-house'. These are 'off-the-shelf' products that are normally used in repairing procedures.
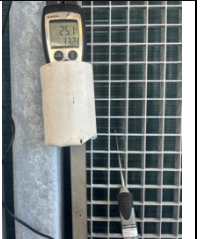
Controllers and data logs

To log data and send it to the needed environment two types are considered. First, there is the collection of data, which happens in a controller, second is the transformation of this to the online environment. See below.

Brand	Type	Description	Image
DIXELL XR 570 C	Controller	Mainly used in refrigeration and air conditioning systems. It is specified as temperature and humidity control and at Coolworld it is mainly used as a measurement controller. In this setup, it is detached from a data log.	
Coolworld RM04010	Server	This is a specific module with a wireless connection to save data of different controllers and send it to an online environment (XWeb) for real-time monitoring and analysis. This data can be downloaded.	--

Temperature Meters

For the determination of energy in flows, the temperature is needed. For this, three different types are considered. One is a permanent installation, the probe, second is for temporary measurements such as the infrared and double mete. All of them are summed up in the table below.

Brand	Type	Description	Image
Dixell	Probe	Temperature probes are attached to pipes and in environmental air to measure the temperature of heat and cold flows within various parts of the facility. These probes are placed either in air streams of heat exchangers or on piping with insulation tape.	
Hioki	Infrared	With this meter, the adequacy and constructiveness of the data generated by temperature probes are checked. It is also used for immediate temperature measurements on-site.	
Testo 922	Double K type A	Testo double input temperature difference sensor is used to determine two individual temperatures and measure the ΔT.	

Electrical Energy Meters

For the determination of energy, AC clamps are used. For this, two types are considered: one with a datalogging function, and the other without. Both of them are summarized below.

Brand	Type	Description	Image
Hioki	AC clamp	Used for short-term energy determination and checking on amperage. The Fluke FC3000i, which includes data logging, is employed for long-term energy determination.	
Fluke FC3000i	AC Clamp	Can be used for longer measuring processes like days and weeks. This clamp was able to measure over different cables at the same time. With wireless connectivity, a log could be shared with a mobile device.	--

Flow Meters

A few different flow meters have been used during the testing. Each circuit has its flow meter installed. The following table (F.4) shows which flow meters are used within the testing facility. Airflow meters are also included in this scheme, but this of course has a tolerance that it could differ from the actual wind speed due to turbulence.

13

Brand	Type	Description	Image
Endress & Hauser Proline P 300	Electro-magnetic	Is used for the flow in a cold liquid circuit.	
Siemens	Pressure	Cooling machines flow	--
Testo 410-1	Anemometer	Airflow cooling machine outlet	

Calculation Programs - Excel/MATLAB

For data processing, both MATLAB and Excel can be used. To facilitate easy implementation, an Excel layout has been chosen at other facilities, which allows data to be implemented to calculate different outputs for measurements.

Visualisation Programs - Excel/ Python/ SankeyMATIC

Visualisation programs are used to give an overview of the current energy needs and measurements and to also complete energy flow overviews. Data measurements are produced in Excel and Python to create consistency in the layout. This approach is not mandatory but is preferred, especially for papers such as this one. More detailed information on this strategy and the positioning of sensors can be found in the next sections

Target measurements

- Flow determination with:
  - Flow meters
- Temperature measurements
  - Determine:
    - The temperature on outside of the piping and approach inside temp, since industrial, is valid, at marked spots
    - Insulation of piping
    - Delta T (in -/- outlet)
- Voltage measurements
  - Determine actual energy usage
  - Use as validation
- Machine measurements
  - Validation checks with:
    - Electricity usage for cooling characteristics
    - DaikinOnsite

Measurement points:

Explanation layout:
1. Is measure point
a. Option 1
b. Option 2

Temperature:

Glycol: (1 heat exchanger)
1. Inlet temperature glycol machine
    a. Machine thermometer – built-in
    b. Piping thermometer – temporarily
2. Outlet temperature glycol machine
    a. Machine – built-in
    b. Piping thermometer – temporarily
3. Inlet glycol heat exchanger
    a. Piping thermometer permanent (long cable/ wireless)
    b. Infrared thermometer
4. Outlet glycol heat exchanger
    a. Piping thermometer permanent (long cable/ wireless)
    b. Infrared thermometer

Air:
1. Inlet temperature air in the machine
    a. Ambient temperature around the machine (thermometer in the corner)
2. Outlet temperature air machine
    a. Thermometer stick
3. Inlet air underside of heat exchanger – see picture
    a. Through existing PVC piping – permanent
    b. Infrared thermometer – temporarily
4. Outlet air upper side of the heat exchanger – see picture
    a. Through existing PVC piping – permanent
    b. Infrared thermometer – temporarily

All the temperature outlets, so for the probes, will be mounted in the corresponding spot in the Remote Monitoring Modem (RM)

Glycol:
1. Inlet flow glycol machine = Outlet
    a. Siemens flow meter (built-in)
    b. Pump characteristics (approach)
2. Inlet glycol heat exchanger = Outlet
    a. Pump characteristics (approach)
    b. Flow meter (temporarily)

Air: Very turbulent, better to use Glycol
1. Inlet flow machine = same for outlet (can you assume this?)
    a. Machine flow meter, amount of air being pushed (datasheet) – calculate on:
        i. Environment temperature
        ii. Power for fans
        iii. Fans wind displacement
    b. Anemometer
2. Inlet air heat exchanger = same for the outlet
    a. Fan flow meter, amount of air pushed by fans (datasheets – calculate on:
        i. Environment temperature
        ii. Power for fans
        iii. Fans wind displacement
    b. Anemometer

Energy:
1. Energy cooling machine
    a. Machine output (read)
        i. Fans on top of the machine
    b. Amperage meter machine with Hoiki
    c. Determine with Enthalpy – Pressure Diagrams
2. Energy fans on heat exchanger roof
    a. Amperage meter on connection (one-time measurement)
3. Pump for:
    a. Machine glycol (changes per machine)
    b. Glycol heat exchanger roof (one-time measurement/ if the temperature is +/- constant (viscosity))

Results

Graphs

Remote monitoring login information can be found on a specific website, you can ask your local logistics or service operator for this information. In this case study it was with the help of. Site: http://cwrm01040.coolworld-rentals.net/

Figures such as the following are possible to make.
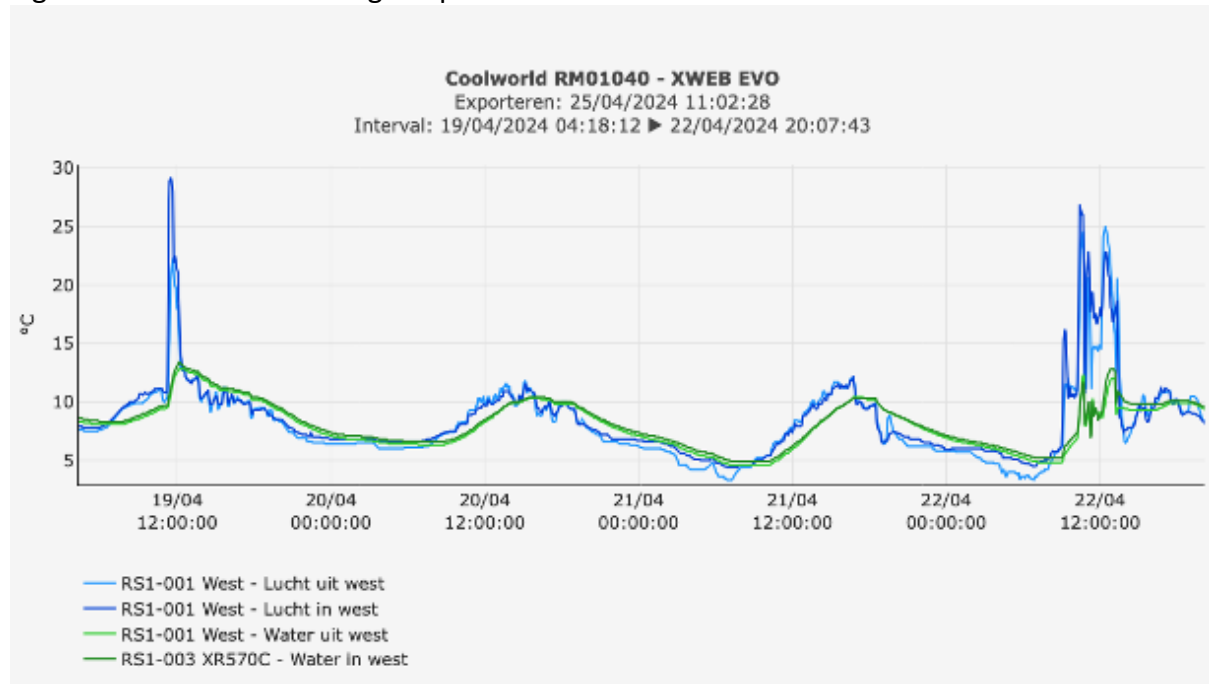
This overview shows the water in and outlet temperature and air in and outlet temperature. With this and the help of MATLAB or Excel, one can create more detailed information such as a temperature profile of Delta T between 10 am and 4 pm, working hours. More can be found in the corresponding paper.
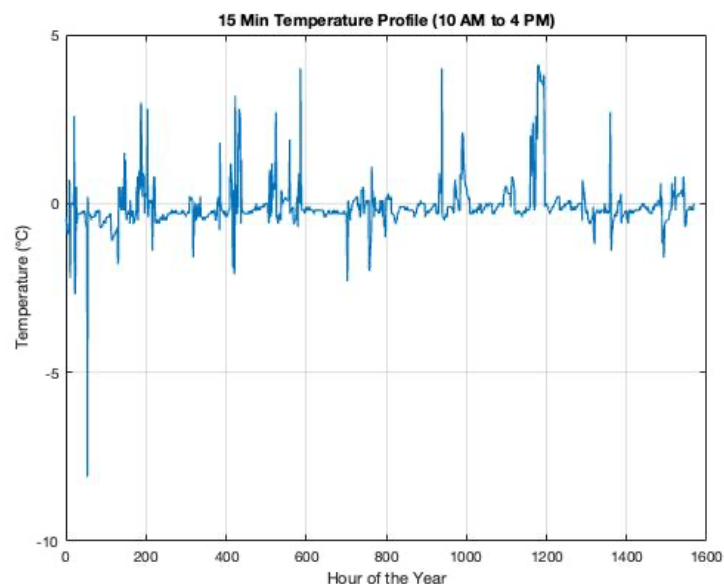
Problem:

It was found that the current testing method is not recovering as much energy as suggested. The temperature profile depicts that there are also losses when Delta T is below zero.

The heat profile showcases this with the areas below zero being losses.
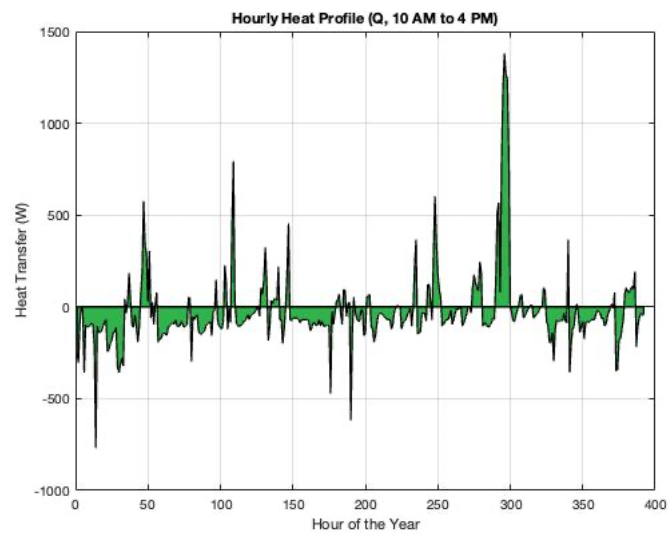
Solution:

A solution is proposed, in this case, more heat capture can be obtained by changing the testing setup, as can be seen below, this is yet not optimal, since it is still lost as can be seen, due to the bulging curtain.

$DT_{heat-ex.}$ and $DT_{coolmachine}$ on 10-04-2024

$Q_{heat-exchanger}$, $Q_{coolmachine}$, and P_{el} on 10-04-2024
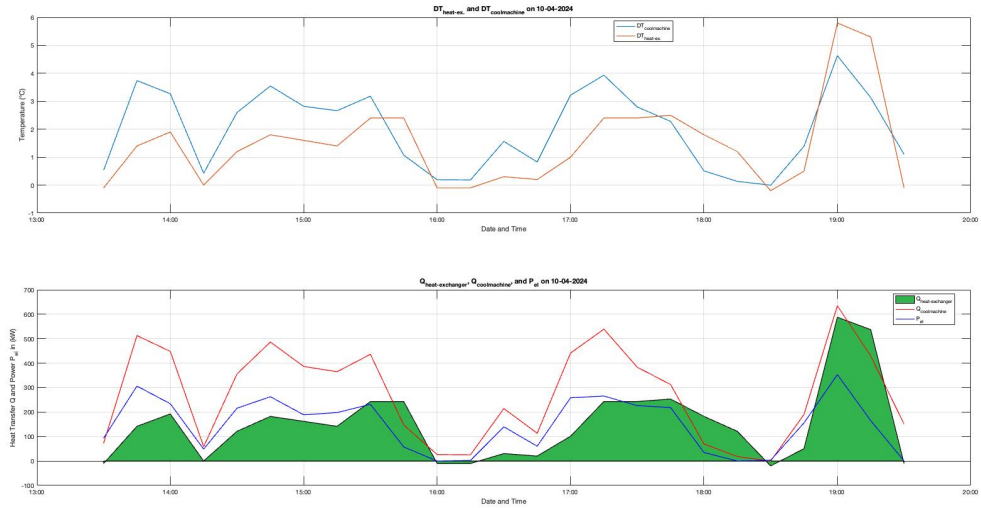
When looking at this graph different schedules with different measurements are visible. More details of this are to be find in the attached paper, explaining on different set ups and heat recovery with it.

Discussion/ Remarks

Temperature sensors
- The sensors are not always calibrated or fully insulated.

Measuring
- Approaches needed to be made for example for flow

Case study
- This is a case study with an example solution. So not every possible solution or method to it is given.

FAQ

1. What supplier is used to buy elements and tools?
   a. Find current suppliers used, to have the easiest communication internally and externally.
2.

Attachments

An initial description is given of how to for example specify measurement tools, to find their belonging stock numbers, this is not worked out any further since it goes into details that are not of any necessity.

Temperature
With the temperature sensors that are currently already being used for repairing purposes, the following group of products needs to be ordered from the warehouse manager or lent for temporary usage. This list is based on 2 heat exchangers for heat recovery in the facility. Some products will need to be ordered and can be found in the second subpart of this chapter.

Log system

Name	Type	Sort	Type number	Needed
CO	Controller	Built-in controller	12744	3
PO	Power to modem etc.	Power supply		1
RM	Modem/ antenna	Remote Monitor	RM01040	1

Thermometers 2 heat exchangers:

Name	Type	Sort	Type number	Needed
MA	Machine (internal)	Machine in and out	X	
IR	Infrared	Infrared sensor	X	1
ST	Stick	Sensor (Wireless)	X	1
TS	Temp sensor	Sensor (wired)	21661	8

Flow Meters/ air

Name	Type	Sort	Type number	Needed
CH	Chiller	Internal meter	X	X
FM	Flowmeter	Anemometer	X	X
PM	Pump	Internal meter	X	X
TF	Flowmeter	Internal Tube meter		

Amperage/multi-meters

Name	Type	Sort	Type number	Needed
AM	Ampere meter	Fluke		1

Side tools:

Name	Type	Sort	Type number	Needed
LA	Laptop	Inside pump	X	1
DP	Data program	Excel	X	1
PA	Paste	Conductive Paste	X	1
TA	Tape	Armaflex	X	1

From external suppliers
Since this step is not chosen in the process, only descriptive advice is given.

Temperature
- Tube clamp temperature sensors
- Air temperature sensors
- Wire extensions
- Infrared thermometer (for checking purposes)
- Wired or wireless log meter

Can be ordered from local/ regional sensor suppliers

Thermometers 1 heat exchanger:

Name	Type	Sort	Available	Needed
BS	Buisstok	Sensor	1	1
BKG	Buisklem Glycol	Sensor (cable)	….	4
BKA	Buisklem Air	Sensor (wireless)	….	2
MA	Machine	Machine in and out	1	1
IR	Infrared	Infrared sensor	1	

Flow Meters/ air

Name	Type	Sort	Available	Needed
PM	Pump	Inside pump	X	x
FM	Flowmeter		X	X

Amperage/multi-meters

| Name	Type	Sort	Available	Needed
MM	Multimeter	Inside pump	1?	
FM	Flowmeter		X	X

# Working principles PV, solar collector and PVT

J.1. PV

To understand this process, first, a small description of the working principle of a PV panel is written which can be found below.

The generation of electricity in PV cells starts when sunlight, which consists of photon energy, penetrates the thin p-type layer, reaching the p-n junction. Here, the photon energy from sunlight is enough to create multiple electron-hole pairs, disrupting the junction's thermal equilibrium. When electron density increases on the n-type side and hole density rises on the p-type side of a junction, the p-n junction starts to function as a miniature battery. This creates a potential difference, referred to as the photo-voltage. Connecting a small load across this junction results in a modest current flow. In Figure J.1a below this is illustrated:
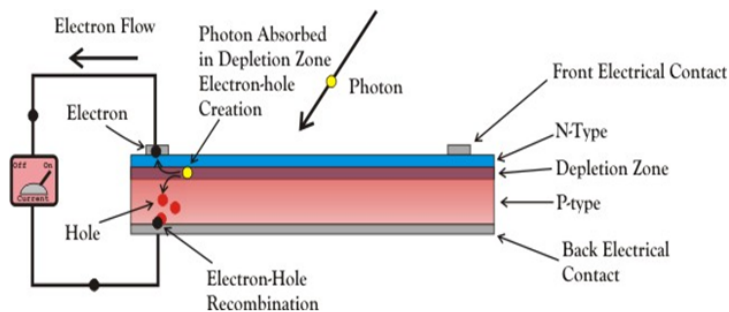
(a) The working principle of a PV solar cell schematically illustrated, source: Sharaf, Yousef, and Huzzayin [46]
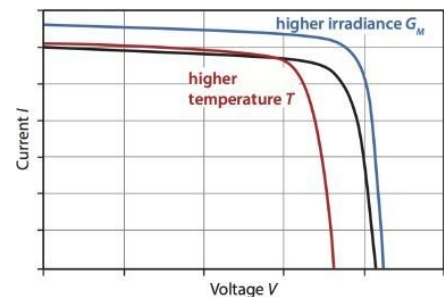
(b) Effect of increased temperature T or irradiance G_M on the I-V curve., source: Smets, Jäger, et al. [3]

Figure J.1: Working principle of a PV cell and Current - Voltage diagram

Temperature significantly impacts a PV cell's performance, primarily by increasing the circuit's resistance, which then reduces electron mobility, this affects the open-circuit voltage, the temperature coefficient, and can degrade the cell's material. In this paper, only the electron mobility and associated power output are taken into consideration and not the amount of cell degradation and therewith its lifespan.

J.1.1. Buildtype

A few examples of PV solar techniques are summed up in the following paragraphs a short sum-up on this can be seen in Table J.1 [20].

**Table J.1:** Performance and Characteristics of Different Types of PV Cells

Type	Eff. (%), η_{el}	Wp (W)	NL Market	Costs	Temp. Coeff. (%/°C),γ
Monocrystalline (m-Si)	15-22	250-350	High	Higher upfront costs	-0.4 to -0.5
Polycrystalline (p-Si)	12-18	200-300	Moderate	Cost-effective	-0.4 to -0.5
Thin-Film (a-Si)	10-13	N/A	Limited	Lower production costs	-0.35 to -0.38
CIGS	15-22	150-250	Increasing	Competitive	-0.32 to -0.36
Multijunction	>30	500-1000	Specialized	High	Varies

Different types of PV cells exhibit varying performance characteristics: **Monocrystalline panels**, known for high efficiency (15-22%) and higher costs, are constructed from a single silicon crystal, offering uniform energy conversion that decreases slightly with temperature increases. **Polycrystalline panels**, made from multiple silicon crystals, are more cost-effective with efficiencies ranging from 12-18% and also show reduced performance at higher temperatures. **Thin-film panels**, including amorphous silicon and CIGS (Copper Indium Gallium Selenide), offer lower efficiencies (10-13% for a-Si and 15-22% for CIGS) but benefit from lower production costs and minimal temperature impact, suitable for flexible applications and irregular surfaces. **Multijunction solar cells** utilise multiple layers to capture a broader spectrum of sunlight, achieving efficiencies over 30%, but are primarily used in specialised settings like space applications due to their high cost. These distinctions underscore the trade-offs between cost, efficiency, and suitability for specific applications.

For monocrystalline and polycrystalline solar panels, the temperature coefficient typically ranges from -0.3% to -0.5%. This means that for every degree Celsius above the standard testing conditions (STC), the efficiency of these panels decreases by the specified percentage. Thin-film solar panels, including CIGS cells, generally have lower temperature coefficients, ranging from -0.2% to -0.3%, indicating a more stable performance in varying temperatures. Numbers can be found in Table J.1.

J.2. Solar Thermal Collector

For solar panels collecting solar heat, the amount of collection depends on the total solar irradation, minus the amount of losses. Figure J.2 Shows a visualisation of each component.
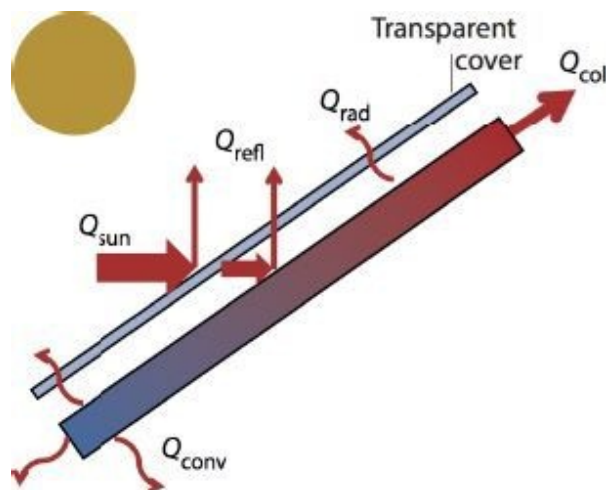
Figure J.2: Solar collector collection and losses, source: [3]

In equation form this can be written as in Equation J.1, below.

$$Q_{\text{col}} = Q_{\text{sun}} - Q_{\text{refl}} - Q_{\text{conv}} - Q_{\text{rad}} \tag{J.1}$$

In which the losses are as defined in the equations that are stated in Appendix A. Some are rewritten, see the following equations. The solar radiation absorbed by the collector is also found in **??**

$$Q_{\text{sun}} = I \cdot A \tag{J.2}$$

where I is the solar irradiance (W/m^2), and A is the area of the solar collector (m^2).

The **reflected** solar radiation:

$$Q_{\text{refl}} = \rho \cdot Q_{\text{sun}} \tag{J.3}$$

where ρ is the reflectivity of the collector surface (dimensionless).

The **convective** heat loss from the collector: see Equation A.4

$$Q_{\text{conv}} = h_c \cdot A \cdot (T_{\text{s}} - T_{\text{a}}) \tag{J.4}$$

where h_c is the convective heat transfer coefficient (W/(m^{2}K), T_{surface} is the temperature of the collector surface (K), and T_{air} is the ambient air temperature (K).

The **radiative** heat loss from the collector: see Equation A.8.

$$Q_{\text{rad}} = \varepsilon \cdot \sigma \cdot A \cdot (T_{\text{s}}^4 - T_{\text{a}}^4) \tag{J.5}$$

where ε is the emissivity of the collector surface (dimensionless), σ is the Stefan-Boltzmann constant, T_{s} is the temperature of the collector surface (K), and T_{a} is the ambient air temperature (K).

Total heat generation can then be derived as:

$$Q_{col} = A \cdot I \cdot (1 - \rho) - h_c \cdot A \cdot (T_s - T_a) - \epsilon \cdot \sigma \cdot A \cdot (T_s^4 - T_a^4) \tag{J.6}$$

Then the efficiency of the collector is determined by two factors, namely:

1. The extent to which sunlight is converted into heat by the absorber
2. The magnitude of heat losses to the surroundings

This gives the efficiency for the collector, being:

$$\eta_{col} = \frac{Q_{col}}{Q_{sun}} \tag{J.7}$$

In a different way, one could use the absorptivity of the solar collector, which is stated by the absorptance coefficient α, to define the energy generation, this gives

$$Q_{col} = I \cdot A \cdot \alpha \tag{J.8}$$

Which makes the same as taking all losses from the actual solar irradiance that are lost in the collector. This can be described as the Removal Factor (FR) as well.

J.2.1. Buildtype
Different types of solar collectors exist, and are named below in Table J.2, [47]
Solar collector technologies vary in efficiency, operational temperature ranges. **Glazed Flat-Plate Collectors** feature a glass cover that enhances efficiency to 70-75% by reducing heat loss, suitable for domestic hot water systems with operational temperatures between 30-80°C. **Unglazed Flat-Plate Collectors**, are less expensive and without a cover, they can achieve 60-65% efficiency and are optimal for pool heating up to about 35°C. **Evacuated Tube Collectors** offer superior insulation and efficiencies of 70-90%, operating effectively up to over 100°C, making them ideal industrial applications. **Concentrated Solar Power (CSP)** systems, utilising mirrors or lenses to concentrate sunlight, generate steam

Table J.2: Typical efficiencies, operational temperature ranges, price, and market shares of various solar collector types in NL.

Type	Eff. (%) η_{th}	Operational T (°C)	NL Market	Costs
Glazed Flat-Plate Collector	70-75	30-80	High	Higher upfront costs
Unglazed Flat-Plate Collector	60-65	Up to about 35	Moderate	Cost-effective
Evacuated Tube Collector	70-90	Up to over 100	Increasing	Competitive
Concentrated Solar Power (CSP)	15-25	300-500	Specialised	High
Solar Air Collector	30-70	50-90	Limited	Lower production costs

for electricity with efficiencies between 15-25%, operating at high temperatures (300-500°C) and are primarily used in large-scale power generation. **Solar Air Collectors**, used for space heating, vary in efficiency from 30-70% and use air as the working fluid, which are therefore not considered any further. Heat loss for the storage tank can be calculated with Equation J.9

$$Q_{\text{loss}} = U \cdot A_{surface} \cdot \Delta T, \tag{J.9}$$

For U a global heat exchange number is usually used. But since this calculation is included in subsection 2.6.2 this one will be used instead and built in.

So the total amount of storage needed depends on the energy consumption. Since seasonal storage is too much, the scope is derived to a day and a week of use. Based on this the storage capacity is made, based. Combined with the energy losses, a total of the storage demand is calculated

$$Q_{\text{storage}} = Q_{\text{consumption}} + Q_{\text{loss}} \tag{J.10}$$

J.2.2. The working principle

The working principle of a PVT module has partly been explained in section 1.3. For this research it has been decided to showcase only the model chosen to work with out the MATLAB model that will be elaborated on in the paragraphs.

The energy generation is based on both thermal and electrical energy that is collected by the sun's solar radiation. It can therefor be seen as a combination of above-mentioned's working principles. Though a small alteration need to be considered. Namely the interaction between the two types of modules. The lay out is as follows, see Figure J.3a.

(a) PVT collector layout, source: [48]   **(b)** PVT collector layout, source: [49]
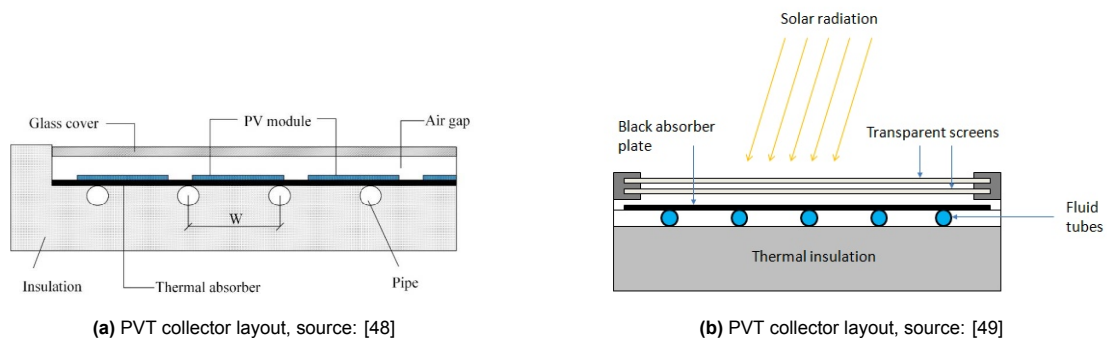
Figure J.3: Working principle of a PV cell and Current - Voltage diagram

For comparison the layout of a solar collector cross section is shown beside from it in Figure J.3b. From this point of view it is easy to understand the difference, and how their energy generation is. Which is

effectively for thermal energy Equation J.8

In PVT panels, the total energy output is comprised of two parts: the electrical energy generated by the photovoltaic cells and the thermal energy captured by the thermal system. With the equations from, Appendix A, combined with section 4.2 and section 4.3 the following output equations are defined for the PVT collector.

J.2.3. PV Thermal: Working Principle

As the name already suggests, is this type of module the combination of the two above-mentioned types of panels combined. A fully working principle will therefore not be given since many different types and combinations exist. A few examples are given in the section below, after which one type is chosen and of which a more detailed description will be given.

J.2.4. Buildtype

Different types of PVT panels exist, a few are named in the paragraphs below, a distinction will be made between them, and a decision for which panel would be the most interesting to implement in the Coolworld Rentals ecosystem for sustainable energy generation. Most panel types are based on existing PV types and collector types and make a PVT panel when combined.

Table J.3: Overview of PVT Panel Types and Characteristics

Type	Eff (%), η_{el}	Eff (%), η_{th}	NL Market	Costs	Op. T (°C)
Uncovered PVT Collector	15-23	45-70	Moderate	High	25-95
Covered PVT Collector	12-18	45-70	Moderate	High	30-120
Concentrated	18-25	50-75	Specialised	Higher upfront	80-250
PCM Integrated	15-20	-	Low	Higher upfront	30-55
Water-Based	15-23	40-80	High	Moderate to high	30-90
Air-Based	15-23	10-25	Limited	Lower production costs	40-85

PVT (Photovoltaic Thermal) panels integrate photovoltaic modules with thermal systems to simultaneously generate electrical and thermal energy, enhancing overall efficiency. **Uncovered PVT Collectors** and **Covered PVT Collectors** share similar thermal efficiencies (45-70%) but differ in electrical efficiency (15-23% for uncovered vs. 12-18% for covered) and operational temperatures, with covered versions capable of higher maximum temperatures, up to 120°C. **Concentrated PVT (CPVT) Systems** use optics to focus sunlight onto high-efficiency cells, offering elevated electrical (18-25%) and thermal efficiencies (50-75%) at higher operational temperatures (80-250°C), making them ideal for regions with intense solar irradiance. **PCM Integrated PVT Systems** are baseed on phase change materials to store and release thermal energy effectivelybut this is out of scope due to a different working fluid at Coolworld Waalwijk. Lastly, **Water-Based PVT Systems** are prominent for their high thermal efficiency range (40-80%) and moderate costs, contrasting with **Air-Based PVT Systems**, which offer lower thermal efficiency (10-25%) but are less expensive and suitable for lower temperature applications (40-85°C), but the latter will also not fit in the curren setup at Coolworld

K
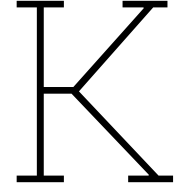
MATLAB method:

Initially, we define ϕ_0 as the latitude and λ_0 as the longitude of the observer's position. To model the Sun's trajectory as observed from Earth, we commence by identifying the time interval D, elapsed since the most recent noon at Greenwich. The source *Solar Energy: The physics and engineering of photovoltaic conversion technologies and systems* [127] underscores the significance of D in calculating the solar path. The Julian Date JD, which originates from the 24th of November, 4717 BC in the Gregorian calendar, is used to determine D:

$$D = JD - 2451545 \tag{K.1}$$

Subsequent to establishing the time interval, we proceed to calculate the Sun's mean longitude θ and the mean anomaly g. The mean anomaly is influenced by the Earth's elliptical orbit:

$$\theta = 280.459° + 0.98564736° \cdot D \tag{K.2}$$

$$g = 357.529° + 0.98560028° \cdot D \tag{K.3}$$

To determine the Sun's ecliptic longitude λ_S:

$$\lambda_S = \theta + 1.915° \sin(g) - 0.020° \sin(2 \cdot g) \tag{K.4}$$

A transformation of coordinates from ecliptic to equatorial is necessary for practical application in an Earth-based system, accomplished through the angle ϵ:

$$\epsilon = 23.439° - 0.00000036° \cdot D \tag{K.5}$$

The calculation of Terrestrial Time T is essential, marking the centuries since the latest Greenwich noon:

$$T = \frac{D}{36525} \tag{K.6}$$

The Greenwich Mean Sidereal Time (GMST) is first computed, setting the stage for the Local Mean Sidereal Time (LMST) calculation:

$$GMST = 18.697374558 + 24.06570982441908 \cdot h \cdot D + 0.000026 \cdot h \cdot T^2 \tag{K.7}$$

$$\theta_L = GMST \cdot \frac{15°}{\text{hour}} + \lambda_0 \tag{K.8}$$

Finally, with the precise date, time, and observer's geolocation, the Sun's position in the sky, including altitude a_S and azimuth A_S:

$$\sin(a_S) = \cos(\phi_0)\cos(\theta_L)\cos(\lambda_S) + [\cos(\phi_0)\sin(\theta_L)\cos(\epsilon) + \sin(\phi_0)\sin(\epsilon)]\sin(\lambda_S) \tag{K.9}$$

$$\tan(A_S) = \frac{-\sin(\theta_L)\cos(\lambda_S) + \cos(\theta_L)\cos(\epsilon)\sin(\lambda_S)}{-\sin(\phi_0)\cos(\theta_L)\cos(\lambda_S) - [\sin(\phi_0)\sin(\theta_L)\cos(\epsilon) - \cos(\phi_0)\sin(\epsilon)]\sin(\lambda_S)} \tag{K.10}$$

$$\tan(A_S) = \begin{cases} \frac{\sin(\lambda_S)}{\sin(\theta_L)} & \text{if } \sin(\lambda_S) > 0 \text{ and } \sin(\theta_L) > 0, \\ \frac{\sin(\lambda_S)}{\sin(\theta_L)} & \text{if } \sin(\lambda_S) < 0, \\ \frac{\sin(\lambda_S)}{\sin(\theta_L)} & \text{if } \sin(\lambda_S) > 0 \text{ and } \sin(\theta_L) < 0, \end{cases} \tag{K.11}$$

$$A_S = \begin{cases} \arctan(\tan(A_S)) & \text{if } \sin(\lambda_S) > 0 \text{ and } \sin(\theta_L) > 0, \\ \arctan(\tan(A_S)) + 180° & \text{if } \sin(\lambda_S) < 0, \\ \arctan(\tan(A_S)) + 360° & \text{if } \sin(\lambda_S) > 0 \text{ and } \sin(\theta_L) < 0. \end{cases} \tag{K.12}$$

$$\tan(A_S) = \begin{cases} \frac{\sin(\lambda_S)}{\sin(\theta_L)} & \text{if } \sin(\lambda_S) > 0 \text{ and } \sin(\theta_L) > 0, \\ \frac{\sin(\lambda_S)}{\sin(\theta_L)} & \text{if } \sin(\lambda_S) < 0, \\ \frac{\sin(\lambda_S)}{\sin(\theta_L)} & \text{if } \sin(\lambda_S) > 0 \text{ and } \sin(\theta_L) < 0, \end{cases} \tag{K.13}$$

$$A_S = \begin{cases} \arctan(\tan(A_S)) - 180° & \text{if } \sin(\lambda_S) > 0 \text{ and } \sin(\theta_L) > 0, \\ \arctan(\tan(A_S)) & \text{if } \sin(\lambda_S) < 0, \\ \arctan(\tan(A_S)) + 180° & \text{if } \sin(\lambda_S) > 0 \text{ and } \sin(\theta_L) < 0. \end{cases} \tag{K.14}$$

K.0.1. Electrical, temperature efficiency

The effect of the temperature on the PV module's performance can be defined by information from the datasheet of the panel, which can be found in: **??** and below in Table 4.2. By implementing a temperature related coefficient, such as V_{oc}, I_{sc}, P_{mpp} of the efficiency η, one can determine the belonging cell temperature T_M by the following equations respectively, in which A_M is the module's area.

$$V_{oc}(T_M, G_{STC}) = V_{oc} + \left(\frac{\partial V_{oc}}{\partial T}\right)_{STC} (T_M - T_{STC}), \tag{K.15}$$

$$I_{sc}(T_M, G_{STC}) = I_{sc} + \left(\frac{\partial I_{sc}}{\partial T}\right)_{STC} (T_M - T_{STC}), \tag{K.16}$$

$$P_{mpp}(T_M, G_{STC}) = P_{mpp} + \left(\frac{\partial P_{mpp}}{\partial T}\right)_{STC} (T_M - T_{STC}), \tag{K.17}$$

$$\eta(T_M, G_{STC}) = \frac{P_{mpp}(T_M, G_{STC})}{G_{STC} A_M}, \tag{K.18}$$

All types of names for solar irradiation

Table K.1: Types of Solar Radiation and Their Notations

Type of Radiation	Notation	Abbreviation	Description
Global Horizontal Irradiance	G_{hem} or G'	GHI	Total amount of shortwave radiation received from above by a horizontal surface. This includes both direct solar irradiance and diffuse horizontal irradiance.
Direct Normal Irradiance	G_{b} or I_{b}	DNI	The amount of solar radiation received per unit area by a surface that is always held perpendicular (normal) to the rays that come in a straight line from the direction of the sun at its current position in the sky.
Diffuse Horizontal Irradiance	G_{d} or I_{d}	DHI	The component of solar radiation received from the sky (excluding the solar disk) on a horizontal surface.
Global Tilted Irradiance	G_{t}	GTI	Total amount of shortwave radiation received per unit area on a plane that is tilted at an angle to the horizontal.
Reflected Irradiance	G_{r}	-	Solar radiation that has been reflected from the ground or other surfaces onto the receiving surface.
Spectral Irradiance	G_{λ}	-	The irradiance of a specific wavelength or band of wavelengths of solar radiation. It is often described as a function of wavelength.
Extraterrestrial Irradiance	G_0	-	The solar irradiance outside the earth's atmosphere on a plane perpendicular to the rays of the sun. This value is approximately 1361 W/m^2, also known as the solar constant.
Direct Tilted Irradiance	$G_{\text{b}}(\theta)$	DTI	The portion of the direct normal irradiance that is incident on a tilted plane.
Hemispherical Irradiance on a Tilted Plane	$G_{\text{hem,t}}$	-	The sum of direct and diffuse irradiance on a tilted plane.

L

PVT Panel Datasheet

TECHNISCHE GEGEVENS

Warmtepomp

Omschrijving	Eenheid	VWS 36/4.1 230V · brine/water	VWF 57/4 400V · brine/water
Prestaties (NEN 14511 B0/W35)			
Merk		Vaillant	Vaillant
Verwarming	kW	2,7	5,3
Elektrisch vermogen	kW	0,7	1,3
sCOP		4,7*	5,0*
*Conform gelijkwaardigheidsverklaring op bcrg.nl			
Dimensies			
Hoogte	mm	720	1183
Breedte	mm	440	595
Diepte	mm	430	600
Netto gewicht	kg	59	145
Aansluitmaten			
Verwarming		22 mm	G 1 1/2"
Broncircuit		22 mm	G 1 1/2"
Elektrische gegevens			
Spanning	V	230	400
Frequentie	Hz	50	50
Afzekerwaarden	At	16	3 x 16/25
Aanloopstroom	A	23	15
Beschermingsgraad	IP	20	10B
Maximaal elektrisch vermogen	kW	1,1	2,5
Naverwarmer	kW	2 – 6**	2–9
Geluidsdruk	dB(A)	34 (op 2m afstand)	30 (op 2m afstand)
** In het geval van een all-electric systeem			
Koude circuit			
Koudemiddel		R 410 A	R 410 A
Type compressor		Rolzuiger	Scroll
Broncircuit			
Vulling		Water/Glycol	Water/Glycol
Percentage	Glycol	30%	30%
Brondebiet (ΔT 3 K)	l/h	620	1290
Restopvoerhoogte bron (ΔT 3 K)	mbar	590	620
Opgenomen vermogen pomp	W	3 – 70	25 – 75
Energielabel bronpomp		A	A
Cv-circuit			
Vulling /		Water	Water
Cv-debiet (ΔT 5 K)	l/h	465	920
Restopvoerhoogte bron (ΔT 5 K)	mbar	620	650
Opgenomen vermogen pomp B0/W35	W	21	25
Energielabel cv-pomp		A	A
Maximale cv-temperatuur	°C	55	65

TECHNISCHE GEGEVENS

Boilervat

Omschrijving	Eenheid		
Merk		DEJONG	DEJONG
Model		WPS 200	WPS 300
Inhoud	L	181	283
Energielabel		B	B
Stilstandverlies EN 12897	W	48	55
Afmetingen (H x D)	cm	149 x 60 incl. isolatie	180 x 67,5 incl. isolatie
Gewicht leeg	kg	41	61
Gewicht vol	kg	222	344

TECHNISCHE GEGEVENS

PVT-paneel

Merk zonnepaneel		DMEGC
Model		Full black mono DM325G1-60BB
Elektrisch vermogen	Wp	325
Afmetingen	mm	1.002 x 1.665 x 40
Materiaal thermische collector		Polypropyleen
Inhoud thermische collector	L	13,6
Vloeistof thermische collector		Water-propyleenglycol mengsel
Stagnatietemperatuur	°C	70
Gevuld gewicht Volthera paneel	kg	40
Merk optimizer		SolarEdge

De thermische prestatie van het Volthera PVT-paneel is getest door TÜV Rheinland te Keulen in november 2018 conform EN ISO 9806:2013.

COP Volthera PVT-systeem

		VWS 36/4.1			VWF 57/4		
Glycol temperatuur ↓	Afgifte temperatuur →	35 °C	45 °C	55 °C	35 °C	45 °C	55 °C
-5 °C		3,4	2,7	2,2	4,2	3,2	2,6
0 °C		3,9	3,1	2,5	4,7	3,7	3,0
5 °C		4,5	3,4	2,9	4,9	4,1	3,3
10 °C		5,2	3,9	3,2	5,3	4,2	3,6
15 °C		6,0	4,5	3,5	5,8	4,5	3,8
20 °C		7,0	5,0	4,0	6,3	5,0	4,2

M

ISO 9806:2017

A.14.2 Test results

Maximum ball diameter without damage (if ice ball testing)	mm

Maximum drop height (1 digit precision) without damage (if steel ball testing)	m

Any evident problems, damages and failures according to Clause 17
(description and photos)

Other observations and remarks

A.15 Final inspection

Evaluate and rate each potential problem as described in Clause 17.

Table A.5 — Final inspection record

Collector component	Potential problem	Evaluation
a) Collector box/fasteners	Cracking/warping/corrosion/rain penetration/permanent deformation/Accumulation of humidity/etc.	
b) Mountings/structure	Strength/safety/loosening/fatiguing/etc.	
c) Seals/gaskets	Cracking/loss of adhesion/elasticity/brittleness/etc.	
d) Cover	Cracking/breaking/crazing/buckling/delamination/permanent warping and deformation/outgassing/etc.	
e) Absorber as a whole	Deformation/corrosion/buckling/etc.	
f) Absorber coating	Cracking/crazing/blistering/discolouration/peeling/flaking/etc.	
g) Reflectors	Deformation/cracking/crazing/blistering/discolourtion/buckling/peeling/flaking/etc.	
h) Absorber tubes and headers/Flow passages/hoses inside the collector	Deformation/corrosion/leakage/loss of bonding/irreversible swelling/etc.	
i) Absorber mountings	Permanent deformation/corrosion/rupture/etc.	
j) Insulation	Water retention/outgassing/swelling/degradation/scorching/singeing/any other detrimental changes that could adversely affect collector performance/fouling/etc.	
k) Corrosion and other deterioration caused by chemical action. Anywhere in the collector	Corrosion shall be considered severe if it impairs the function of the collector or if there is evidence that it will progress	
l) Retention of water. Anywhere in the collector	Excessive retention of water anywhere in the collector	
m) Heat pipes	Loss of fluid/loss of pressure/severe deformation/etc.	
n) Self-protection systems	Any problem	
o) Other components	Any other abnormality resulting in a reduction of thermal performance or service life time	

N
Test characteristics

During testing some procedures need to be taken into consideration, a small sum up of these can be found in this paragraph. The first is, the average value of the surrounding air speed, taking into account spatial variations over the collector and temporal variations during the test period, shall be less than 4 m/s. Furthermore The dew point is for QDT not of importance as well as the mean collector temperature to stay within $\pm$ 3 K from the ambient air temperature.

What is of importance is written in the following table, Table **??**, which is written in ISO9806-2017, 23.5.

**Table N.1:** Measured quantities during testing

	SST liquid	SST air	WISC*/ QDT
Hemispherical solar irradiance at the plane of the collector	X	X	X
Diffuse solar irradiance at the plane of the collector (only outdoors)	X	X	X
Angle of incidence of direct solar radiation (only outdoors)	X	X	X
Airspeed parallel to the plane of the collector	X	X	X
Temperature of the ambient air	X	X	X
Temperature of the heat transfer fluid at the collector inlet and outlet	X	X	X
Flow rate of the heat transfer fluid	X	–	X
Dew point temperature of the surrounding air	–	X	–
(Relative) humidity of the fluid at the collector inlet and outlet	–	X	–
The mass flow rate of the heat transfer fluid at the collector inlet (only closed loop)	–	X	–
The mass flow rate of the heat transfer fluid at the collector outlet	–	X	–
Static pressure of the heat transfer fluid at the inlet and outlet of the solar collector	–	X	–
Absolute pressure of the ambient air	–	X	–
Long wave thermal irradiance in the collector plane	–	–	X (WISC only)

A change of the inlet temperature can be done after a test has been completed. The inlet temperature should be stable within $\pm$ 1K during each test.

Weather conditions are described as in 23.6.2 in which multiple day types are described. Testing should be done in a minimum length of 3 hours, but does not have to be consecutive. The several parts should be at a minimum length of 30 minutes.

- **Day type 1:** Conduct testing with clear skies, ensuring the incident angle varies from just over 60 degrees to a point where the beam irradiance's angle modifier changes by no more than 2% from the normal incidence value.

- **Day type 2:** Perform at least one test with variable cloud coverage, which could range from partial to complete cloud cover, or under completely clear conditions. This sequence may occur at an increased operational temperature or under standard η_0-conditions.
- **Day type 3 (1 or 2 days):** Collect data with the collector operating at an average temperature, paired with unobstructed sunny conditions.
- **Day type 4:** Record measurements while the collector operates at elevated temperatures, in the presence of clear skies.

O
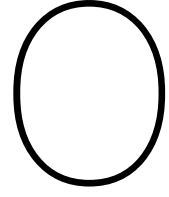
Thermal performance collector: ISO9806

Useful power extracted in the collector is mentioned in Equation O.1. With this later efficiency can be defined.

$$\dot{Q}_{prod} = \dot{m} \cdot C_p \cdot \Delta T \qquad (O.1)$$

Then the thermal efficiency is determined for the QDT method by calculating $\dot{Q}_{loss}$ as follows in Equation O.2

$$\dot{Q} = A_g \left[\frac{\eta_{0,b} K_b(\theta_L, \theta_T) G_b + \eta_{0,b} K_d G_d - a_1(\vartheta_m - \vartheta_a) - a_2(\vartheta_m - \vartheta_a)^2 - a_3 u'(\vartheta_m - \vartheta_a) +}{a_4(E_L - \sigma T_a^4) - a_5\left(\frac{d\vartheta_m}{dt}\right) - a_6 u' G_{hem} - a_7 u'(E_L - \sigma T_a^4) - a_8(\vartheta_m - \vartheta_a)^4} \right] \qquad (O.2)$$

With the following parameters

- A_G is the gross area of the collector.
- $\eta_{0,b}$ is the peak collector efficiency for beam irradiance.
- $K_b(\theta_L, \theta_T)$ is the incidence angle modifier for direct beam irradiance.
- G_b is the beam (direct) solar irradiance.
- K_d is the incidence angle modifier for diffuse radiation.
- G_d is the diffuse solar irradiance.
- $a_1, a_2, \ldots, a_8$ are empirical coefficients for the collector's heat loss which are defined below.
- ϑ_m is the mean fluid temperature.
- ϑ_a is the ambient air temperature.
- u' is the reduced wind speed.
- E_L represents the long-wave radiation exchange with the environment.
- σ is the Stefan-Boltzmann constant.
- T_a is the ambient temperature.
- G is the global solar irradiance.
- $\frac{d\vartheta_m}{dt}$ represents the rate of change of the mean fluid temperature.

The Concentration Ratio C_R plays a role in defining these a-parameters. For a PVT panel, this ratio is considered between 1.1 and 2.5, as can be read in [50]. Since this is lower than 20, based on [7], a_1, a_2 and a_5 are mandatory and a_8 can be set to 0.

The TüV report is first made as a SST method for the Sunbeam (flat roof) setup, in which the testing environment is isolated from the sun and only produces artificial conditions with wind speeds between 2 and 2 m/s, namely 0.1, 2.4 and 2.8 m/s, besides, the thermal panel is partly covered (with the PV

Coefficient	Description	Units
a_1	Heat loss coefficient	W/(m^{2}K)
a_2	Temperature dependence of the heat loss coefficient	W/(m^{2}K^2)
a_3	Wind speed dependence of the heat loss coefficient	J/(m^{3}K)
a_4	Sky temperature dependence of the heat loss coefficient	—
a_5	Effective thermal capacity	J/(m^{2}K)
a_6	Wind speed dependence of the zero loss efficiency	s/m
a_7	Wind speed dependence of IR radiation exchange	W/(m^{2}K^4)
a_8	Radiation losses	W/(m^{2}K^4)

part). This means that by [7] a few heat loss coefficients are set to zero. These are: a_3, a_4, a_6 and a_7. Furthermore, it is specifically named in the report that a_5 is not taken into consideration since the method is SST, in which thermal capacity (a_5) is not measured. Based on this test report, in the dark, the formula for $\dot{Q}$ follows in the next Equation O.3

$$\dot{Q} = A_G \left[\eta_{0,b} K_b(\theta_L, \theta_T) G_b + \eta_{0,b} K_d G_d - a_1(\vartheta_m - \vartheta_a) - a_2(\vartheta_m - \vartheta_a)^2 - a_3 u'(\vartheta_m - \vartheta_a) \right] \qquad \text{(O.3)}$$

With this equation, and the parameters formed by testing, done by TÜV as can be found in Appendix Q, the heat loss coefficients could be determined. Later with these, the total thermal efficiency of the panel calculated and checked, and used to approach the testing performances at Coolworld Waalwijk. The parameters are:

- $\eta_{0,hem}$ = 0
- a_1 = 48.61 with σ = 0.0391 $W/(m^2 K$
- a_3 = 13.07 with σ = 0.176 $W s/(m^3 K$
- $dotm$ = 202 kg/h

The equation below shows what the overall equation is that is used to calculate the performance while testing, based on ISO9806-2017 and the corresponding heat coefficients.

$$\dot{Q} = A_G \left[\eta_{0,b} K_b(\theta_L, \theta_T) G_b + \eta_{0,b} K_d G_d - a_1(\vartheta_m - \vartheta_a) - a_3 u'(\vartheta_m - \vartheta_a) \right] \qquad \text{(O.4)}$$

These numbers are again calculated to see if they correspond correctly and used in this paper. For u' the related wind speed is: u - 3 m/s. Equation O.4 will then be:

$$\dot{Q} = 1.94 \left[48.61(\vartheta_m - \vartheta_a) - 13.07 u'(\vartheta_m - \vartheta_a) \right] \qquad \text{(O.5)}$$

The numbers are checked and correspond correct, only small rounding-off differences are noticeable. After, the last few coefficients could be defined, which resulted in the following parameters:

Symbol	Value	Standard deviation	Unit
η_{hem}^*	0.101	-	-
η_{ab}	0.102	0.003	-
K_d^{***}	1.0	-	-
a_1^{**}	52.14	0.564	W/(m^{2}K)
a_2^{**}	0	-	W/(m^{2}K^2)
a_3^{**}	15.77	0.339	Ws/(m^{3}K)
a_4^{***}	0	-	-
a_5^{**}	12467	2984	Ws/(m^{2}K)
a_6^{**}	0.035	-	s/m
a_7^{***}	0	-	s/m
a_8^{***}	0	-	W/(m^{2}K^4)
C/A	-	-	Ws/(m^{2}K)

Table O.1: Incidence Angle Modifier

Angle [°]	0	10	20	30	40	50	60	70	80*	90
$K_d(\theta, 0)$ trans	1.00	1.00	1.00	1.00	0.99	0.99	0.98	0.49	0	-
$K_d(\theta, 0)$ longi	1.00	1.00	1.00	1.00	0.99	0.99	0.98	0.49	0	-

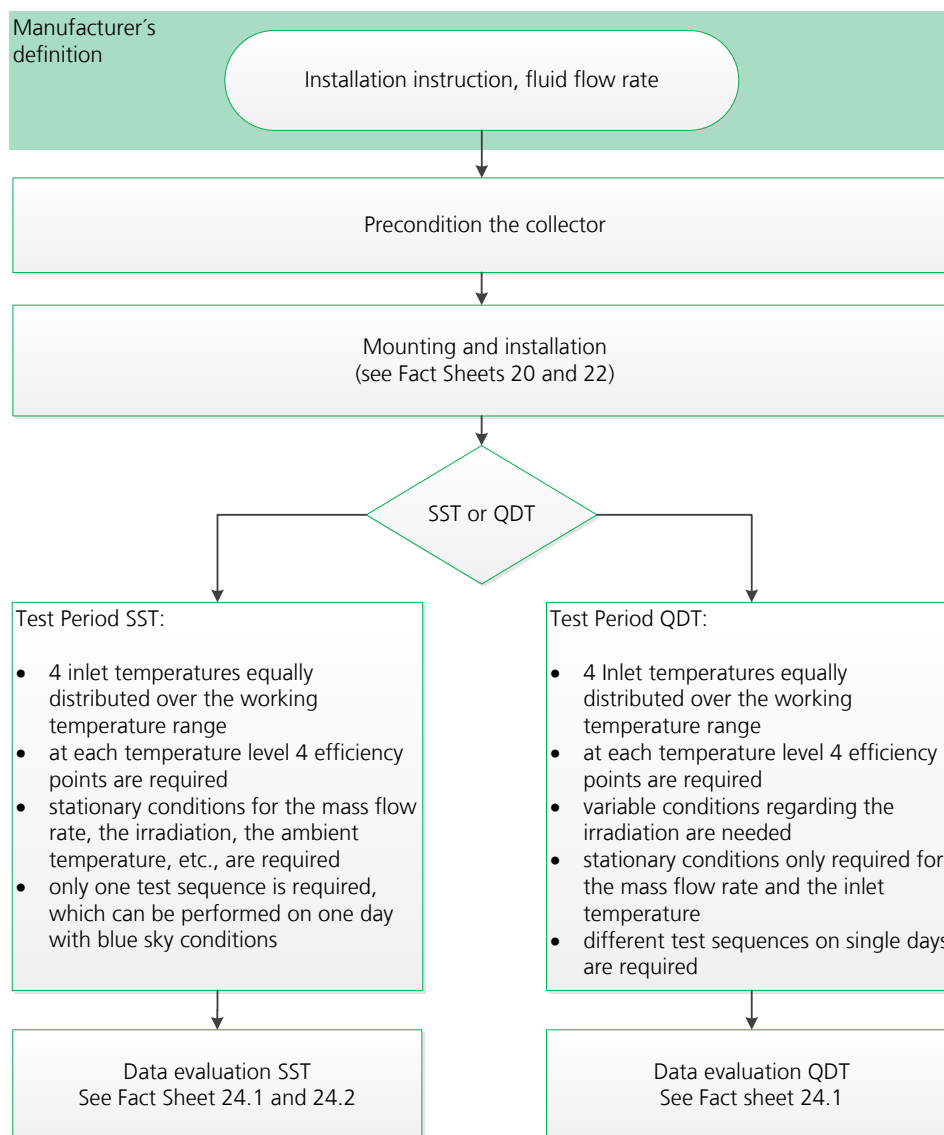# P

Guide to Standard ISO 9806:2017

23 Performance Test Procedures

The thermal performance of a collector shall either be tested according to the Steady-State Testing (SST) or the Quasi-Dynamic Testing (QDT) procedure as given in ISO 9806:2017.

Procedure

Manufacturer´s definition

> Installation instruction, fluid flow rate

↓

> Precondition the collector

↓

> Mounting and installation
> (see Fact Sheets 20 and 22)

↓

◇ SST or QDT ◇

Test Period SST:

- 4 inlet temperatures equally distributed over the working temperature range
- at each temperature level 4 efficiency points are required
- stationary conditions for the mass flow rate, the irradiation, the ambient temperature, etc., are required
- only one test sequence is required, which can be performed on one day with blue sky conditions

↓

Data evaluation SST
See Fact Sheet 24.1 and 24.2

Test Period QDT:

- 4 Inlet temperatures equally distributed over the working temperature range
- at each temperature level 4 efficiency points are required
- variable conditions regarding the irradiation are needed
- stationary conditions only required for the mass flow rate and the inlet temperature
- different test sequences on single days are required

↓

Data evaluation QDT
See Fact sheet 24.1

"Tips and Tricks"

- In case of SAHC, it is important to measure the time constant first because it can reduce the time effort for testing significantly and avoid failures in testing;

- In case of liquid heating FPCs, usually a "time constant" of 10 minute is sufficient. The time constant shall be long enough to make sure that the steady state conditions have been reached;
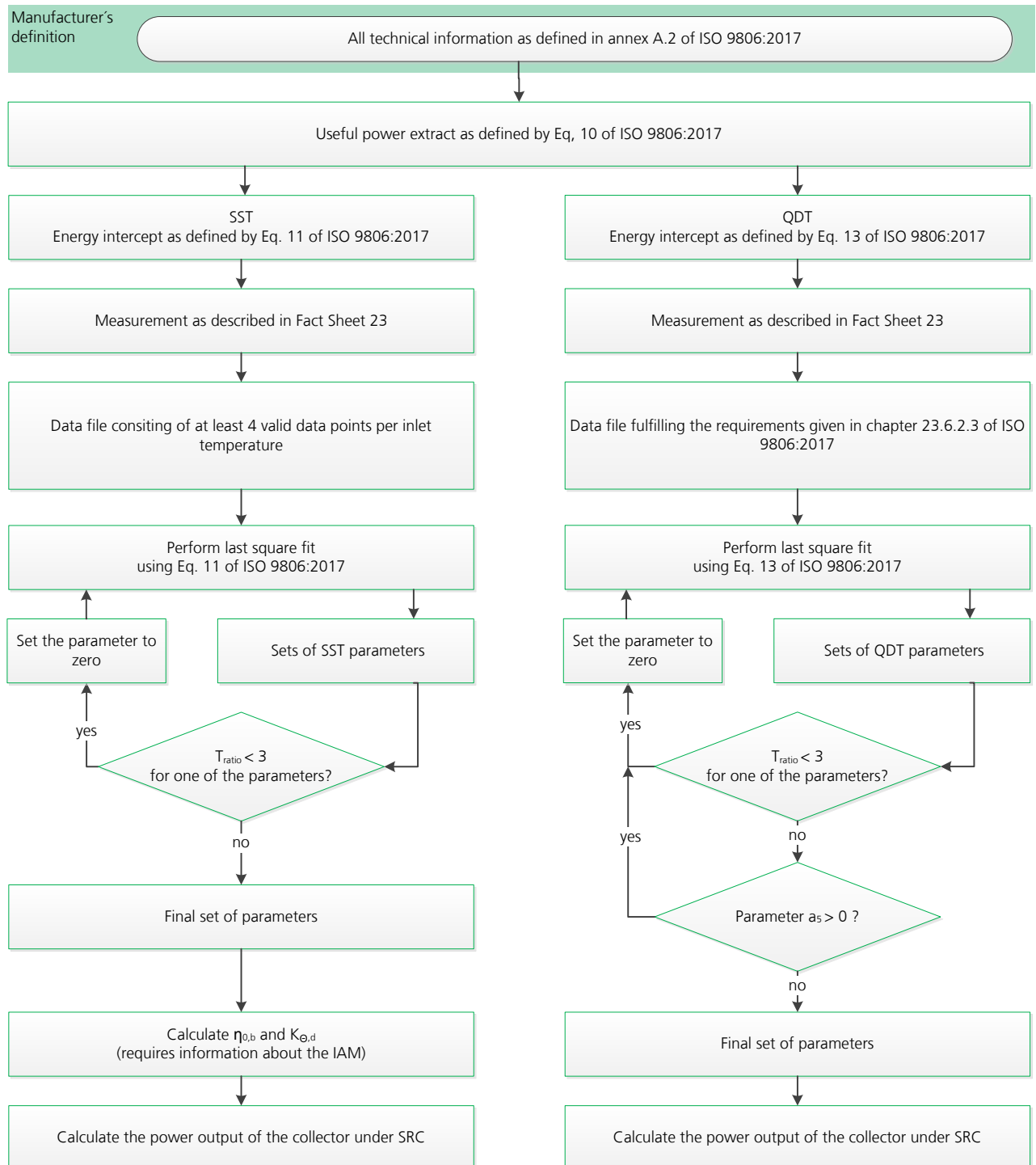
24.1 Computation of Parameters (liquid heating collectors)

This Fact Sheet contains information about the computation of collector parameters including the power extracted $\dot{Q}$, the solar energy intercepted, and information about modelling the instantaneous efficiency and the power output of liquid heating collectors.
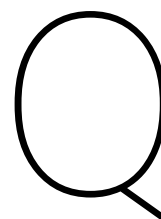
Procedure

Manufacturer´s definition	All technical information as defined in annex A.2 of ISO 9806:2017

Useful power extract as defined by Eq, 10 of ISO 9806:2017

SST	QDT
Energy intercept as defined by Eq. 11 of ISO 9806:2017	Energy intercept as defined by Eq. 13 of ISO 9806:2017
Measurement as described in Fact Sheet 23	Measurement as described in Fact Sheet 23
Data file consiting of at least 4 valid data points per inlet temperature	Data file fulfilling the requirements given in chapter 23.6.2.3 of ISO 9806:2017
Perform last square fit using Eq. 11 of ISO 9806:2017	Perform last square fit using Eq. 13 of ISO 9806:2017

Set the parameter to zero — Sets of SST parameters

$T_{ratio} < 3$ for one of the parameters? yes / no

Final set of parameters

Calculate $\eta_{0,b}$ and $K_{\Theta,d}$ (requires information about the IAM)

Calculate the power output of the collector under SRC

Set the parameter to zero — Sets of QDT parameters

$T_{ratio} < 3$ for one of the parameters? yes / no

Parameter $a_5 > 0$? no

Final set of parameters

Calculate the power output of the collector under SRC

Q

TüV report Alius Volthera EVO Collector

TÜVRheinland®

Prüfbericht-Nr.: *Test report no.*:	**DE23S2GS 001**	**Auftrags-Nr.:** *Order no.*:	3001 01078	Seite 1 von 9 *Page 1 of 9*
Kunden-Referenz-Nr.: *Client reference no.*:	4660	**Auftragsdatum:** *Order date:*	2023-02-17	

Auftraggeber: *Client*:	Alius Energ BV (for add. information see page 3)
Prüfgegenstand: *Test item*:	Solar thermal PVT collector
Bezeichnung / Typ-Nr.: *Identification / Type no.*:	Volthera EVO + DM405M10-54HBB + Aelex
Auftrags-Inhalt: *Order content*:	A collector dark performance test following EN ISO 9806:2017 should be performed.
Prüfgrundlage: *Test specification*:	EN ISO 9806:2017 Solar energy - Solar thermal collectors - Test methods

Wareneingangsdatum: *Date of sample receipt*:	2023-03-14
Prüfmuster-Nr.: *Test sample no:*	see "List of test samples"
Prüfzeitraum: *Testing period*:	2023-03-22 – 2023-06-12
Ort der Prüfung: *Place of testing*:	Cologne
Prüflaboratorium: *Testing laboratory*:	Solar Energy Assessment Center Cologne
Prüfergebnis*: *Test result*:*	Pass

geprüft von: *tested by*:	X *[signature]* Signiert von: Juergen Sommer	**genehmigt von:** *authorized by*:	X *[signature]* Signiert von: Ulrich Fritzsch
Datum: *Date:* 2023-08-07		**Ausstellungsdatum:** *Issue date:* 2023-08-07	
Stellung / Position:	Sachverständige(r)/Expert	**Stellung** / Position:	Sachverständige(r)/Expert

Sonstiges / *Other*:	EN 12975:2022

Zustand des Prüfgegenstandes bei Anlieferung: *Condition of the test item at delivery*:	Prüfmuster vollständig und unbeschädigt *Test item complete and undamaged*

* Legende:	P(ass) = entspricht o.g. Prüfgrundlage(n)	F(ail) = entspricht nicht o.g. Prüfgrundlage(n)	N/A = nicht anwendbar N/T = nicht getestet
* Legend:	*P(ass) = passed a.m. test specification(s)*	*F(ail) = failed a.m. test specification(s)*	*N/A = not applicable N/T = not tested*

	Anmerkungen
	Remarks

1	Alle eingesetzten Prüfmittel waren zum angegebenen Prüfzeitraum gemäß eines festgelegten Kalibierungsprogramms unseres Prüfhauses kalibriert. Sie entsprechen den in den Prüfprogrammen hinterlegten Anforderungen. Die Rückverfolgbarkeit der eingesetzten Prüfmittel ist durch die Einhaltung der Regelungen unseres Managementsystems gegeben. Detaillierte Informationen bezüglich Prüfkonditionen, Prüfequipment und Messunsicherheiten sind im Prüflabor vorhanden und können auf Wunsch bereitgestellt werden. *The equipment used during the specified testing period was calibrated according to our test laboratory calibration program. The equipment fulfils the requirements included in the relevant standards. The traceability of the test equipment used is ensured by compliance with the regulations of our management system. Detailed information regarding test conditions, equipment and measurement uncertainty is available in the test laboratory and could be provided on request.*
2	Wie vertraglich vereinbart, wurde dieses Dokument nur digital unterzeichnet. Der TÜV Rheinland hat nicht überprüft, welche rechtlichen oder sonstigen diesbezüglichen Anforderungen für dieses Dokument gelten. Diese Überprüfung liegt in der Verantwortung des Benutzers dieses Dokuments. Auf Verlangen des Kunden kann der TÜV Rheinland die Gültigkeit der digitalen Signatur durch ein gesondertes Dokument bestätigen. Diese Anfrage ist an unseren Vertrieb zu richten. Eine Umweltgebühr für einen solchen zusätzlichen Service wird erhoben. *As contractually agreed, this document has been signed digitally only. TUV Rheinland has not verified and unable to verify which legal or other pertaining requirements are applicable for this document. Such verification is within the responsibility of the user of this document. Upon request by its client, TUV Rheinland can confirm the validity of the digital signature by a separate document. Such request shall be addressed to our Sales department. An environmental fee for such additional service will be charged.*
3	Prüfklausel mit der Note * wurden an qualifizierte Unterauftragnehmer vergeben und sind unter der jeweiligen Prüfklausel des Berichts beschrieben. Abweichungen von Prüfspezifikation(en) oder Kundenanforderungen sind in der jeweiligen Prüfklausel im Bericht aufgeführt. *Test clauses with remark of * are subcontracted to qualified subcontractors and descripted under the respective test clause in the report.* *Deviations of testing specification(s) or customer requirements are listed in specific test clause in the report.*

4	**Revision History**			
	Revision	*Date*	*Nature of changes*	*Page*
	-	07/08/2023	Original issue	

Prüfbericht-Nr.: DE23S2GS **001**	Seite 3 von 9
Test report no.:	*Page 3 of 9*

Produktbeschreibung
Product description

| 1	**Auftraggeber** *Client*	AliusEnergy BV Meerheide 101 5521 DX Eersel Netherlands	
2	**Produktdetails** *Product details*	**Allgemeine Informationen ;** General Information	
		Brand name	Alius Energy
		Type name	Volthera EVO + DM405M10-54HBB + Aelex
		Construction type/Category	PVT collector
		Year of production	2023
		Hydraulic Designation Code	-
		Dimensionen / Gewicht ; Dimension / Weight	
		Dimension (l / w / h) [mm]	1708 / 1134 / 30 (PV) 70 (PVT)
		Gross area [m²]	1.94
		Aperture area [m²]	1.94
		Absorber area [m²]	n.n.
		Weight empty [kg]	n.n.
		Fluid content [l]	n.n.
		Flow rate (recommended) [kg/s]	n.n.
		Absorber tube orientation	Mainly horizontal
		Flow pattern	Two parallel serpentine absorber
		Einsatzmöglichkeit; Intended use / Limitations	
		Maximum operating temperature [°C]	n.n.
		Maximum operating pressure [kPa] at max. temperature of operation	n.n.
		Minimum tilt angle [°]	n.n.
		Maximum tilt angle [°]	n.n.
		Recommended heat transfer medium	n.n.
		Collector mounting	n.n.
		Other limitations	n.n.
3	**Technische Dokumentation** *Technical documentation*	-	

TÜVRheinland®

Produktbeschreibung
Product description

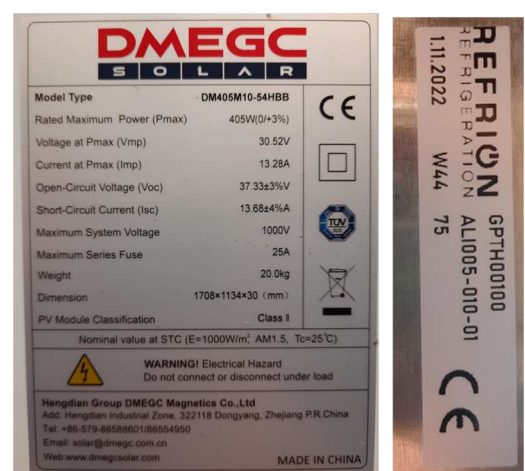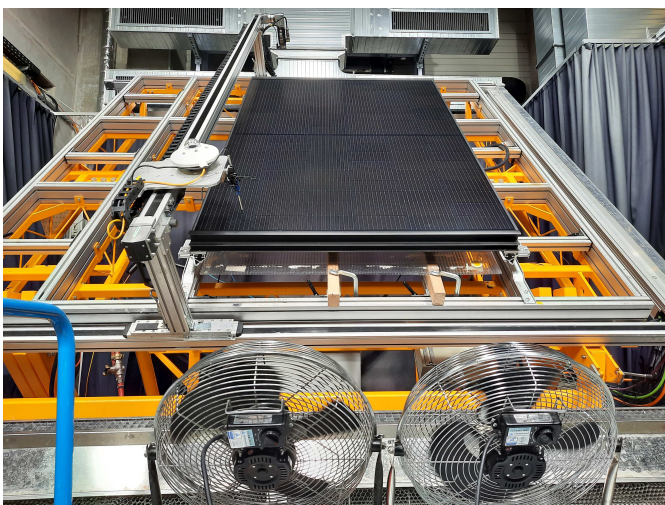| 4	**Verwendete Materialien** *Used materials*	R&D Samples
5	**Produktionsstandort** *Manufacturing site(s)*	AliusEnergy BV (see Point 1)
6	**Sonstiges** *Other*	Test sample(s), as well as sample information, description, product details and intended usage was provided by customer.
7	**Prüfmusterbereit-stellung**: *Test sample obtaining*	☒ Sending by customer ☐ Sampling by TÜV Rheinland Group ☐ others:
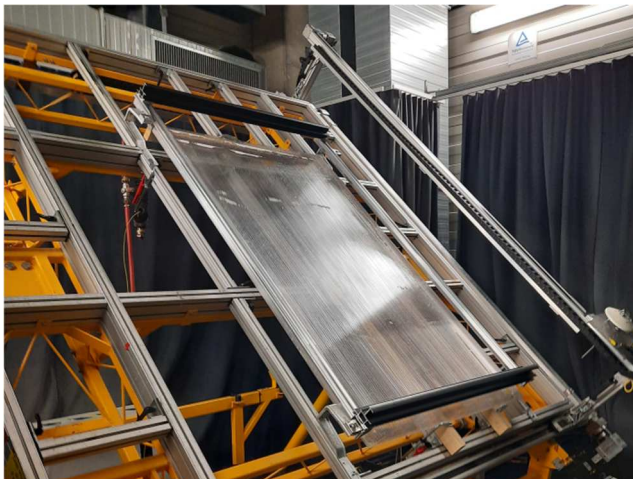
Test set up	Ventilation unit
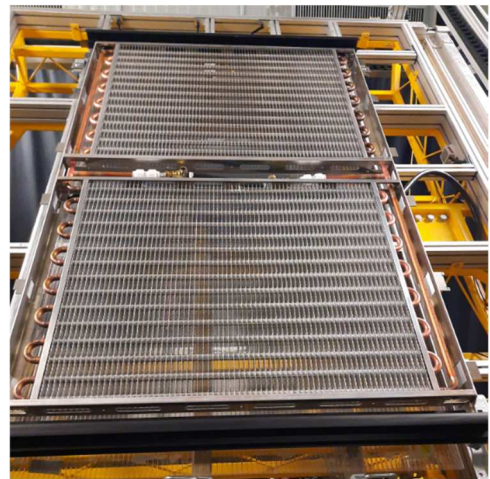
Test set up	

Prüfbericht-Nr.: DE23S2GS **001** *Test report no.:*			Seite 5 von 9 *Page 5 of 9*
Absatz *Clause*	**Anforderungen - Prüfungen /** *Requirements - Tests*	**Messergebnisse – Bemerkungen/** *Measuring results - Remarks*	**Ergebnis** *Result*
-	**General remarks and subblementary information**		

Measuring uncertainties		
All results only refer to the test samples that were subjected to testing. The extended total measuring uncertainty for the outdoor performance test is: $\eta \leq \pm\ 2.8\ \%$ (for irradiation levels above 700 W/m²) The extended total measuring uncertainty (k=2) for the indoor performance test is: $\eta \leq \pm\ 2\ \%$	—

-	**List of test samples**		

Sample No.	Sample S/N	Remarks / constructional characteristics	
HV2023001262	DMWUBBUFA1231AL00425	PV Module	
HV2023001267	ALI005-010-01 1.11.2022 W44 75	Heat Exchanger	

Absatz *Clause*	Anforderungen - Prüfungen / *Requirements - Tests*	Messergebnisse – Bemerkungen/ *Measuring results - Remarks*	Ergebnis *Result*
23b	**Dark performance testing of fluid heating collectors – Indoor testing – full wind**		

Test date [DD/MM/YYYY]	23/03/2023 /// 24/03/2023	
Method used for determination acc. to	<u>Following</u> Clause 23.4.2 "Steady-state testing of liquid heating collectors"	
Used type of lamps	ATLAS MHT 4010 (not relevant)	
Shading of long wave radiation by	Artificial cold sky (not relevant)	
Collector tilt angle [° from horizontal]	45	
Orientation of the collector during test	Portrait	—
Used fluid	Water	
Minimum/ **Mean**/ Maximum irradiance [W/m²]	0 / **0** / 0	
Minimum/ **Mean**/ Maximum collimation [W/m²] (for total test area; less than 30° angle)	- / **0%** / - (of irradiation lies in the angle of beam < 30°)	
Mean Long wave irradiance "IRnet" [W/m²]	0	
Mean wind speed [m/s]	0.4/ 1.9/ 2.4 (with artificial wind generation)	
Mean mass flow [kg/s]	0.056	
Supplementary information:		

Sample No. HV2023001262 HV2023001267	Collector performance coefficients		
	Value	Standard deviation	Unit
$eta_{0,hem}$	0	-	-
$eta_{0,b}$	0	-	-
K_d	0	-	-
a_1	51.62	0.564	W/(m²K)
a_2	0	-	W/(m²K²)
a_3	16.10	0.339	Ws/(m³K)
a_4	0	-	-
a_5	-***	-	Ws/(m²K)
a_6	0	-	s/m
a_7	0	-	s/m
a_8	0	-	W/(m²K^4)
C/A	-***	-	Ws/(m²K)
Nominal flowrate during the Measurement $\dot{m}$ [kg/h]		202	

Supplementary information: ***as the test was only performed as steady state indoor test, the determination of thermal capacity is not possible.

According to the standard and with reference to the wind speed requirements for covered collectors, the related wind speed u' is calculated u'=u -3 m/s. If u will be used, the performance will be under estimated!

Absatz *Clause*	**Anforderungen - Prüfungen /** *Requirements - Tests*	**Messergebnisse – Bemerkungen/** *Measuring results - Remarks*	**Ergebnis** *Result*

Collector power output [W] full wind	
Dark performance output at varying wind speed ranges	

$\vartheta_m - \vartheta_a$ [K]	No wind 0m/s	Low wind 1.5 m/s	mean wind 3 m/s	High wind 5 m/s	—
-10	64.5	533.0	1001.5	1626.2	
0	0.0	0.0	0.0	0.0	
10	-64.5	-533.0	-1001.5	-1626.2	

Peak Power per unit $\dot{Q}_{peak}$ [W]	**0**	

Collector power output	—

Power Curve PVT @ 0 W/m² full-wind
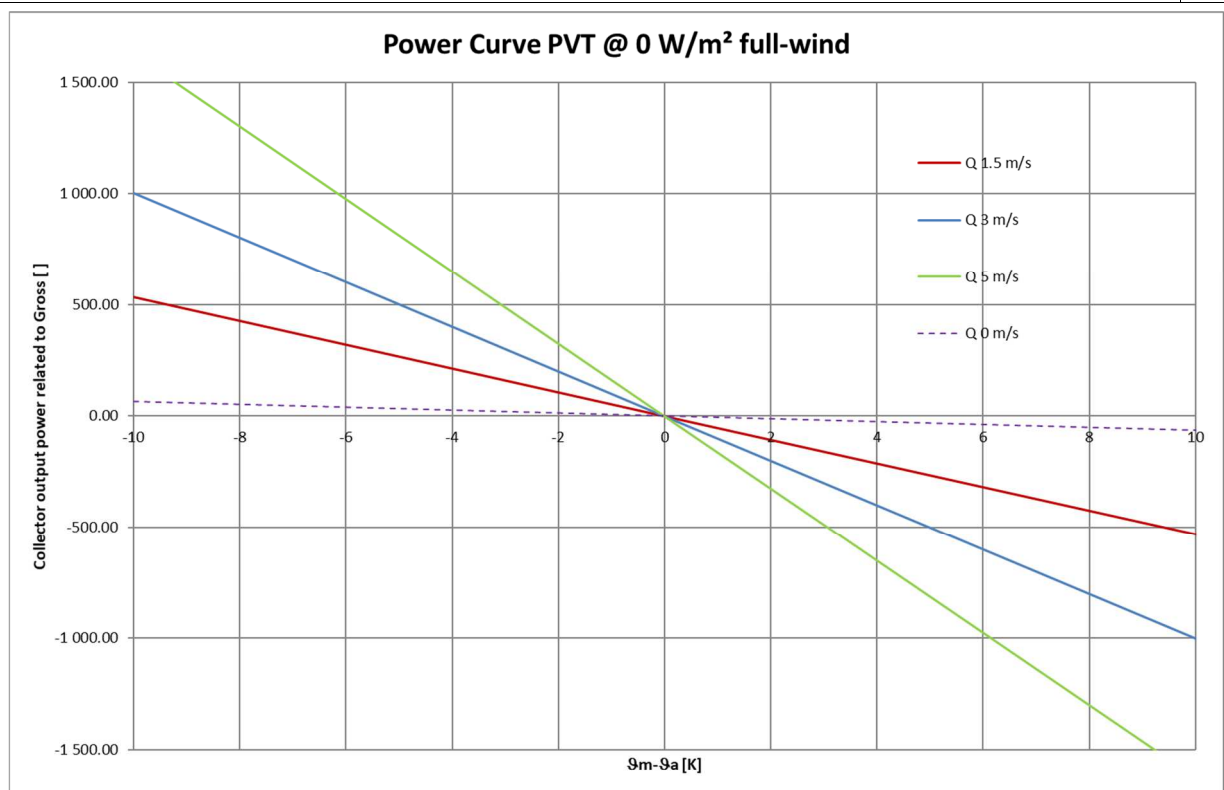
Supplementary information:

| **Prüfbericht-Nr.:** DE23S2GS **001** *Test report no.:*		Seite 8 von 9 *Page 8 of 9*

Absatz *Clause*	**Anforderungen - Prüfungen /** *Requirements - Tests*	**Messergebnisse – Bemerkungen/** *Measuring results - Remarks*	**Ergebnis** *Result*
-	**Additional normative information**		

Collector performance table – full wind												—
Date	UTC	G	t_a	U	m_{dot}	t_{in}	t_e	t_m	t_m-t_a	T*m	Q_{dot}	eta g
YY-MM-DD	hh:mm	W/m²	°C	m/s	kg/s	°C	°C	°C	K	m²*K/W	W	- - -
2023-03-23	15:59		c	2.4	0.0548	14.86	17.84	16.35	-8.43		684.8	
2023-03-23	16:10		24.92	2.4	0.0548	14.66	17.74	16.20	-8.72		708.9	
2023-03-23	17:05		24.26	2.4	0.0554	16.59	18.85	17.72	-6.55		524.1	
2023-03-23	17:26		24.14	2.4	0.0553	16.55	18.80	17.67	-6.47		522.3	
2023-03-23	18:11		24.13	2.4	0.0564	20.50	21.57	21.04	-3.09		253.8	
2023-03-23	18:36		24.11	2.4	0.0563	20.49	21.55	21.02	-3.09		249.9	
2023-03-23	19:27		24.10	1.9	0.0548	14.71	17.11	15.91	-8.20		552.6	
2023-03-23	19:48		23.97	1.9	0.0548	14.58	16.96	15.77	-8.20		546.4	
2023-03-23	20:34		23.83	1.9	0.0554	16.51	18.34	17.42	-6.41		425.4	
2023-03-23	20:55		23.70	1.9	0.0554	16.51	18.32	17.42	-6.29		419.9	
2023-03-23	21:41		23.96	1.9	0.0565	20.47	21.30	20.89	-3.08		194.8	
2023-03-23	22:02		23.83	1.9	0.0565	20.48	21.29	20.88	-2.95		190.2	
2023-03-23	22:40		23.95	1.9	0.0572	24.39	24.30	24.35	0.40		-21.5	
2023-03-23	23:01		23.96	1.9	0.0571	24.40	24.31	24.35	0.39		-20.8	
2023-03-24	15:49		24.48	0.4	0.0545	16.55	17.16	16.86	-7.62		138.9	
2023-03-24	16:10		24.47	0.4	0.0545	16.58	17.20	16.89	-7.58		140.6	
2023-03-24	20:41		24.63	0.4	0.0558	20.48	20.76	20.62	-4.01		64.0	
2023-03-24	21:02		24.62	0.4	0.0558	20.49	20.76	20.63	-3.99		63.0	

Supplementary information: -

Power Curve PVT @ 0 W/m² full-wind
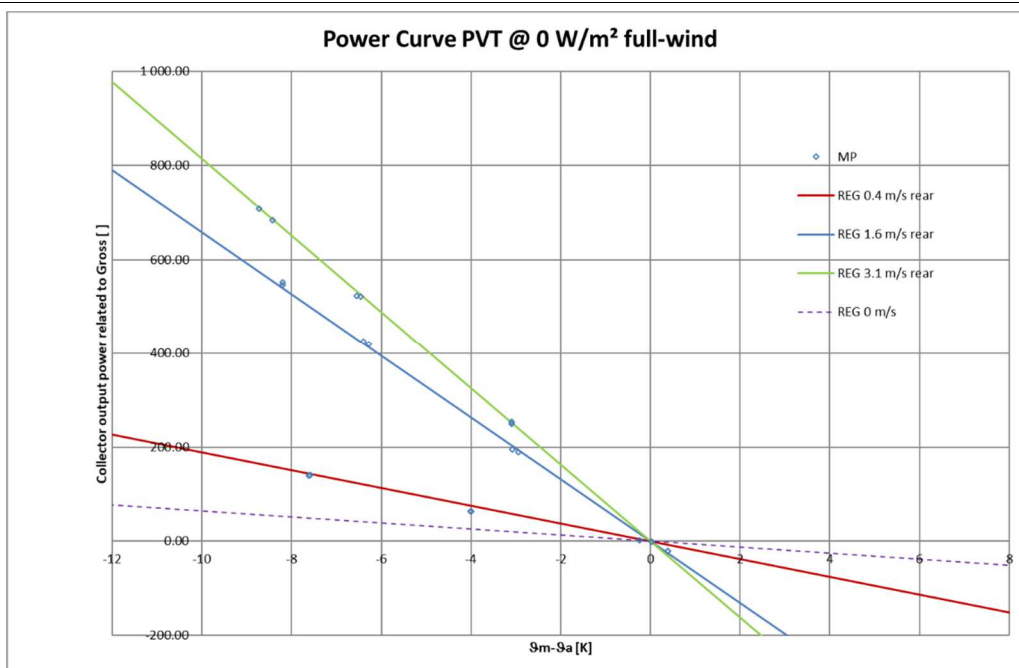
Supplementary information: -

--- Blank page ---

Test report no.: **DE23S2GS 001**

Page 9 of 9

--- End of report ---